2017

Experimental study fo white heat line formation in burned bone using fourier transform infrared spectroscopy

BOSTON UNIVERSITY

SCHOOL OF MEDICINE

Thesis

EXPERIMENTAL STUDY OF WHITE HEAT LINE FORMATION IN BURNED BONE USING FOURIER TRANSFORM INFRARED SPECTROSCOPY

by

MEGAN ANNE GOUGH

B.A., University of South Carolina, 2013

Submitted in partial fulfillment of the

requirements for the degree of

Master of Science

2017

Approved by

First Reader

James T. Pokines, Ph.D., D-ABFA
Assistant Professor
Program in Forensic Anthropology
Department of Anatomy and Neurobiology

Second Reader

Gary Reinecke, M.A. (SSA ret. FBI)
Instructor
Program in Forensic Anthropology
Department of Anatomy and Neurobiology

Third Reader

Sabra Botch-Jones, M.S., M.A., ABFT-FTS
Instructor
Program in Biomedical Forensic Sciences
Department of Anatomy and Neurobiology

DEDICATION

This work is dedicated to my parents, James and Maureen Gough, my husband Will, my sister Reid, and the rest of my family and friends for supporting me throughout this entire process. Thank you for all of your unconditional love and encouragement. I could not have accomplished this without you.

ACKNOWLEDGMENTS

The completion of this project would not have been possible without the assistance of many. First and foremost, I would like to thank my thesis committee. Thank you to Dr. Pokines, Agent Reinecke, and Professor Botch-Jones for lending your expertise, support, and guidance to my thesis.

A special thank you goes to Chief Michael Cassidy for supervising the experimental burning process out in Holliston and to Dr. Donald Siwek for his help in the laboratory during the processing of my samples. In addition, I would like to thank Dr. Farzad Mortazavi for his advice and assistance with my project's statistical analysis.

Finally, I would like to extend my gratitude to Krehbiels Specialty Meats, Inc. in McPherson, Kansas for providing me the sheep and pig bones utilized in this research.

EXPERIMENTAL STUDY OF WHITE HEAT LINE FORMATION IN BURNED BONE USING FOURIER TRANSFORM INFRARED SPECTROSCOPY

MEGAN ANNE GOUGH

ABSTRACT

In the anthropological analysis of burned bone, the presence of a white heat line aids in determining a bone's physical condition prior to burning, distinguishing between those burned fleshed or wet versus dry. However, while the relationship between this thermal signature and a bone's physical condition has been studied, there is a lack of research concerning the chemical composition of white heat lines.

The present study assessed the composition of white heat lines that form on burned bone using Fourier transform infrared spectroscopy (FTIR) with the potassium bromide (KBr) pellet method. The present study examined the effects of soft tissue and the retention of bone's organic material, including naturally-occurring grease and water, on the development and appearance of a white heat line. Experimental remains consisted of isolated long bones from white-tailed deer (*Odocoileus virginianus*), elk (*Cervus canadensis*), sheep (*Ovis aries*), and pig (*Sus scrofa*) in five physical conditions – fleshed (fresh bones with adhering soft tissue), very wet (recently defleshed bone, greasy), partially wet (defleshed, slight grease retention), dry (defleshed, naturally degreased), and soaked (formerly dry bone immersed in water). These bones were burned over a wood fire made within a 55-gallon drum.

After a visual analysis to evaluate white heat line formation, chemical composition was analyzed by determining spectral peak heights of the carbonate (CO_3)

ν3 (1415 cm^{-1}), phosphate (PO_4) ν3 (1035 cm^{-1}), and amide I (1660 cm^{-1}) vibrational bands. These thermal signatures appear to form superficially, measuring approximately 1.5 mm in depth. Results indicate that white heat lines that formed on fleshed bone contain an increased amount of CO_3, PO_4, and amide I in comparison to their unburned controls, while those that formed on very wet bone contain decreased amounts instead.

These findings further our knowledge of how fire modifies physical remains and the effect that bone's physical condition prior to burning has on the development of a white heat line and the resulting compositional changes. In order to build upon the results gained from the present study, continuing research is needed to investigate compositional differences between white heat lines that form on fleshed versus very wet bone and to assess bone's fat content as a possible contributing factor. Additional FTIR research is needed to assess the other vibrational bands of CO_3, PO_4, and amide that are present in bone.

TABLE OF CONTENTS

LIST OF TABLES

LIST OF FIGURES

LIST OF ABBREVIATIONS

β-TCP ..... beta-tricalcium phosphate

BUSM ..... Boston University, School of Medicine

Ca ..... calcium

CO_3 ..... carbonate

FTIR ..... Fourier transform infrared spectroscopy

HRR ..... heat release rate

KBr ..... potassium bromide

kJ/s ..... kilojoules per second

kW ..... kilowatts

MANOVA ..... multi-variate analysis of variance

Mg^{2+} ..... magnesium

Na^{2+} ..... sodium

ORF ..... Outdoor Research Facility

PO_4 ..... phosphate

SNR ..... signal-to-noise ratio

WHL ..... white heat line

CHAPTER 1: INTRODUCTION

Forensic anthropologists often must interpret the sequence of events from the time of death until the discovery of skeletal remains (Ellingham *et al*, 2015; Keough 2013; Keough *et al*., 2015; Ubelaker 2009). The presence of burned bone poses additional concerns, raising questions as to the timing of the burning event and the physical condition of the body prior to burning. Analyzing burned remains is a complicated process, for fire is a destructive force that can damage, alter, or destroy physical remains and the associated evidence (Dirkmaat *et al.*, 2012; Fairgrieve 2008; Symes *et al.*, 2008a). For bodies exposed to fire and heat, the resulting modifications are diverse and extensive (Bohnert *et al.*, 1998; Christensen 2002; Pope 2007; Pope and Smith 2004; Porta *et al.*, 2013). Burned bone may become heavily fractured, fragile, and discolored, making it difficult to distinguish, and subsequently recover, human remains from other burned, nonhuman items (Ubelaker 2009). Once recovered, reconstruction and interpretation of skeletal remains may be problematic due to compound changes in the burned bones' structure, color, and overall size in comparison to their thermally unaltered form.

A variety of events can result in thermally altered remains, including transportation accidents, attempts to conceal criminal activity, accidental fires, and explosions (Symes *et al.*, 2008a; Ubelaker 2009). Fire scenes are often complex, as both the body (or individual skeletal elements) and the surrounding environment are dramatically affected. Furthermore, fire suppression and extinguishing efforts by first

responders typically result in dispersed and additional fragmented remains. Thus, fire scenes pose difficult investigative challenges (Dirkmaat *et al.*, 2012). In a forensic context, these types of events often require a joint effort by individuals from several medico-legal fields, including law enforcement and forensic science, to recover and analyze the burned remains (Cordner *et al.*, 2011; Park *et al*., 2009; Ubelaker *et al.*, 1995).

In a forensic investigation, skeletal remains provide crucial contextual information, especially if the original fire scene has been disturbed (Ellingham *et al.*, 2015). Anthropological analysis of burned bone contributes to a more comprehensive interpretation of the fire scene (e.g., position and orientation of the body), as well as to the reconstruction of events leading to the thermal incident (e.g., condition of the body prior to the event) (Dirkmaat *et al.*, 2012; Ellingham *et al.*, 2015). Depending upon the condition of the remains and which skeletal elements are recovered, a forensic anthropologist may be able to estimate an individual's biological profile, including biological sex, age-at-death, stature, and ancestry (Thompson 2004), as well as describe any potentially individualizing characteristics (e.g., medical device, broken bone, or dental work) (Dirkmaat *et al.*, 2012).

The degree to which remains are burned can be highly variable, as differential burning may occur throughout an entire body or on a single skeletal element (Symes *et al.*, 2008a). However, regardless of the extent, the burning process of soft and hard tissues proceeds in a consistent, identifiable, and predictable pattern (Adelson 1955; Bass 1984; Bohnert 1998; DeHaan 2012; Icove and DeHaan, 2004; Pope 2007; Pope and

Smith, 2004). Combustion of a body starts with the superficial soft tissue layers first, beginning with the skin, before progressing inwards to the muscles, subcutaneous fat, and other deeper tissue layers as the thermal event continues (Pope 2007).

Once the soft tissues have been consumed by the fire, the underlying bone will then undergo heat-induced alterations (Fairgrieve 2008). When exposed to high temperatures, bone's chemical properties are altered, and its structural integrity is then compromised or lost (Symes *et al.*, 2008a). Research on characteristics of burned bone has increased, including descriptive, experimental, and actualistic studies, and it has been established that heat exposure causes significant chemical and mechanical changes to bone, resulting in dehydration, discoloration, shrinkage, warping, fracture, and fragmentation (Bradtmiller and Buikstra, 1984; Buikstra and Swegle, 1989; Goncalves *et al.*, 2011; Holden *et al.*, 1995a, 1995b; Nicholson 1993; Quatrehomme *et al.*, 1998; Symes *et al.*, 2012; Thompson 2004, 2005; Thompson and Chudek, 2007; Walker and Miller, 2005; Wells 1960).

During a thermal event, the gradual shrinkage and destruction of soft tissues causes bone to undergo a series of visible color changes as it dehydrates and becomes exposed to the heat source (Buikstra and Swegle, 1989; Nicholson 1993; Pope 2007; Pope and Smith, 2004; Shipman *et al.*, 1984). Heat-induced color changes occur in set stages as the burning event progresses and the heat exposure continues to modify and reduce bone's organic material (Bonucci and Graziani, 1975). These sequential color changes remain as a permanent signature of thermal modification and are used to distinguish burned bone from unburned (Pope and Smith, 2004). They also depict the

degradation of bony organic material, as well as the location, direction, extent, and progression of the burning event (Alunni *et al.*, 2014; Pope 2007).

Symes *et al.* (2008a) categorize this color change as initial unaltered bone that progresses to a white heat line, heat border, charring, and lastly, calcination. Initially, natural unaltered bone is generally light ivory or beige in color (Mayne Correia, 1997). The first area of heat-modified bone is an opaque white heat line, an occasionally occurring feature that, when it forms, is the area of initial transition from unaltered to thermally altered bone (Keough 2013; Keough *et al.*, 2012, 2015; Symes *et al*., 1999a, 1999b, 2008a, 2014a). Adjacent to the white heat line is the heat border, a translucent off-white or yellow boundary that may have been protected from direct contact with the heat source by overlying, yet receding soft tissue (Symes *et al.*, 2008a). The width of the heat border is generally broader than that of the white heat line. Burned bone then becomes charred and black in color as a result of the carbonization of skeletal material and incineration of organic components, primarily collagen (Buikstra and Swegle, 1989; Herrmann 1977; Nelson 1992; Shipman *et al.*, 1984; Symes *et al.*, 2014a). Calcination is a continuation of the combustion process, resulting in bone that is gray with blue tints, to gray, and then finally white, indicating a complete loss of all organic compounds and moisture (Binford, 1963; Buikstra and Swegle, 1989; Nelson 1992; Shipman *et al*., 1984; Quatrehomme *et al.*, 1998).

Analysis of thermally altered bone has rapidly increased due to experimental studies and forensic cases (Bohnert *et al.*, 1998; Cattaneo *et al.*, 1999; Christensen 2002; Correia 1997; Fairgrieve 2008; Holden *et al.*, 1995; Pope and Smith, 2004; Thompson

2005; Ubelaker 2009). While researching circumstances that surround sets of remains at the time of burning, several observational and experimental studies have distinguished between bones burned in one of three conditions: fleshed (fresh bones encased in adhering soft tissue), green or wet (defleshed shortly before burning, greasy), and dry (defleshed and degreased) (Asmussen 2009; Cain 2005; Buikstra and Swegle, 1989; Keough *et al.*, 2012; Keough *et al.*, 2015; Pope 2007; Pope and Smith, 2004; Symes *et al.*, 2008a; Symes *et al.*, 2014a). Knowledge of a bone's prior physical condition contributes to anthropological examinations of burned skeletonized remains and interpretation of the sequence of events leading to the thermal modification (Ellingham *et al.*, 2015; Ubelaker 2009).

Methods for determining a bone's physical condition prior to burning can include evaluating heat-induced fracture and cracking patterns (Symes *et al.*, 2008b; Symes *et al.*, 2012), changes in surface texture (Cain 2005), dimensional transformations such as shrinkage and expansion (Shipman *et al.*, 1984; Thompson 2005), warping of overall bone morphology (Fairgrieve 2008; Goncalves *et al.*, 2011), deformation of bone's microstructural features (Bradtmiller and Buikstra, 1984), and macroscopic gradient color changes (Buikstra and Swegle, 1989; Nicholson 1993; Shipman *et al.*, 1984). Many researchers agree that similar thermal characteristics exist among bones burned while fleshed or wet that may differentiate them from those burned dry. However, there are fewer physical differences that will reliably distinguish between the former, for bone burned fleshed versus wet (Asmussen 2009; Bennett, 1999; Buikstra and Swegle 1989; Cain 2005; Pope 2007; Stiner *et al.*, 1995).

Recent studies indicate that the formation of a white heat line aids in determining a bone's physical condition prior to burning (Keough 2013; Keough *et al.*, 2012, 2015; Symes *et al.*, 2008, 2014). Notably, experiments suggest that one may differentiate between bones burned fleshed or wet versus dry, making the white heat line an important source of information in anthropological analysis regarding the relative timing of burning. Symes *et al.* (2008a) note that a white heat line may form with fleshed burned remains as the heat causes muscle and other soft tissues to retract, exposing the bone to the heat source. Other researchers observed similar burn patterns in fully fleshed bodies, either fresh or in early decomposition, noting that a white heat line was not present when bone burned in the absence of soft tissue (Keough *et al.*, 2012; Pope 2007; Symes *et al.*, 1999a). However, Keough (2013) and Keough *et al.* (2015) found that distinct white heat lines formed on remains burned in early to advanced decompositional stages, with bone conditions ranging from fleshed or partially fleshed, to wet and lacking extensive soft tissue protection.

However, while the relationship between bone's physical condition prior to burning and white heat line formation has been studied, there is a lack of research concerning the chemical or physical composition of this thermal signature. Due to its proximity to the heat source in a burning event, previous research suggests that this area of bone has undergone some dehydration and molecular alteration (Symes *et al*., 2014a), resulting in a reduced organic component (Pope 2007; Pope and Smith, 2004; Symes *et al.*, 2008a). The present study will expand upon previous research concerning the formation of a white heat line on burned bone in relation to bone's physical condition

prior to burning. Additionally, this research will be the first to investigate the chemical composition of white heat lines.

Research Objectives

The present study investigates the effects of soft tissue and the retention of bone's organic material, including naturally-occurring grease and water, on the development and appearance of a white heat line for bones thermally altered by burning. Skeletal remains for this project consist of 108 isolated long bones from four animal species: white-tailed deer (*Odocoileus virginianus*), elk (*Cervus canadensis*), sheep (*Ovis aries*), and pig (*Sus scrofa*). Of these 108 long bones, 96 were burned as the experimental samples, while the remaining 12 were used as the thermally unaltered controls.

These long bones were burned over a wood fire while in five physical conditions with differing amounts of organic material present: (1) fleshed (fresh bones encased in adhering soft tissue); (2) very wet (recently defleshed bone that is still greasy); (3) partially wet (defleshed with slight grease retention); (4) dry (defleshed and naturally degreased); (5) soaked (formerly dry bone immersed in water). Ten percent of the bones for each sample group were set aside as thermally unaltered controls.

The goal of the present study is to determine the chemical composition of white heat lines. The hypothesis tested is that a white heat line forms from inorganic minerals deposited on or near the bone's surface, resulting from the evaporation of moisture in advance of the expanding carbonized bone. These lines will manifest under analysis as an increase of carbonate (CO_3) and phosphate (PO_4) (representing the mineral component

of bone), as well as a lack of the organic component Amide I (from proteins found in type I collagen, the main organic phase), in comparison to thermally unaltered bone and burned bone that does not develop a white heat line.

The quantity of these three components were calculated based on the spectral peak heights of the carbonate (CO_3) ν3 (1415 cm^{-1}), phosphate (PO_4) ν3 (1035 cm^{-1}), and amide I (1660 cm^{-1}) vibrational bands using Fourier Transform Infrared Spectroscopy (FTIR). Spectral peak peaks for CO_3, PO_4, and amide I will then be compared between the unburned controls, burned bones that develop a white heat line, and burned bones that do not develop this thermal signature for each of the five sample groups. The current study will contribute to forensic anthropological investigations of thermally altered remains and further the field's understanding of how a bone's physical condition prior to burning affects why and/or how a white heat line may form.

The current study will further the field's understanding of how fire and heat modify physical remains, specifically, with regards to the effect that bone's physical condition prior to burning has on the resulting heat-induced compositional changes. The presence of this thermal signature is utilized in forensic anthropological investigations of thermally altered remains regarding the relative timing of burning and yet limited research has been conducted to determine why or how it forms. Assessing the composition of white heat lines, or in its absence the junction of unburned and charred bone, will further delineate the chemical changes that bone undergoes during the beginning and middle stages of a thermal event.

CHAPTER 2: PREVIOUS RESEARCH

Bone Biology

Bone Composition

Bone is a composite material consisting of three main components: an organic phase, an inorganic phase, and water (Farlay and Boivin 2012). The organic component, representing approximately 25-30% of bone's mass, is comprised predominately of type 1 collagen (90%), as well as a small percentage of other non-collagenous proteins (10%) (Pearson and Lieberman 2004). Collagen is a fibrous, structural protein and the most abundant protein found in the human body (Miller 1984). In bone, the collagen molecules intertwine to form flexible and slightly elastic fibers (White *et al.,* 2012).

These organic components exist within a dense, inorganic matrix comprised mainly of calcium phosphate as a poorly formed crystalline hydroxyapatite ($Ca_{10}(PO_4)_6(OH)_2$) (D'Elia *et al.,* 2007; Etok *et al.,* 2007; Michel *et al.,* 1995; Mkukuma *et al.,* 2004; Wopenka and Pasteris 2005; Wright and Schwarcz 1996). This inorganic mineral phase accounts for 60-70% of bone's mass (Pearson and Lieberman 2004; Wang *et al.,* 2010) and contains several major elements: calcium (Ca^{2+}), phosphate ($PO4^{3-}$), and carbonates ($CO3^{2-}$) (LeGeros and LeGeros 1983; LeGeros *et al.,* 1968). These three major elements comprise 40%, 18%, and 6-7% of bone's mass, respectively. Minor elements are also present, including magnesium (Mg^{2+}) and sodium (Na^{2+}), as well as trace elements that can be introduced into the body through one's diet. Living bone also contains blood vessels, nerve tissue, fats, and other tissues that promote growth and enable bone to continually repair and remodel itself throughout life in response to

stressors or injury (Currey 2002). The organic phase contributes to bone's flexibility and elasticity, while the inorganic matrix is responsible for the tissue's rigidity, hardness, and strength (Dirkmaat *et al.,* 2012; Nala *et al.,* 2003; White *et al.,* 2012). Together, bone's organic and inorganic components create a strong, supportive, yet semi-flexible skeletal frame that is capable of withstanding tensile and compressive forces while enabling locomotion (Symes *et al.,* 2008a).

Bone Structure

In the adult skeleton, the gross anatomical structure of mature bones can be subdivided into compact and trabecular bone (Hillier and Bell 2007). Compact, or cortical, bone is solid and dense, generally found in the walls of bone diaphyses and on external bone surfaces (Bell *et al.,* 2001; White *et al.,* 2012). In contrast, trabecular, or cancellous, bone is spongy, porous, and lightweight with a honeycomb structure. Formed by, and named after, tiny bony spicules called trabeculae, trabecular bone is found in the epiphyses of long bones, in short bones, and layered within flat bones. Both bone types have an identical molecular and cellular composition; differences arise in their porosity and structural layout.

During life, the outer surface of bone is covered by a tough, vascularized membrane called the periosteum (White *et al.,* 2012). This tissue layer coats most bone surfaces, except for those covered by cartilage and/or in areas of articulation where bones connect at a joint. It is not present on dry bones. The periosteum serves to nourish the bone and helps anchor tendons and muscles. Within the diaphyses of long bones is a

hollow space called the medullary cavity. This inner bony surface is lined with a membrane, the endosteum, and contains yellow marrow in adults.

Mature bone, both compact and trabecular, is made up of lamellar bone tissue (White *et al.*, 2012). This tissue is named for its orderly and organized structure produced by the repeated addition of uniform bone layers, or lamellae, during growth (Boyde 1980; Currey 2003; Jowsey 1968). Compact bone, due to its dense composition, cannot be nourished by diffusion from surface-level blood vessels (White *et al.*, 2012). Instead, it utilizes Haversian systems, fundamental functional units consisting of Haversian canals and their concentrically arranged lamellae and canal networks (Currey 2003; Enlow 1962). At its core, each system contains a large, hollow Haversian canal, or secondary osteon, that contains blood, lymph vessels, nerves, and marrow (White *et al.*, 2012). These main canals are linked by additional, smaller canals, including canaliculi and Volkmann's canals, that radiate outward and create a network to supply nourishment to cells throughout the bone. In contrast, trabecular bone lacks a Haversian system, instead receiving nutrition from blood vessels in the surrounding marrow spaces.

Nonhuman mammalian bone is generally composed of plexiform, or fibrolamellar, bone (Enlow and Brown 1956, 1957, 1958; Currey 1960; de Ricqlès 1977; Stover *et al.*,1992). Commonly found among younger individuals, plexiform bone, especially that found under the insertion of strong muscles, may remodel into lamellar bone later in an animal's life (Currey 2002). This type of bone tissue is characteristic of large, fast-growing animals, such as cows, pigs, and sheep, as well as dogs and other carnivores (Currey 2003). It can also be found in the bones of primates, although less

frequently, and rarely in humans (e.g., fetal bone) (Hillier and Bell 2007). In developing humans, primary fibrolamellar bone may be laid down initially, but it is soon remodeled and replaced by lamellar bone (Currey 2002). As opposed to the organized and concentric Haversian system, plexiform bone exhibits a more disorganized and linear brick-shaped structure. This structure results from the dense arrangement of rectilinear vascular spaces that form from alternating layers of parallel-fibered, or woven, and lamellar bone tissues (Hillier and Bell 2007). Plexiform bone may also contain scattered Haversian systems, but they lack the concentric and evenly spaced alignment as seen in mature human bone.

Bone Functions

Bones, and the skeletal system that they comprise, serve a variety of functions for the human body (Symes *et al.*, 2008a, 2014b). Structurally, bones act as essential components of the musculoskeletal system and help to support the body, give it shape, and protect the internal organs (Currey 2002; White *et al.*, 2012). Mechanically, bones assist in movement by providing attachment points for muscles, tendons, and ligaments, as well as functioning as levers upon which the muscles act (Currey 2002; Pearson and Lieberman 2004). The skeletal system also functions as production centers of blood cells, storage facilities for fat and marrow, and as reservoirs of important elements for the body (e.g., calcium) (White *et al.*, 2012).

Thermal Alteration

Fire and Combustion

In order to interpret more accurately thermal damage caused to biological remains from burning, it is important to understand the fundamentals of fire. Fire is an exothermic oxidation reaction occurring between a fuel and an oxidizer, commonly the oxygen in the surrounding air (DeHaan 2006). This process of combustion can generate a sufficient amount of heat to be self-sustaining, as well as produce readily detectable energy in the form of additional heat and light (i.e., flames). A fire's heat output, or heat release rate (HRR), is measured in kilojoules per second (kJ/s) or kilowatts (kW) and can indicate the size or power of a fire (Icove and DeHaan 2004). This oxidation reaction has four requirements in order for a fire to occur: (1) combustible material (fuel), (2) adequate ignition temperature (heat), (3) sufficient oxygen (air), and (4) a suitable environment for maintaining these conditions (Holck 2005). If all four conditions are not present, a fire cannot be sustained.

Stages of Fire Development

The development of a fire is separated into four phases; these are based largely on a fire's HRR, as well as the timeframe in which they occur (Fairgrieve 2008). Each phase exhibits specific characteristics that can be recognized by fire investigators and utilized to evaluate a fire scene. The first phase, incipient ignition, takes place when heat, oxygen, and a fuel source combine and combustion occurs, starting a fire (Icove and DeHaan 2004). Next, additional fuel becomes involved, and in combination with

available ventilation, causes the fire to grow and its HRR to increase as greater amounts of heat and flame are produced. Once the fire is fully developed, it reaches a steady state wherein the maximum rate of burning is reached (DeHaan 2006). This hottest stage will continue for as long as there is a sufficient amount of oxygen and/or other fuels to support the fire's burning intensity and its heat and flame production. Lastly, the natural decay of a fire occurs when all available sources of fuel are consumed and the combustible materials have degraded, resulting in a decreased HRR and the eventual extinguishment of the fire.

Fire Types

Fire is categorized as two basic forms, flaming and smoldering (Han *et al.*, 2016). For the former, a flame is the visible product of a gaseous fuel burning in the presence of oxygen (Symes *et al.*, 2008a). It is the result of a gas-gas reaction made visible due to the effects of the heat produced. A flaming fire is the most common type of destructive fire, capable of spreading at very high speeds with high rates of heat release. Smoldering occurs due to the oxidation of a solid fuel in direct contact with oxygen. This solid-gas reaction can occur on the surface of fuel and/or within the matrix of a porous solid (e.g., charcoal). Even in the absence of flames, a smoldering fire can produce charring on the object burned (Fairgrieve 2008).

Fire Temperatures

Assessment of a fire's temperature can be problematic; due to the movement and 'flicker' of a flaming fire, it is difficult to measure the temperature of a flame at any one point as the temperature fluctuates rapidly (Symes *et al.*, 2008a). Therefore, it is recommended that one measure the average flame temperature instead. Average flame temperatures vary considerably based on the fuel used and their measured 'heat of combustion'. Generally, the average flame temperature for most fuels when burned in the air is in the range of 800-1000ºC. Common exceptions include methanol, whose flame temperatures can be in the range of 1200ºC, charcoal, and some plastics such as styrene and polyurethane, which can reach 1400ºC. Additionally, fires that occur in oxygen-enriched atmospheres can produce very high flame temperatures.

Heat Transfer

When substances ignite in a fire, including soft and hard tissues, it is due to the transfer of heat from one object to another (Fairgrieve 2008). Heat transfer can occur through four methods: conduction, convection, radiation, or superimposition (Symes *et al.*, 2008a). Conduction is a process by which thermal energy, specifically heat, passes from a warmer area of a solid material to a cooler one through direct physical contact (DeHaan 2006). During convection, heat transfer occurs as the result of liquids or gases moving from a warmer location to a cooler one (Fairgrieve 2008). Radiation is the transmission of electromagnetic waves from a warmer to a cooler surface. Lastly, superimposition is a combination of effects from two or more of the aforementioned

methods of heat transfer. Once heat is transferred to an object its temperature rises, beginning initially at its heated surface and progressing further into the object as the heat penetrates via conduction. The rate of heat transfer determines how quickly thermal damage is inflicted upon the biological tissues affected by a fire.

Soft Tissue Modification

The degree of heat-induced modifications to soft tissue can be highly variable, as differential burning commonly occurs throughout a whole body, or on a single skeletal element, highlighting the effects of exposure variability (Symes *et al.*, 2008a). Burn morphology of a body or skeletal element is affected by several factors, including the condition of the body or skeletal element prior to burning (e.g., fleshed, decomposed, or skeletonized) and its organic composition (Baby 1954; Binford 1963; Keough *et al.*, 2012, 2015; Symes *et al.*, 1999; Thurman and Wilmore 1980), the position and proximity of the body in relation to the fire (Fojas *et al.*, 2011), presence of broken bones, dismemberment, restraints or confinement (Fairgrieve 2008), duration of exposure to fire (Symes *et al.*, 1999), and intensity of the heat (Bohnert *et al.*, 1998). Additionally, various types of soft tissue respond differently to the thermal event based on relative depth and protection within the body or skeletal element, differential thickness of the tissue, as well as moisture and organic content (Pope 2007).

However, while the degree to which remains are burned may vary, the combustion process of soft tissues occurs in a recognizable, consistent, and predictable pattern (Adelson 1955; Bass 1984; Bohnert 1998; DeHaan 2012; Icove and DeHaan

2004; Pope 2007; Pope and Smith 2004). The burning process affects the most superficial soft tissue layers first, before progressing inwards to deeper tissue layers as the thermal event continues (Pope 2007). Initially, the skin is first impacted by the fire, leading to the dilation of the dermal and epidermal blood vessels, formation of skin blisters, and the eventual slippage and gloving of the epidermis from the dermis (Fairgrieve 2008). During this time, the hair is also affected, becoming charred and eventually consumed by the fire. The heat removes moisture from the skin and alters its organic composition and elasticity (Pope 2007), causing the skin to turn black and brittle as it chars (Thompson 2003). At this point in the burning process, heat-induced contractures can cause the skin to rupture and split (Fairgrieve 2008), occurring anywhere on the body (DeHaan 2006). Due to the fire's dehydrating effects, the epidermis and dermis contract, causing the ruptured skin margins to pull away, which exposes the underlying subcutaneous fat, muscle, ligaments, tendons, and hard tissues (DeHaan and Nurbakhsh 2001; Pope 2007; Pope and Smith 2004). No bleeding occurs at the site of these skin ruptures due to the coagulation of blood vessels from the heat (Fairgrieve 2008).

As the burning progresses, heat-induced dehydration in the muscle tissues causes their proteins to denature, resulting in a shortening of the deeper connective tissues (e.g., muscles, tendons, and ligaments) and postmortem muscle contractions (Crow and Glassman 1996; Eckert *et al.,* 1988; Ubelaker 2009). With continued combustion, the major, dominant flexor muscles overpower the contractions of the weaker extensor muscles, repositioning the body's extremities in the direction of the more powerful

muscle masses (DeHaan 2006; Icove and DeHaan 2004; Thompson 2003). The body may exhibit a general pose of extreme flexion, referred to as the "pugilistic posture" or "pugilistic pose" (Adelson 1955; Pope 2007; Symes *et al.,* 2008b; Ubelaker 2009), so-named as the upper body of a burn victim resembles that of a defensive boxing position (Dirkmaat *et al.,* 2012). This characteristic pose can occur as soon as ten minutes into burning (Bohnert *et al.,* 1998; Crow and Glassman 1996), resulting in the increased exposure of some anatomical areas and the shielding of others, depending upon the depth of the soft tissue and the specific posture assumed by the body (Symes *et al.,* 2008a). A full "pugilistic Pose" may not be attained if the muscles cannot react naturally to the heat and are somehow obstructed (e.g., lying against an object or facedown) or if the relationship between the muscles and bones has been compromised (e.g., broken bone prior to thermal event) (Dirkmaat *et al.,* 2012).

Once the skin and muscles undergo direct charring, turning black from the carbonization of organic materials, there is a loss of tissue mass and burning continues deeper, eventually reaching the internal organs and bones (Herrmann and Bennett 1999; Pope and Smith 2004; Richards 1977). As the thermal event progresses, the soft tissues and periosteum shrink away from their bony attachments, receding along the diaphysis, and gradually exposing the bone to the advancing heat (Pope 2007).

The differential protection of soft tissues, from the repositioning of the body's extremities in the "pugilistic pose", contributes to the manifestation of a normal burn pattern that forms when a fleshed body is exposed to fire (Symes *et al.,* 1999, 2001, 2008b, 2014a). Whole bodies burn first in areas with minimal soft tissue protection and

greater exposure before advancing to areas shielded by a greater amount of tissue (Symes *et al.,* 2008a). Thermal damage generally affects the distal ends of limbs first, before continuing along bone shafts to the proximal, and better protected, areas of the body (Pope 2007). However, areas of articulation may exhibit "joint shielding" in which the tissues are protected from burning (Symes *et al.,* 2014a). This phenomenon can occur anywhere on the body where two bones articulate at a joint, except in cases of dismemberment prior to burning. Areas of the body or skeletal element with the greatest amount of soft tissue density and/or those insulated from the fire are the last to be consumed (Fairgrieve 2008).

Stages of Heat Modification to Bone

Once the soft tissues have been consumed by the fire, including the epidermis, dermis, adipose, muscle, periosteum, and other connective tissues, the underlying bone will begin to undergo heat-induced alterations (Fairgrieve 2008). The anatomical distribution and differential thickness of the body's soft tissues affect which bones become exposed and when during a thermal event (Pope and Smith 2004). Boney surfaces covered by a thicker layer of muscle and other soft tissues are generally protected from the heat's effects longer than bone that is covered with a thinner layer of tissue.

When exposed to high temperatures, bone's chemical properties are altered, and its structural integrity is compromised or lost (Symes *et al.,* 2008a). The loss of chemical and structural properties for both organic and inorganic components is a complex process

not yet fully understood (Thompson 2005). Researchers remain uncertain of the exact chemical reactions, as well as the number and timing of transitions, that bone undergoes during burning. However, based on descriptive, experimental, and actualistic studies, it has been established that heat exposure causes significant chemical and mechanical changes to bone, resulting in dehydration, discoloration, shrinkage, warping, fracture, and fragmentation (Bradtmiller and Buikstra 1984; Buikstra and Swegle 1989; Goncalves *et al.,* 2011; Holden *et al.,* 1995a, 1995b; Nicholson 1993; Quatrehomme *et al.,* 1998; Symes *et al.,* 2012; Thompson 2004, 2005; Thompson and Chudek 2007; Walker and Miller 2005; Wells 1960). These heat-induced changes are variable and can fluctuate depending upon the interaction of several factors, including the bone's intrinsic properties, the intensity and duration of the thermal event, and whether the bone comes in direct contact with flames (Dirkmaat *et al.,* 2012).

Bone's reaction to heat can be described in four stages of a sequential process, defined by observed structural and compositional changes, as bone degrades (Thompson 2005). The first stage of the heat-induced modifications, dehydration, is characterized by the breaking of hydroxyl-bonds and the removal of both loosely-bound water (physisorbed) and bonded water (chemisorbed) from the hydroxyapatite mineral. Dehydration results in shrinkage of the bone's overall size, warping of its dimensions, weight loss, and fracture patterns at 100 to 600º C. Next, during the decomposition stage the organic components of bone (e.g., amino acids and collagen) are removed through the process of pyrolysis, or thermochemical decomposition (Bonucci and Graziani 1975; Civjan *et al.,* 1971). Occurring at 500 to 600º C, decomposition introduces heat-induced

color changes, a second phase of mass loss, reduction in mechanical strength, as well as changes in porosity (Thompson 2004). Continued exposure to the heat and fire leads to inversion, characterized by the loss of carbonates ($CaCO_3$) around 700 to 1100º C. Additionally, the hydroxyapatite recrystallizes and converts to beta-tricalcium phosphate (β-$Ca_3(PO_4)_2$ or β-TCP) (Bonucci and Graziani 1975; Civjan *et al.,* 1971; Grupe and Hummel 1991; Harbeck *et al.*, 2011; Herrmann 1977; Munro *et al.,* 2007; Ou *et al.*, 2013). The final stage, fusion, is characterized by the melting and coalescing of the crystal matrix at temperatures of 1000º and higher (Thompson 2005).

The terms dehydration, decomposition, inversion, and fusion were initially applied to burned bone by Shipman *et al.* (1984), building upon the earlier thermogravimetric research of Bonucci and Graziani (1975). The utility of these phases was later supported by Mayne Correia (1997) who added temperature ranges for each stage of thermal modification as gathered from her review of previous studies. Thompson (2004) modified these ranges based upon his own experimental work, proposing that the decomposition stage occurs at 300-800º C, inversion at 500-1100º C, and fusion at temperatures above 700º C. Thompson (2004) also states that these four stages do not in themselves fully explain all of the fundamental changes that occur in bone as a result of burning. He does, however, suggest that all heat-induced changes can be classified as occurring within one of these stages.

Heat-Induced Color Changes

During a thermal event, bone undergoes a sequence of macroscopic color changes as it dehydrates and becomes exposed due to the gradual shrinkage and destruction of soft tissues (Buikstra and Swegle 1989; Nicholson 1993; Pope 2007; Pope and Smith 2004; Shipman *et al.*, 1984). Heat-induced color changes occur in constant and set stages as the burning event progresses, delineating the advancement of thermal alteration as heat modifies and reduces bone's organic component (Bonucci and Graziani 1975). Burning does not uniformly encompass a bone's entire surface at one time; instead, it begins superficially and proceeds inward as the heat penetrates deeper into the bone (Pope 2007). Upon extinguishment of the fire, these sequential color changes remain as a permanent, diagnostic signature of thermal modification and are used to distinguish burned bone from unburned (Pope and Smith 2004). They also depict the degradation of bony organic material, as well as the location, direction, extent, and progression of the burning event (Alunni *et al.*, 2014; Pope 2007).

Symes *et al.* (2008a) categorize the color change progression as initial unaltered bone, then a white heat line, brown heat border, charring/carbonization, and finally, calcination. Natural unaltered bone is generally light ivory or beige in color (Mayne Correia 1997). The first heat-induced color changes follow the margins of soft tissue as heat exposure causes it to withdraw, exposing the bone (Pope and Smith 2004). Continued heat then alters the bone, beginning with the denaturation of organic materials, including collagen, proteins, water, and lipids (Pope 2007). This area of modified bone is the heat border, a translucent, off-white or yellow boundary that may have been protected

from direct contact with the heat source by overlying, yet receding, soft tissue (Symes *et al.*, 2008a). Variable in width, this border likely occurs due to the chemical alteration of the bone as organic compounds undergo initial pyrolysis during heat exposure (Pope and Smith 2004; Symes *et al.*, 1996). Adjacent to the heat border is an opaque white heat line, an occasionally occurring thermal signature that forms along the junction between heat-altered and thermally unaltered bone (Keough 2013; Keough *et al.*, 2012, 2015; Symes *et al*., 1999a, 1999b, 2008, 2014). When it forms, this macroscopic color change characteristic is the area of initial transition from unaltered to thermally altered bone. The width of the white heat line is generally narrower than that of the heat border.

Burned bone then transitions from brown to black in color as a result of the carbonization of skeletal material and organic pyrolysis, primarily of collagen (Buikstra and Swegle 1989; Nelson 1992; Shipman *et al.*, 1984; Symes *et al.*, 2014a). Charred bone, also referred to as carbonized or smoked, has come in direct contact with heat and flames, severely reducing its moisture content (Herrmann 1970). While the organic component of charred bone has been modified extensively (Herrmann 1977), in some cases the charred area may appear greasy due to persisting organic material and the release of marrow from the inner medullary cavity (Pope 2007). During this phase the periosteum is also destroyed (Fairgrieve 2008). Calcination is a continuation of the combustion process, resulting in bone that is gray with blue tints, to gray, and then finally white, indicating a complete loss of all organic materials and moisture (Buikstra and Swegle 1989; Nelson 1992; Shipman *et al*., 1984; Quatrehomme *et al.*, 1998). Calcined bone, therefore, is comprised primarily of inorganic hydroxyapatite crystals and the other

mineral components of bone (Pope 2007). As a result, calcined bone is extremely fragile, exhibiting a brittle, glasslike overall structure that is commonly accompanied by fracturing, shrinkage, and/or deformation (Binford, 1963; Buikstra and Swegle 1989; Nelson 1992; Shipman *et al*., 1984).

This full spectrum of color change can occur throughout a set of skeletal remains or on a single bone (Symes *et al.*, 2008a; Ubelaker 2009). Bones exposed to the thermal event the longest generally show the greatest amount of heat-induced degradation (Symes *et al.*, 1996). However, if a fire burns long and/or hot enough, the entirety of a set of remains, or a single bone, will eventually become charred and calcined (Symes *et al.*, 2008a). Thick cortical bone (e.g., diaphysis of the femur) is more durable than thinner cortical bone overlying trabecular structures (e.g., skull) and has a higher chance of survival (Pope 2007). Thin cortical layers may be completely destroyed prior to discovery.

White Heat Lines

Recent studies indicate that the presence of a white heat line aids in determining a bone's physical condition prior to burning (Keough 2013; Keough *et al.*, 2012, 2015; Symes *et al.*, 2008, 2014). Notably, experiments suggest that one may differentiate between bones burned fleshed or wet versus dry, making the white heat line an important source of information in anthropological analysis regarding the relative timing of burning. Symes *et al.* (2008a) note that a white heat line may form with fleshed burned remains as the heat causes muscle and other soft tissues to retract, exposing the bone to

the heat source. Other researchers observed similar burn patterns in fully fleshed bodies, either fresh or in early decomposition, noting that a white heat line was not present when bone burned in the absence of soft tissue (Keough *et al.*, 2012; Pope 2007; Symes *et al.*, 1999a). However, Keough (2013) and Keough *et al.* (2015) found that distinct white heat lines formed on remains burned in early to advanced decompositional stages, with bone conditions ranging from fleshed or partially fleshed, to wet and lacking extensive soft tissue protection. While white heat lines did form on partially fleshed remains or wet bone in advanced decomposition, this thermal signature formed most often in fresh remains or during the early stages of decomposition, when a combination of soft tissues and muscular structures were present (Keough 2013; Keough *et al.*, 2015). Keough (2013) and Keough *et al.* (2015) suggest that fresh tissue, still adhering to the underlying bone, is needed for a white heat line to form. In advanced decomposition, the nature of the soft tissue and denatured periosteum may allow the tissue to burn away with less resistance, preventing the creation of a distinctive white heat line.

The presence of a white heat line can also indicate that a bone is from a forensic context, for archaeological remains rarely exhibit this color gradient after being subjected to years or decades of taphonomic processes (Symes *et al.*, 2008a). Archaeological burned bone can become stained by the mineral deposits in its burial environment, making its appearance different than that of freshly burned bone (Pope 2007). Additionally, a white heat line may be the only remaining indication that a bone was burned. Due to taphonomic processes (e.g., burial or prolonged weathering), or movement and handing, the more fragile charred and calcined sections of bone may break

off, leaving the unburned portion and area of initial transition from thermally unaltered to thermally altered bone.

In their experiments, Keough (2013) and Keough *et al.* (2015) were the first to test the relationship of heat-related signatures, including the white heat line, to bone's physical condition prior to burning. Previously, other authors had documented, but did not quantify, the formation of a white heat line during experimental studies (Pope 2007) or forensic cases (Symes *et al.*, 1999a, 1999b). While the relationship between this thermal signature and the physical condition of bone has been studied, there is a lack of research concerning the chemical or physical composition of this feature. Previous research suggests that, due to its proximity to the heat source during a burning event, this area of bone has undergone some dehydration and molecular alteration, resulting in a reduced organic component (Pope 2007; Pope and Smith 2004; Symes *et al.*, 2008a).

Heat-Induced Color Changes and Burning Temperature

Surface color change is often used to identify thermally altered bone from both archaeological and forensic contexts (Ellingham *et al.*, 2015; Gilchrist and Mytum 1986; Squires *et al.*, 2011). Researchers commonly utilize the *Munsell Soil Color Chart* (2012) in order to standardize descriptions when recording the color changes present on bone (Bennett 1999; Quatrehomme *et al.*, 1998; Shipman *et al.*, 1984; Thurman and Willmore 1980). According to the Munsell Color Theory, each color is comprised of three attributes: hue (color), value (lightness or darkness of a color), and chroma (saturation or brilliance of a color).

Earlier research focusing on heat-induced color changes was based predominantly on observational studies and developed within an archaeological framework aimed at interpreting cultural cremation practices (Baby 1954; Webb and Snow 1945). More recently, systematic studies have been conducted to determine the type of burning environments likely to result in certain bone color changes (Buikstra and Swegle 1989; Shipman *et al.,* 1984; Walker and Miller 2005). A key factor investigated is the influence of burning temperature. Previous research indicates that surface color change cannot be used as the sole indicator of the maximum temperature to which a bone was exposed, as a simple one-to-one correlation does not exist between heat-induced color change and burning temperature (Symes *et al.,* 2008a). The actual temperatures at which these heat-induced color changes occur, or were concluded by researchers to have occurred, have varied greatly among different studies due to differences in the bones' physical condition and the interaction of several environmental factors, including oxygen availability, positioning near the heat source, maximum temperature the bone reached, duration of exposure time, soil composition, and presence of organic materials or metals in the surrounding soil (Devlin *et al.,* 2006; Dunlop 1978; Quatrehomme *et al.,* 1998; Squires *et al.,* 2011; Stiner *et al.,* 1995; Walker and Miller 2005).

While the color of burned bone does not signify an exact burning temperature, it can be interpreted in regards to its position along the heat-induced color change gradient. The color of burned bone, along with structural modifications and the appearance of additional heat signatures, such as a white heat line or heat border, can then indicate the degree of burning (Hanson and Cain 2007; Harbeck *et al.,* 2011; Herrmann 1977; Holden

et al., 1995a, 1995b; Pope and Smith 2004; Quatrehomme *et al.,* 1998; Stiner *et al.,* 1995). Shipman *et al.* (1984) suggest that changes in the three color components (hue, value, chroma) are produced by alterations to the chemical composition of bone due to heating and are likely attributable to decomposition of the organic component. Walker and Miller (2005) state that the color of burned bone appears to demonstrate the bone's level of decomposition, as opposed to the temperature of the fire. Additionally, these authors suggest that heat-induced color change may predict the presence and content of collagen, and perhaps other biomolecules, in burned bone.

Determining Bone Condition Prior to Burning

Knowledge of a bone's physical condition prior to burning contributes to anthropological examinations of burned skeletonized remains and interpretation of the sequence of events leading to the thermal modification (Ellingham *et al.,* 2015; Ubelaker 2009). Much of the initial research on thermal modification to human skeletal remains was developed within an archaeological framework, with the objective to interpret cultural cremation practices (Symes *et al.,* 2008a). This early research focused predominantly on determining the conditions under which bone was exposed to fire, such as the burning methods used, temperatures reached, and whether the physical remains were in a dry, defleshed yet fresh, or fleshed state at the time of burning (Baby 1954; Binford 1963; Krogman 1943; Thurman and Willmore 1980; Webb and Snow 1945). Early archaeological research helped to form the basis of current practices used by forensic anthropologists in the analysis of burnt skeletal remains.

In one of the first anthropological studies on burned bone, Krogman (1943a; 1943b) highlighted the role of the physical anthropologist in identifying human skeletal remains for forensic contexts. These articles discussed variation in heat-induced alterations to wet and dry bone, examining differences in bone coloration, fracture morphology, and surface alteration in relation to the thickness of the overlying soft tissues. Soon after, other researchers applied Krogman's observations to archaeological studies in order to develop cultural interpretations. Webb and Snow (1945) utilized Krogman's techniques in their study of the cremation practices of prehistoric peoples in the Ohio River area, focusing on the Adena and Hopewell people. After consulting with Krogman, Webb and Snow concluded that while some overlap was present, the Hopewell cremations predominantly involved defleshed, dry bones while the Adena cremations were generally carried out using fleshed bodies.

Baby (1954) later tested Webb and Snow's (1945) results, examining cremated remains from different Hopewell sites in Ohio. Baby also incorporated experimental research by using a crematory furnace to compare heat alteration patterns between two unembalmed cadavers (fleshed and defleshed) and dry bone samples. Based on the patterns present in his experimental work, Baby concluded that the Hopewell practiced cremation mainly on fleshed bodies, contradicting Webb and Snow's (1945) earlier work. These two conflicting interpretations represent the necessity for examining multiple variables when analyzing thermally-altered bone, as well as the need for continued experimental research in this area. Subsequent cremation studies incorporated the analysis of additional factors such as body position, firing temperatures, and

characteristics of perimortem versus postmortem fractures (Binford 1972; Krogman 1949; Stewart 1979; Trotter and Peterson 1995; Wells 1960; Van Vark 1970).

As research capabilities advanced, quantitative traits of thermal modifications to bone began to be investigated (Binford 1963; Van Vark 1970). Due to a rapidly increasing number of both experimental and actualistic studies in this research area, several factors for determining a bone's physical condition prior to burning can be utilized. These methods include evaluating heat-induced fracture and cracking patterns (Symes *et al.*, 2008b; Symes *et al.*, 2012; Thurman and Willmore 1980; Whyte 2001), changes in surface texture (Cain 2005), bone's dimensional transformations (e.g., shrinkage and expansion) (Gilchrist and Mytum 1986; Shipman *et al.*, 1984; Thompson 2005; Wells 1960), warping of overall bone morphology (Fairgrieve 2008; Goncalves *et al.*, 2011; Kennedy 1996; Spennemann and Colley 1989; Thurman and Willmore 1980), deformation of bone's microstructural features (Absolonová *et al.*, 2012; Bradtmiller and Buikstra, 1984), macroscopic gradient color changes (Buikstra and Swegle 1989; Nicholson 1993; Shipman *et al.*, 1984), and the appearance of additional thermal signatures (e.g., white heat line, heat border, or joint shielding) (Keough 2013; Keough *et al.*, 2012, 2015; Symes *et al.*, 1999). Many researchers agree that similar thermal characteristics exist among bones burned while fleshed or wet, enabling one to differentiate them from those burned while dry (Asmussen 2009; Bennett, 1999; Baby 1954; Buikstra and Swegle 1989; Cain 2005; Pope 2007; Stiner *et al.*, 1995; Webb and Snow 1945). However, among the two former bone conditions, researchers have found

fewer heat-induced differences that will reliably distinguish between bone that is burned while fleshed versus bone that is burned wet.

Perimortem and Postmortem Intervals

When determining circumstances that surround a set of remains at the time of burning, several observational and experimental studies have distinguished between bones burned in one of three conditions: fleshed (fresh with soft tissue), wet (fresh, retains organic content, also referred to as green), and dry (defleshed and degreased) (Asmussen 2009; Cain 2005; Buikstra and Swegle 1989; Keough *et al.,* 2012; Keough *et al.,* 2015; Pope 2007; Pope and Smith 2004; Symes *et al.,* 2008a; Symes *et al.,* 2014a). In forensic contexts, this determination of bone condition prior to burning assists in assigning a temporal classification when interpreting skeletal modifications (e.g., trauma or taphonomic processes) in relation to the time of death (Symes *et al.,* 2008a). Establishing whether a skeletal modification took place when the bone was fleshed, wet, or dry is used to delineate the defect as having occurred either perimortem, making it forensically significant, or postmortem (Dirkmaat *et al.,* 2008).

Use of these temporal concepts, perimortem and postmortem, differs in various medico-legal settings (Dirkmaat *et al.,* 2008). For members of law enforcement and medical examiners, defining the perimortem interval is based solely upon the time surrounding the death event. The term 'postmortem' is then utilized in clinical environments once somatic death occurs and life functions cease. In contrast, forensic anthropologists use the term 'perimortem' in osteological analysis when describing

changes that occur to wet or fresh bone, despite somatic death having already occurred (Dirkmaat *et al.,* 2008; Symes *et al.,* 2014b). As applied in the field of forensic anthropology, the terms 'perimortem' and 'postmortem' depend upon the condition of a bone when a defect occurred, and may not coincide with the death event (Nawrocki 2009; Symes *et al.,* 2008a). These two classifications are based upon a relative sequence of events as bone degrades, transitioning from viscoelastic and fresh to dry and brittle, regardless of the chronological time elapsed (Currey 2002; Reilly and Burnstein 1974). The perimortem period is not defined by a physiological death or fixed amount of time, but rather the changes that occur during the variable process of decomposition. This temporal classification can be quite broad and extends as long as the bone remains moist and retains its viscoelastic properties, lasting anywhere from weeks to years after the time of death (Symes *et al.,* 2014a; 2014b). The perimortem interval, as utilized by forensic anthropologists, therefore overlaps with the clinical postmortem period.

After death, when bone starts to decay, its biochemical composition changes over time, particularly in regard to the preservation of its organic matrix and loss of moisture (Dirkmaat *et al.,* 2008). This process in which bone transitions from wet to dry, and the perimortem to postmortem temporal periods for describing bone tissue response, is gradual and continuous, varying greatly in relation to the depositional context (Nawrocki 2009; Symes *et al.,* 2008a). There is not a set time period for when bone will lose its organic component; this taphonomic change varies in different context, depending upon the interaction between the bone and its environment.

Fourier Transform Infrared Spectroscopy

Multiple analytical techniques have been developed that can be used to examine the compositional changes that bone undergoes during thermal alteration. Fourier transform infrared spectroscopy (FTIR) is a versatile and well-established analytical technique that can be used to characterize a wide range of substances, whether in solid, liquid, or gas form (Stuart 2004). In this method, a FTIR introduces an infrared light source to the sample, inciting the molecular bonds to vibrate and rotate at characteristic frequencies. Some of the infrared radiation is absorbed by the sample, while the rest is passed through, or transmitted. The instrument then absorbs and detects these differences in the amount of energy, creating a spectrum of these frequencies. This spectrum is a plot of transmittance to wavenumber and represents the molecular absorption and transmission of the sample. Vibrations created correspond to the resulting absorption bands shown on the obtained infrared spectrum.

No two unique molecular structures produce the same infrared spectrum. The specific frequencies that a given molecule absorbs is distinct due to its chemical makeup and vibrational modes which differ from other molecules (Griffiths and de Haseth 2007). One notable exception is enantiomers, two compounds whose molecular structures have a non-superimposable, mirror-image relationship to each other. Therefore, FTIR can be used to identify said molecule when characterizing known or unknown materials. Positive identification of a sample can be accomplished through manual interpretation of the spectrum and/or computer-assisted comparison with appropriate reference spectra from a library or database.

Transmission Sample Preparation Technique

A commonly used sample preparation technique for examining solids is transmission FTIR (Stuart 2004). For this technique, the sample is prepared for analysis using alkali halide discs, mulls, or films, depending up on the nature of the sample. The use of alkali halide discs involves mixing dry alkali halide powder with the sample, before grinding the mixture into a powder using an agate mortar and pestle. This mixture is then placed into a hydraulic or hand press and subjected to pressure, causing it to coalesce and producing a clear, transparent disc. For this method, potassium bromide (KBr) is the most commonly utilized alkali halide. To prepare a sample for analysis, a ratio of 1:100 of sample to KBr should be followed. Approximately 2 mg of sample mixed with 200 mg of KBr is sufficient to form a disc.

Advantages of FTIR

Fourier transform spectroscopy has two fundamental benefits in comparison to other infrared techniques, the Fellgett (multiplex) and Jacquinot (throughput) advantages (Griffiths and de Haseth 2007). The *Fellgett advantage* results from the FTIR spectrometer's ability to measure spectral information from all wavelengths simultaneously. A complete spectrum can be collected rapidly, with multiple scans averaged, in the time it would take a dispersive infrared instrument to conduct a single scan (Stuart 2004). This ability to take multiplex measurements versus direct measurements observed sequentially leads to an improved signal-to-noise ratio (SNR)

due to the accumulation of successive scans. The *Jacquinot advantage* results from the total source output being passed through a sample continuously. FTIR spectrometry does not require the use of a slit or restricting device like dispersive infrared instruments, instead utilizing a circular aperture with a larger area. This enables a higher throughput of radiation, and the resulting substantial gain in energy at the instrument's detector leads to higher signals and improved SNRs, allowing absorbances to be measured more accurately. The combination of the Fellgett and Jacquinot advantages leads to higher-quality results obtained by FTIR (Griffiths and de Haseth 2007).

FTIR and Osteological Analysis

For the analysis of bone, FTIR allows for the simultaneous examination of all tissue components, as both mineral and organic constituents produce distinctive absorption peaks (Carden and Morris 2000; Donnelly 2011; Ellingham *et al.*, 2015; Gamsjäger *et al.*, 2009; Paschalis 2009; Paschalis *et al.*, 2011). FTIR is a well-established method that has been utilized for quantitative and qualitative analysis of bone in a variety of research areas, including to assess variations in health and disease (Boskey and Camacho 2007; Boskey and Mendelsohn 2005; Morris and Finney 2004), calculate and compare bone compositional parameters (e.g., mineral-to-matrix, carbonate-to-phosphate, and carbonate-to-amide ratios) (Gadaleta *et al.*, 1996; Gourion-Arsiquad *et al.*, 2013; Isaksson *et al.*, 2010; Paschalis *et al.*, 1996, 1997), and determine crystallinity indices (Surovell and Stiner 2001; Wright and Schwarcz 1996). This analytical technique has also been used to identify the composition of bone material, both inorganic (Álvarez-

Lloret *et al.*, 2006; Bigi *et al.*, 1997; Kuhn *et al.*, 2008; Rey *et al.*, 1989; Tanasescu *et al.*, 2015; Turunen *et al.*, 2011, 2014; Walters *et al.*, 1990) and organic (D'Elia *et al.*, 2007; Nakada *et al.*, 2010; Pestle *et al.*, 2014; Salesse *et al.*, 2014; Weiner and Bar-Yosef 1990). A typical FTIR spectrum of fresh bone is shown in Figure 2.1.

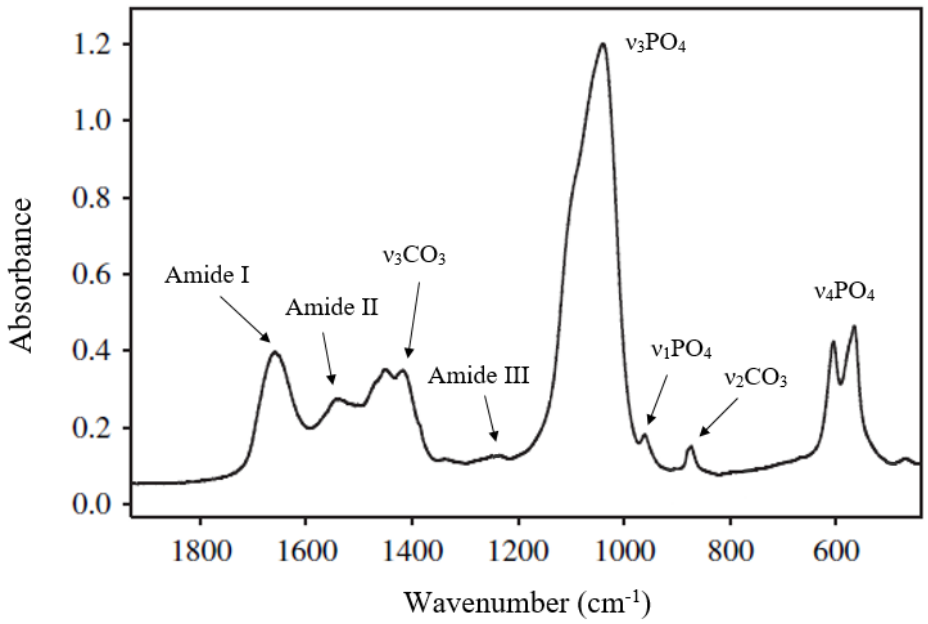

Figure 2.1. Typical FTIR spectra of fresh bone (adapted from Lebon *et al.*, 2010:2267).

Archaeologically, FTIR has been applied to numerous sites in order to evaluate diagenesis of skeletal materials (Beasley *et al.*, 2014; Howes *et al.*, 2012; Reiche *et al.*, 2003), distinguish between modern and archaeological remains (Nagy *et al.*, 2008; Patonai *et al.*, 2013), reconstruct settlement behavior, including the use of burning bones as fuel and seasonal habitation of sites (Butler and Dawson 2013), and determine depositional processes and distribution of bones (Schiegl *et al.*, 2003; Stiner *et al.*, 2001; Weiner *et al.*, 1993).

FTIR and Analysis of Burned Bone

For burned and cremated bones, FTIR has been used in experimental studies to assess heat-induced compositional changes (Figueiredo *et al.,* 2010; Mkukuma *et al.,* 2004; Piga *et al.,* 2016; Snoeck *et al.,* 2014; Wang *et al.,* 2010; Younesi *et al.,* 2011) and modifications to the crystalline microstructure (Munro *et al.,* 2007; Olsen *et al.,* 2008; Stiner *et al.,* 1995; Thompson *et al.,* 2011, 2013) in relation to the degree of burning. This analytical technique has utility in both modern and archaeological contexts, helping researchers to identify burnt bone in archaeological assemblages (Stiner *et al.,* 1995), differentiate burning effects from black mineral oxide staining, notably that of manganese (Schiegl *et al.,* 2003; Shahack-Gross *et al.,* 1997), interpret funerary cremation practices (Piga *et al.,* 2010; Squires *et al.,* 2011; Van Strydonck *et al.,* 2015), and compare diagenetic and thermal-alteration modifications (Lebon *et al.,* 2010) and determine if a bone deposit was an *in situ* accumulation or had been moved to a secondary dump site (Schiegl *et al.,* 2003).

Previous research suggests that FTIR also yields information that may potentially be used to reconstruct burning events, including oxygen availability (Walker and Miller 2005) and the presence of fuel (Snoeck *et al.,* 2016). Ellingham *et al.,* (2016) utilized this technique to investigate the effect of soft tissue and varying exposure times on the prediction of burning temperatures for burnt bone. Additionally, researchers have used FTIR to characterize high versus low intensity burnings for archaeological remains (Butler and Dawson 2013; Piga *et al.,* 2015; Snoeck *et al.,* 2014; Thompson *et al.,* 2009).

Determining the composition of white heat lines contributes to previous studies on thermally altered bone and enables new avenues of research in this field. This new research can expand on topics such as the reconstruction of thermal events; interpretation of the circumstances surrounding the death and/or physical condition of a fire victim; and further delineation of bone's altered chemical properties as it undergoes burning. Increased research on the development and formation of white heat lines has implications for numerous fields including forensic anthropology, taphonomy, zooarchaeology, and the medico-legal community.

CHAPTER 3: MATERIALS AND METHODS

In order to investigate the effects of soft tissue, naturally-occurring grease, and water retention on the formation and appearance of a white heat line, osteological remains in five physical conditions (fleshed, very wet, partially wet, dry, and soaked) (see below) were utilized in this study. Experimental samples consisted of isolated long bones from white-tailed deer (*Odocoileus virginianus*), elk (*Cervus canadensis*), sheep (*Ovis aries*), and pig (*Sus scrofa*). The four animal species selected for this research all belong to the Order Artiodactyla, even-toed ungulates, and share similar bone structures.

Animal Models as Human Analogues

Animal remains are often utilized as human analogues in experimental research due to the difficulties associated with acquiring and using human cadaveric material (Marceau 2007; Thompson 2003). These difficulties include a paucity of human cadaveric material, legal and ethical complications attached to the use of human remains in experimental work, and legal constraints outlining their involvement in destructive studies. In contrast, animal remains are usually more accessible, with the capability to select for certain variables such as developmental age and limb type, as well as fewer restrictions and regulations regarding their use (Pope 2007).

Animal analogues have been used in a variety of research areas, including cremation or burning studies (Buikstra and Swegle 1989; DeHaan and Nurbakhsh 2001; Thompson 2003, 2005; Thompson *et al.*, 2009, 2011), investigations of decomposition

rates (Schotsmans *et al.*, 2012, 2014), thanatochemistry (Dekeirsschieter *et al.*, 2009), weathering (Marceau 2007), entomological activity (Grassberger and Frank 2004), and effects of different burial microenvironments (Forbes *et al.*, 2005a, 2005b, 2005c; Stuart *et al.*, 2005; Wilson *et al.*, 2007).

Animal species frequently used as human analogues include pig, sheep, white-tailed deer, and goat (*Capra hircus*) (Thompson 2002, 2003, 2005; Mayne 1990). Pig is most common in forensic experiments due to its many physical similarities with humans (de Gruchy and Rogers 2002; DeHaan 1997; DeHaan and Nurbakhsh 2001; DeHaan *et al.*, 1999; Herrmann and Bennett 1999), such as the fat-to-muscle ratio, body mass, and general physiology (France *et al.*, 1992; Rodriguez and Bass 1985; Schoenly *et al.*, 1991). Additionally, porcine soft tissue size and composition, relative hairlessness, skin structure, and subcutaneous fat layer are also comparable to that of humans (Aerssens *et al.*, 1998; Schotsmans *et al.*, 2012, 2014).

For the investigation of burning on hard tissues, animal models are useful for replicating and examining differential heat-induced modifications to bone, including color changes (Buikstra and Swegle 1989; Pope 2007). Mayne (1990) suggests that sheep are the most appropriate choice for cremation or burning research, because their bone density and microstructure are more comparable to humans than that of other accessible species. Multiple researchers have incorporated sheep bone into their thermal-alteration studies, generally burning the long bones or ribs (Abdel-Maksoud 2010; Ellingham *et al.*, 2015, 2016; Koon *et al.*, 2003; Thompson 2005; Thompson *et al.*, 2009, 2011, 2013; Thompson and Chudek 2007).

In addition to sheep, Marceau (2007) concludes that both deer and pig bone can serve as suitable models in forensic experiments due to their geometric and densitometric similarities to human bone. Of these two species, Marceau (2007) also found that deer bone responds to subaerial weathering in a manner more similar to human bone than pig bone. Although less frequently, cervid bone has been utilized in several thermal-alteration studies (Bennett 1999; Horocholyn 2013; Munro *et al.*, 2007, 2008; Whyte 2001). Therefore, it was concluded that white-tailed deer, elk, sheep, and pig long bones would serve as suitable models in the current research to investigate heat-induced modifications to bone.

Osteological Samples

The first sample group consists of eight sheep and ten pig metapodials, fleshed and encased in soft tissue with the hide and hair present. The author obtained these 18 fleshed animal specimens from Krehbiels Specialty Meats, a processing plant in McPherson, Kansas, a few days after the animals were butchered. These bones were shipped frozen, and once received, they were placed in a facility freezer at Boston University School of Medicine (BUSM) until the experimental work could be performed. The bones were then allowed to thaw for several days prior to burning. This sample includes both adult and subadult individuals, as some of the distal metapodial epiphyses are not fused.

The second sample group consists of 30 isolated, very wet elk femora previously purchased by the Forensic Anthropology Program under the Department of Anatomy and

Neurobiology at BUSM. These bones were greasy with minimal amounts of soft tissue adhering but with the marrow intact. They had been manually processed prior to the program acquiring them, with a majority of the soft tissue removed with hand tools, but no additional thermal alteration (e.g., boiling). These bones were stored in a facility freezer at the Boston University Outdoor Research Facility (ORF) located in Holliston, Massachusetts until the experimental work could be performed. The bones were then allowed to thaw for several days prior to burning.

The third sample group consists of 30 partially wet white-tailed deer metapodials. These bones were already defleshed and partially dry from undergoing decomposition in a forested environment for approximately 1.5 years after deposition at the ORF. This sample includes both adult and subadult individuals, as some of the distal metapodial epiphyses are not fused.

The fourth sample group consists of 15 dry white-tailed deer metapodials. These bones were already defleshed and dry from undergoing decomposition in a forested environment in eastern Massachusetts. This sample includes both adult and subadult individuals, as some of the distal metapodial epiphyses are not fused.

The fifth sample group consists of 15 soaked white-tailed deer metapodials. These bones were immersed in tap water and placed in plastic tubs to soak for three days prior to burning. The soaked bones were selected from the dry sample group, and as such, were already defleshed and dry from undergoing decomposition in a forested environment in eastern Massachusetts. This sample includes both adult and subadult individuals, as some of the distal metapodial epiphyses are not fused.

The partially wet, dry, and soaked bone samples underwent decomposition in similar forested environments and were all in Weathering Stage 0 following Behrensmeyer (1978). Bone surfaces did not exhibit cracking, flaking, or sun bleaching due to weathering, and there was sometimes slight dried soft tissue and fur still adhering.

Experimental Burning

Ten percent of the bones in each sample group, approximated when necessary, were set aside as thermally unaltered controls for the burned experimental bones. Three controls were used for the very wet and partially wet sample groups, and two controls were used for the fleshed, dry, and soaked sample groups. Thermal experimentation of all bone samples took place at the ORF. This 32-acre facility offers a secure area away from most human disturbances in which to conduct research. Prior to burning, each bone was given a label identifying its sample group and its individual number within that group. The partially wet, dry, and soaked samples were labeled using black permanent marker directly on the bone. For the fleshed and very wet samples, aluminum tags, etched with the identifying information, were attached to the unburned end of the bone using stainless steel wire. Due to the presence of subadult samples lacking distal epiphyses, the fused proximal end was burned for all bones. Each bone was also photographed prior to and following burning.

Burning of all experimental bones for this project took place at the Holliston Fire Department Training Facility, located near the ORF. In order to contain the fire, the experimental bone samples were placed on stainless steel wire mesh and burned over a

wood fire made within a 55-gallon drum. The bones were burned by sample group with the fire rebuilt between each group, and during burning if necessary, using wood available from the area. Due to space constraints with the 55-gallon drum, the very wet bones were burned in three groups, the fleshed and partially wet bones in two groups each, and the dry and soaked bones in one group each. Bones remained on the fire until they exhibited charring, allowing enough time for a white heat line to form potentially. Approximately halfway through burning, they were flipped over to ensure a more even exposure to the heat source.

In order to record the maximum temperature that each bone and the fire reached, a ThermoTech TT1610 Non-Contact Digital Infrared Laser Temperature Thermometer (Thermo Fisher Scientific Inc., Waltham, MA) was used before the bones were placed on the fire, once the bones were flipped partway through, and when they were removed from the steel wire mesh at the end of burning. Additionally, the total burn time for each sample group was also noted and whether the fire needed to be rebuilt during burning, and if so, at what time. Once removed from the fire, the burned bones were then allowed to cool at the ORF for several hours to ensure safe handling before being placed in individual plastic bags and transported to BUSM, along with the controls, for storage and processing.

Visual Analysis

After burning the experimental bone samples, a subsequent macroscopic visual analysis was conducted to assess the formation and appearance of a white heat line. In

order to conduct this analysis, the fleshed and very wet experimental bones, as well as their unburned controls, were first defleshed using a dermestid beetle (*Dermestes maculatus*) colony available through the Department of Anatomy and Neurobiology at BUSM. The partially wet, dry, and soaked bones did not require additional processing prior to the visual analysis. For each of the experimental bones from all five sample groups, the formation of a white heat line was then scored using a binary system, as either present (1) or absent (0). If present, the maximum and minimum widths of the white heat line were measured, as well as its depth into the bone's surface. Additionally, the percentage of the bone's burned diaphyseal circumference exhibiting a white heat line was classified as ≤ 25%, 25-50%, 50-75%, or 75-100%. Visual analysis of all bone samples for the current study was completed in laboratory facilities available through the Forensic Anthropology program at BUSM.

FTIR Analysis

FTIR Sample Preparation

Fourier transform infrared spectroscopy (FTIR) was used to analyze the chemical composition of white heat lines in comparison to the experimental burned bones that do not develop this thermal signature, as well as the unburned controls. Specifically, the transmission method was used in which the sample is prepared into a pellet before being placed directly into the path of the infrared beam. As the infrared beam passes through the sample, the transmitted energy is measured and an infrared spectrum is generated. Since white heat lines appear to form only on the outer surface of bone, superficial

samples for all osteological materials were obtained using a WEN 2305 Rotary Tool Kit (WEN Products, Elgin, IL) with a grinding attachment. In order to prevent contamination between samples, a new grinding attachment was used for each bone. For the experimental bones, samples were taken directly from the white heat line, and if not present then an area from the junction of charred and thermally unaltered bone was obtained. The middle of the diaphysis was used as the sampling site for the unburned controls. Ground bone samples were collected using wax paper and stored in individual glass vials prior to FTIR analysis.

In order to prepare each bone sample for FTIR analysis, approximately 2 mg of bone powder was manually ground with 200 mg of infrared spectroscopic grade KBr using a mortar and pestle. The KBr powder was stored in a desiccator, with working portions removed as needed. This mixture was then placed into a Thermo Scientific™ hand press (Thermo Fisher Scientific Inc., Waltham, MA), using a 7 mm die set, and applying pressure for 30 seconds to form a transparent pellet. In order to prevent contamination between samples, the laboratory equipment used to create the pellets was cleaned between each bone sample with alcohol preparation pads.

FTIR Spectral Analysis

All bone samples, the experimental burned and their controls, were analyzed using FTIR and the transmission method. FTIR absorbance spectral data was obtained using a Thermo Scientific™ Nicolet™ 6700 FT-IR Spectrometer and Thermo Scientific™ OMNIC™ Spectra Software (Thermo Fisher Scientific Inc., Waltham, MA).

Interferences from the KBr and environment were removed by collecting background spectra of a homogenous KBr pellet and subtracting it from all bone sample spectra. Spectra for the background scans and each bone sample were recorded between 2000 cm^{-1} and 400 cm^{-1}, at a resolution of 4 cm^{-1}, and an averaging of 64 scans. An automatic baseline correction and smoothing were performed on each of the spectra in order to ensure a level baseline and to decrease the noise level, respectively.

The resulting infrared spectra obtained from the experimental and control bone samples were compared to previous authors' research in order to identify the presence of CO_3, PO_4, and amide I (Butler and Dawson 2013; Garvie-Lok *et al.*, 2004; Koon *et al.*, 2003; Lebon *et al.*, 2010; Nagy *et al.*, 2008; Olsen *et al.*, 2008; Thompson *et al.*, 2009, 2011, 2013; Wright and Schwarz 1996). Spectral peak heights of these three components were determined for each bone at the ν3 CO_3 (1415 cm^{-1}), ν3 PO_4 (1035 cm^{-1}), and amide I (1660 cm^{-1}) vibrational bands using the OMNIC™ Spectra Software (Thermo Fisher Scientific Inc., Waltham, MA). The mean spectral peak heights were then calculated for ν3 CO_3, ν3 PO_4, and amide I, subdivided by bone condition prior to burning, unburned control versus burned experimental, and whether an experimental bone developed a white heat line after burning.

For the current study, the ν3 modes for carbonate and phosphate were chosen, as they represent the strongest infrared bands of these minerals in bone (Rey *et al.*, 1989; Wright and Schwarz, 1996). Additionally, Amide I was selected as it represents the main band of bone's organic matrix and is commonly used to assess the presence of organic material through the infrared analysis of bone (Álvarez-Lloret *et al.*, 2006; Butler and

Dawson 2013; Camacho *et al.*, 1995; Lebon *et al.*, 2010; Pienkowski *et al.*, 1997). Preparation and processing of all bone samples for FTIR analysis was completed in laboratory facilities available through the Biomedical Forensic Sciences program at BUSM.

Statistical Analysis

Several statistical analyses were calculated to assess the data collected in the current study. These analyses were performed using the Statistical Package for the Social Sciences (SPSS), version 20 (SPSS Inc., Chicago, Illinois).

Test for Normality

The statistical normality of the data collected was assessed using a Shapiro-Wilk's W test.

Correlation of Bone Condition and White Heat Line Formation

A Chi-Squared (X^2) Test of Independence was performed to evaluate if there is a relationship between bone's physical condition prior to burning (fleshed, very wet, partially wet, dry, soaked) and white heat line formation.

Multivariate Correlation

A multivariate analysis of variance (MANOVA) test was used to compare the effect of bone's physical condition prior to burning (fleshed, very wet, partially wet, dry,

soaked) on the formation of a white heat line and the spectral peak heights of ν3 CO_3, ν3 PO_4, and amide I.

Post-Hoc Test

Following the MANOVA, a Bonferroni post-hoc test was conducted to compare subgroups of the data set in order to determine which, if any, subgroups differ significantly.

CHAPTER 4: RESULTS

Burning Observations

Table 4.1 lists the observations recorded when the experimental bones were burned. The author documented the temperature of each bone and the fire three times during the burning process: (1) initially, before the bones were placed on the fire; (2) when the bones were flipped partway through; and (3) at the end of burning. Additionally, the length of time for which each sample group was burned, when the bones were flipped, and whether the fire was rebuilt, and if so when, during burning were also noted. Photos of the experimental bones burning on the 55 gallon drum can be found in Appendix A (Figures A.1-A.5).

Due to space constraints with the 55-gallon drum, the experimental fleshed bones were burned in two groups, divided by species. In the first group, the sheep metapodials ranged in initial temperature from 58.0ºF to 69.0ºF (14.4ºC to 20.6ºC) prior to being placed on the fire, between 245.1ºF and 333.6ºF (118.4ºC to 167.6ºC) halfway through burning, and from 163.0ºF to 183.8ºF (72.8ºC to 84.3ºC) once removed from the steel wire mesh at the end of burning. Additionally, the fire temperature was 1,005.1ºF (540.6ºC) in the beginning, 1,090.0ºF (587.8ºC) halfway through burning, and 1,010.9ºF (543.8ºC) when the bones were removed. The sheep metapodials burned for ten minutes, were flipped at six minutes, and the fire was not rebuilt due to its consistently high temperature. For the second group of fleshed bones, the pig metapodials ranged in initial temperature from 58.0ºF to 69.5ºF (14.4ºC to 20.8ºC) prior to being placed on the fire,

between 239.5ºF and 334.5ºF (115.3ºC to 168.1ºC) halfway through burning, and from 145.4ºF to 174.3ºF (63.0ºC to 79.1ºC) once removed from the steel wire mesh at the end of burning. Initially, the fire temperature was 1,170.0ºF (632.2ºC), then 998.4ºF (536.9ºC) halfway through burning, and 860.3ºF (460.2ºC) once the bones were removed. The pig metapodials burned for a total of twenty-three minutes and were flipped halfway at twelve minutes with the fire rebuilt in order to ensure that each bone became partially carbonized.

The experimental very wet bones were burned in three groups, and their initial temperatures prior to being placed on the fire ranged from 57.9ºF to 66.2ºF (14.4ºC to 19.0ºC), 62.0ºF to 69.8ºF (16.7ºC to 21.0ºC), and 61.7ºF to 66.9ºF (16.5ºC to 19.4ºC). Halfway through burning, the very wet bone temperatures varied from 247.7ºF to 308.3ºF (119.8ºC to 153.5ºC), 252.8ºF to 316.4ºF (122.7ºC to 158.0ºC), and 272.3ºF to 328.6ºF (133.5ºC to 164.8ºC). Once removed from the fire, the bones cooled to between 165.9ºF and 208.0ºF (74.4ºC to 97.8ºC), 142.7ºF to 178.1ºF (61.5ºC to 81.2ºC), and 154.4ºF to 221.1ºF (68.0ºC to 103.1ºC) for the three groups. The fire's temperature was initially recorded as 922.1ºF to 984.0ºF (494.5ºC to 528.9ºC), then 888.0ºF to 998.4ºF (475.6ºC to 536.9ºC) once the bones were flipped, and lastly as 620.9ºF to 763.3ºF (327.2ºC to 406.3ºC) when the bones were removed. Total burning time for the very wet bones was 23 minutes, 28 minutes, and 21 minutes for the first, second, and third bone groups, respectively. The very wet bones were flipped approximately halfway through burning, with the fire rebuilt for each group, at 18 minutes, 14 minutes, and 8 minutes.

The partially wet experimental bones were burned in two groups, and prior to being placed on the fire their temperatures ranged from 67.5ºF to 74.3ºF (19.7ºC to 23.5ºC) and 71.6ºF to 75.5ºF (22.0ºC to 29.1ºC). Halfway through burning, the bones were heated to between 204.6ºF and 258.9ºF (95.9ºC to 126.1ºC) and 233.1ºF to 291.4ºF (111.7ºC to 144.1ºC). Once removed from the fire, they cooled from 121.8ºF to 213.1ºF (49.9ºC to 100.6ºC) and 148.2ºF to 219.1ºF (64.6ºC to 103.9ºC). The fire's temperature was initially recorded as 987.2ºF to 1,208.0ºF (530.7ºC to 653.3ºC), then 784.9ºF to 973.1ºF (418.3ºC to 522.8ºC) once the bones were flipped, and lastly as 518.9ºF to 924.6ºF (270.5ºC to 495.9ºC) when the bones were removed. Total burning time for the partially wet bones was 31 minutes and 26 minutes for the first and second groups, respectively. The bones were flipped at 12 and 15 minutes, and both fires were rebuilt at 8 minutes.

The dry experimental bones were burned in one group and ranged in initial temperature from 67.4ºF to 73.2ºF (19.7ºC to 22.9ºC) prior to being placed on the fire, between 203.5ºF and 241.3ºF (95.3ºC to 116.3ºC) halfway through burning, and from 116.9ºF to 146.6ºF (47.2ºC to 63.7ºC) once removed from the steel wire mesh at the end of burning. Additionally, the fire temperature was 956.2ºF (513.4ºC) in the beginning, 708.2ºF (375.7ºC) halfway through burning, and 572.2ºF (300.1ºC) when the bones were removed. The dry bones burned for twelve minutes, were flipped at six minutes, and the fire was not rebuilt.

The soaked experimental bones were burned in one group, and prior to being placed on the fire their temperatures ranged from 62.2ºF to 68.0ºF (16.8ºC to 20.0ºC).

Halfway through burning, the bones were heated to between 201.3ºF and 241.4ºF (94.1ºC to 116.3ºC). Once removed from the fire, they cooled to between 102.0ºF and 168.6ºF (38.9ºC to 75.9ºC). Additionally, the fire temperature was initially 878.5ºF (420.3ºC), 734.6ºF (390.3ºC) halfway through burning, and 685.4ºF (362.9ºC) when the bones were removed. The soaked bones burned for twelve minutes, were flipped at six minutes, and the fire was not rebuilt.

Table 4.1. Temperatures and burning times for experimental burned bones.

Sheep	TEMPERATURE (BONE)			TEMPERATURE (FIRE)			REBUILT	BURN TIME
Metapodials	**Start**	**Flipped**	**End**	**Start**	**Flipped**	**End**	**When (min.)**	**# Min**
Fleshed	Notes: #1-8 (sheep) burned in first group; #9-18 (pig) burned in second group							
F1	63.2ºF 17.3ºC	332.9ºF 167.2ºC	174.5ºF 79.2ºC	1,005.1ºF 540.2ºC	1,090.0ºF 587.8ºC Flipped at 6 min.	1,010.9ºF 543.8ºC	Not rebuilt	10 min. total
F2	58.0ºF 14.4ºC	247.2ºF 119.6ºC	163.0ºF 72.8ºC					
F3	61.0ºF 16.1ºC	298.9ºF 148.3ºC	178.3ºF 81.3ºC					
F4	69.0ºF 20.6ºC	271.4ºF 133.0ºC	171.7ºF 77.6ºC					
F5	59.0ºF 15.0ºC	245.1ºF 118.4ºC	165.4ºF 74.1ºC					
F6	64.0ºF 17.8ºC	333.6ºF 167.6ºC	183.8ºF 84.3ºC					
F7	66.0ºF 18.9ºC	269.7ºF 132.1ºC	167.9ºF 75.5ºC					
F8	UNBURNED CONTROL (SHEEP)							
F9	65.9ºF 18.8ºC	239.5ºF 115.3ºC	168.1ºF 75.6ºC	1,170.0ºF 632.2ºC	998.4ºF 536.9ºC Flipped at 12 min.	860.3ºF 460.2ºC	Once, at 12 min.	23 min. total
F10	68.4ºF 20.2ºC	303.3ºF 150.7ºC	168.7ºF 75.9ºC					
F11	68.5ºF 20.3ºC	331.0ºF 166.1ºC	172.5ºF 78.1ºC					
F12	59.1ºF 15.1ºC	286.5ºF 141.4ºC	165.2ºF 74.0ºC					

Pig	TEMPERATURE (BONE)			TEMPERATURE (FIRE)			REBUILT	BURN TIME
Metapodials	**Start**	**Flipped**	**End**	**Start**	**Flipped**	**End**	**When (min.)**	**# Min**
F13	58.0ºF 14.4ºC	268.4ºF 131.3	145.4ºF 63.0ºC	1,170.0ºF 632.2ºC	998.4ºF 536.9ºC Flipped at 12 min.	860.3ºF 460.2ºC	Once, at 12 min.	23 min. total
F14	69.5ºF 20.8ºC	284.8ºF 140.4ºC	161.7ºF 72.1ºC	1,170.0ºF 637.2ºC	998.4ºF 536.9ºC Flipped at 12 min.	860.3ºF 460.2ºC	Once, at 12 min.	23 min. total
F15	63.6ºF 17.6ºC	334.5ºF 168.1ºC	174.3ºF 79.1ºC					
F16	60.0ºF 15.6ºC	273.7ºF 134.3ºC	159.5ºF 70.1ºC					
F17	62.2ºF 16.8ºC	306.2ºF 152.3ºC	169.8ºF 76.6ºC					
F18	UNBURNED CONTROL (PIG)							
Elk	**TEMPERATURE (BONE)**			**TEMPERATURE (FIRE)**			**REBUILT**	**BURN TIME**
Femora	**Start**	**Flipped**	**End**	**Start**	**Flipped**	**End**	**When (min.)**	**# Min**
Very Wet	Notes: Bones burned in groups - #1-9, #10-20, #21-27							
W1	61.3ºF 16.3ºC	293.6ºF 145.3ºC	165.9ºF 74.4ºC	922.1ºF 494.5ºC	888.0ºF 475.6ºC Flipped at 18 min.	621.3ºF 328.4ºC	Once, at 18 min.	23 min. total
W2	66.2ºF 19.0ºC	301.1ºF 149.5ºC	183.5ºF 84.17ºC					
W3	60.6ºF 15.9ºC	247.7ºF 119.8ºC	190.0ºF 87.8ºC					

Elk	TEMPERATURE (BONE)			TEMPERATURE (FIRE)			REBUILT	BURN TIME
Femora	**Start**	**Flipped**	**End**	**Start**	**Flipped**	**End**	**When (min.)**	**# Min**
W4	63.8ºF 17.7ºC	292.2ºF 144.6ºC	193.4ºF 89.7ºC	922.1ºF 494.5ºC	888.0ºF 475.6ºC Flipped at 18 min.	621.3ºF 328.4ºC	Once, at 18 min.	23 min. total
W5	64.2ºF 17.9ºC	276.4ºF 135.8ºC	182.8ºF 83.8ºC					
W6	57.9ºF 14.4ºC	308.3ºF 153.5ºC	206.9ºF 97.2ºC					
W7	63.1ºF 17.3ºC	272.8ºF 133.8ºC	208.0ºF 97.8ºC					
W8	62.4ºF 16.9ºC	290.1ºF 143.4ºC	182.3ºF 83.5ºC					
W9	58.1ºF 14.5ºC	284.6ºF 140.3ºC	173.9ºF 78.8ºC					
W10	64.4ºF 18.0ºC	257.1ºF 125.1ºC	148.7ºF 64.8ºC	970.7ºF 521.5ºC	998.4ºF 536.9ºC Flipped at 14 min	620.9ºF 327.2ºC	Once, at 14 min.	28 min. total
W11	63.3ºF 17.4ºC	294.6ºF 145.9ºC	170.5ºF 76.9ºC					
W12	68.0ºF 20.0ºC	252.8ºF 122.7ºC	166.8ºF 74.9ºC					
W13	66.7ºF 19.3ºC	265.8ºF 129.9ºC	153.6ºF 67.6ºC					
W14	63.1ºF 17.3ºC	304.7ºF 151.5ºC	178.1ºF 81.2ºC					
W15	62.0ºF 16.7ºC	316.4ºF 158.0ºC	162.7ºF 72.6ºC					
W16	63.3ºF 17.4ºC	312.9ºF 156.1ºC	174.9ºF 79.3ºC					

Elk	TEMPERATURE (BONE)			TEMPERATURE (FIRE)			REBUILT	BURN TIME
Femora	**Start**	**Flipped**	**End**	**Start**	**Flipped**	**End**	**When (min.)**	**# Min**
W17	62.1ºF 16.7ºC	282.0ºF 138.9ºC	159.1ºF 70.1ºC	970.7ºF 521.5ºC	998.4ºF 536.9ºC Flipped at 14 min	620.9ºF 327.2ºC	Once, at 14 min.	28 min. total
W18	65.1ºF 18.4ºC	287.4ºF 141.9ºC	154.3ºF 67.9ºC					
W19	63.7ºF 17.6ºC	291.2ºF 144.0ºC	142.7ºF 61.5ºC					
W20	69.8ºF 21.0ºC	306.2ºF 153.3ºC	159.8ºF 71.0ºC					
W21	65.4ºF 18.6ºC	325.6ºF 163.1ºC	221.1ºF 105.1ºC	984.0ºF 528.9ºC	957.1ºF 513.9ºC Flipped at 8 min.	763.3ºF 406.3ºC	Once, at 12 min.	21 min. total
W22	63.8ºF 17.7ºC	307.2ºF 152.9ºC	165.9ºF 74.4ºC					
W23	66.9ºF 19.4ºC	272.3ºF 133.5ºC	173.8ºF 78.3ºC					
W24	61.7ºF 16.5ºC	328.6ºF 164.8ºC	183.2ºF 84.0ºC					
W25	65.1ºF 18.4ºC	318.1ºF 158.9ºC	172.9ºF 78.3ºC					
W26	62.0ºF 16.7ºC	306.8ºF 152.7ºC	156.0ºF 68.9ºC					
W27	65.2ºF 18.4ºC	313.1ºF 156.2ºC	154.4ºF 68.0ºC					
W28	UNBURNED CONTROL							
W29	UNBURNED CONTROL							
W30	UNBURNED CONTROL							

Deer	TEMPERATURE (BONE)			TEMPERATURE (FIRE)			REBUILT	BURN TIME
Metapodials	**Start**	**Flipped**	**End**	**Start**	**Flipped**	**End**	**When (min.)**	**# Min**
Partially Wet	Notes: Bones burned in groups - #1-11, 12-20, 21-27							
P1	67.5ºF 19.7ºC	223.4ºF 106.3ºC	121.8ºF 49.9ºC					
P2	68.2ºF 20.1ºC	241.9ºF 116.6ºC	183.4ºF 84.1ºC					
P3	73.7ºF 23.2ºC	206.0ºF 96.7ºC	146.3ºF 63.5ºC					
P4	73.0ºF 22.8ºC	226.0ºF 107.8ºC	124.7ºF 51.5ºC					
P5	71.7ºF 22.1ºC	247.5ºF 119.7ºC	198.5ºF 92.5ºC	1,208.0ºF 653.3ºC	784.9ºF 418.3ºC	518.9ºF 270.5ºC	Once, at 15 min.	31 min total
P6	72.1ºF 22.3ºC	218.1ºF 103.4ºC	164.1ºF 73.4ºC					
P7	74.3ºF 23.5ºC	207.3ºF 97.4ºC	154.3ºF 67.9ºC		Flipped at 12 min.			
P8	73.7ºF 23.2ºC	258.9ºF 126.1ºC	200.1ºF 93.4ºC					
P9	69.9ºF 21.1ºC	204.6ºF 95.9ºC	142.9ºF 61.6ºC					
P10	73.4ºF 23.0ºC	220.0ºF 104.4ºC	149.4ºF 65.2ºC					
P11	72.1ºF 22.3º	256.2ºF 124.6ºC	213.1ºF 100.6ºC					

Deer	TEMPERATURE (BONE)			TEMPERATURE (FIRE)			REBUILT	BURN TIME
Metapodials	**Start**	**Flipped**	**End**	**Start**	**Flipped**	**End**	**When (min.)**	**# Min**
P12	75.5ºF 24.2ºC	251.6ºF 122.0ºC	203.5ºF 95.3ºC					
P13	72.1ºF 22.3ºC	279.5ºF 137.5ºC	148.2ºF 64.6ºC					
P14	75.5ºF 24.1ºC	243.4ºF 117.4ºC	151.3ºF 66.3ºC					
P15	73.7ºF 23.2ºC	233.1ºF 111.7ºC	166.4ºF 74.7ºC					
P16	73.4ºF 23.0ºC	289.9ºF 143.3ºC	153.6ºF 67.6ºC	987.2ºF 530.7ºC	973.1ºF 522.8ºC	924.6ºF 495.9ºC	Once, at 8 min.	26 min. total
P17	73.4ºF 23.0ºC	258.2ºF 125.7ºC	181.3ºF 82.9ºC		Flipped at 8 min.			
P18	74.8ºF 23.8ºC	284.9ºF 140.5ºC	152.6ºF 67.0ºC					
P19	73.2ºF 22.9ºC	291.4ºF 144.1ºC	192.8ºF 89.3ºC					
P20	71.6ºF 22.0ºC	254.6ºF 123.7ºC	219.1ºF 103.9ºC					
P21	74.1ºF 23.4ºC	271.9ºF 133.3ºC	171.3ºF 77.4ºC					
P22	71.9ºF 22.2ºC	269.4ºF 131.9ºC	152.1ºF 66.7ºC	870.9ºF 466.1ºC	1,060.7ºF 571.5ºC	732.0ºF 388.9ºC	Once, at 10 min.	34 min. total
P23	73.2ºF 22.9ºC	283.5ºF 139.7ºC	190.4ºF 88.0ºC		Flipped at 10 min.			
P24	73.9ºF 23.3ºC	276.1ºF 135.6ºC	183.5ºF 84.2ºC					

Deer	TEMPERATURE (BONE)			TEMPERATURE (FIRE)			REBUILT	BURN TIME
Metapodials	**Start**	**Flipped**	**End**	**Start**	**Flipped**	**End**	**When (min.)**	**# Min**
P25	71.6ºF 22.0ºC	287.9ºF 142.2ºC	197.1ºF 91.7ºC	870.9ºF 466.1ºC	1,060.7ºF 571.5ºC Flipped at 10 min.	732.0ºF 388.9ºC	Once, at 10 min.	34 min. total
P26	71.0ºF 21.7ºC	273.2ºF 134.0ºC	168.7ºF 75.9ºC					
P27	74.1ºF 23.4ºC	284.8ºF 140.4ºC	195.2ºF 90.7ºC					
P28	UNBURNED CONTROL							
P29	UNBURNED CONTROL							
P30	UNBURNED CONTROL							
Deer	**TEMPERATURE (BONE)**			**TEMPERATURE (FIRE)**			**REBUILT**	**BURN TIME**
Metapodials	**Start**	**Flipped**	**End**	**Start**	**Flipped**	**End**	**When (min.)**	**# Min**
Dry	Notes: Bones burned all at once, #1-13.							
D1	67.4ºF 19.7ºC	203.5ºF 95.3ºC	127.3ºF 52.9ºC	956.2ºF 513.4ºC	708.2ºF 375.7ºC Flipped at 6 min.	572.2ºF 300.1ºC	Not rebuilt	12 min. total
D2	68.1ºF 20.1ºC	211.7ºF 99.83ºC	116.9ºF 47.2ºC					
D3	72.8ºF 22.7ºC	223.9ºF 106.6ºC	129.8ºF 54.3ºC					
D4	71.5ºF 21.9ºC	231.4ºF 110.8ºC	146.6ºF 63.7ºC					
D5	70.1ºF 21.2ºC	217.8ºF 103.2ºC	139.0ºF 59.4ºC					

Deer	TEMPERATURE (BONE)			TEMPERATURE (FIRE)			REBUILT	BURN TIME
Metapodials	**Start**	**Flipped**	**End**	**Start**	**Flipped**	**End**	**When (min.)**	**# Min**
D6	71.0ºF 21.7ºC	208.6ºF 98.1ºC	121.9ºF 49.9ºC	956.2ºF 513.4ºC	708.2ºF 375.7ºC Flipped at 6 min.	572.2ºF 300.1ºC	Not rebuilt	12 min. total
D7	69.6ºF 20.9ºC	221.7ºF 105.4ºC	128.9ºF 53.8ºC					
D8	70.1ºF 21.2ºC	241.3ºF 116.3ºC	138.9ºF 59.4ºC					
D9	70.7ºF 21.5ºC	219.0ºF 103.9ºC	129.0ºF 53.9ºC					
D10	71.7ºF 22.1ºC	234.2ºF 112.3ºC	119.5ºF 48.6ºC					
D11	69.2ºF 20.7ºC	217.9ºF 103.3ºC	129.9ºF 54.4ºC					
D12	73.2ºF 22.9ºC	224.6ºF 107.0ºC	136.7ºF 58.2ºC					
D13	72.8ºF 22.7ºC	230.5ºF 110.3ºC	128.5ºF 53.6ºC					
D14	UNBURNED CONTROL							
D15	UNBURNED CONTROL							

Deer	TEMPERATURE (BONE)			TEMPERATURE (FIRE)			REBUILT	BURN TIME
Metapodials	**Start**	**Flipped**	**End**	**Start**	**Flipped**	**End**	**When (min.)**	**# Min**
Soaked	Notes: Bones burned all at once, #1-13.							
S1	64.4ºF 18.0ºC	207.4ºF 97.4ºC	108.6ºF 52.6ºC	878.5ºF 470.3ºC	734.6ºF 390.3ºC Flipped at 6 min.	685.4ºF 363.0ºC	Not rebuilt	12 min. total
S2	66.3ºF 19.1ºC	201.3ºF 94.1ºC	102.0ºF 38.9ºC					
S3	64.4ºF 18.0ºC	213.8ºF 101.0ºC	121.8ºF 49.9ºC					
S4	64.0ºF 17.8ºC	231.5ºF 110.8ºC	151.1ºF 66.2ºC					
S5	66.2ºF 19.0ºC	221.9ºF 105.5ºC	127.7ºF 53.2ºC					
S6	68.0ºF 20.0ºC	236.9ºF 113.8ºC	152.8ºF 67.1ºC					
S7	66.2ºF 19.0ºC	231.4ºF 110.8ºC	148.6ºF 64.8ºC					
S8	64.9ºF 18.3ºC	229.1ºF 109.5ºC	142.1ºF 61.2ºC					
S9	66.7ºF 19.3ºC	226.3ºF 107.9ºC	140.1ºF 60.1ºC					
S10	65.4ºF 18.6ºC	237.8ºF 114.3ºC	168.6ºF 75.9ºC					
S11	66.7ºF 19.3ºC	231.9ºF 111.1ºC	152.2ºF 66.8ºC					
S12	64.4ºF 18.0ºC	239.8ºF 115.4ºC	163.0ºF 72.8ºC					

Deer	TEMPERATURE (BONE)			TEMPERATURE (FIRE)			REBUILT	BURN TIME
Metapodials	**Start**	**Flipped**	**End**	**Start**	**Flipped**	**End**	**When (min.)**	**# Min**
S13	62.2ºF	241.4ºF	167.3ºF	878.5ºF	734.6ºF Flipped at 6 min.	685.4ºF	Not rebuilt	12 min. total
S14	UNBURNED CONTROL							
S15	UNBURNED CONTROL							

Visual Analysis

The observations recorded for each experimental burned bone assessing the formation of a white heat line are shown in Table 4.2. In the soaked, dry, and partially wet sample groups, none of the experimental burned bones developed a white heat line (Figures 4.1-4.6). For the very wet sample group, 8 out of 27 bones (29.6%) developed a white heat line, compared to 8 out of 16 bones from the fleshed sample group (50.0%). For these eight very wet bones, none of the white heat lines that developed were present throughout the entire circumference of the bone. Where present, their maximum widths ranged from 3 mm to 12 mm, with an average maximum width of 6.75 mm. Additionally, the diaphyseal circumference exhibiting this thermal signature varied among the very wet bones from less than 25% (n = 3) to between 75-100% (n = 1). Images of the burned very wet bones that developed a white heat line are presented in

Figures 4.7-4.14. The very wet bones that did not develop this thermal signature in presented in Figures 4.15-4.16.

For the fleshed bone samples that developed a white heat line, only one bone exhibited this thermal signature throughout its entire circumference, with a minimum width of 2 mm. Where present, maximum widths ranged from 4 mm to 12 mm, with an average maximum width of 8 mm. The diaphyseal circumferences of fleshed bones exhibiting a white heat line varied from 25-50% (n = 2) up to 75-100% (n = 3), with 50-75% (n = 3) and 75-100% (n = 3) occurring most frequently. Images of the burned fleshed bones that developed a white heat line are presented in Figures 4.17-4.24. The fleshed bones that did not develop this thermal signature in presented in Figures 4.25-4.26.

For both the fleshed and very wet samples, the shape and width of white heat lines varied among the bones. Generally, the white heat lines that formed on the fleshed samples were sharply defined, with a greater contrast to the surrounding bone, and exhibited a more uniform width. Conversely, the white heat lines that formed on the very wet samples were more irregular in shape, variable in their width per bone, and often presented with an adjacent heat border. For both bone sample groups, the white heat lines appear to form superficially, as they measure approximately 1.5 mm in depth, and do not penetrate deeply into the bone's surface. Their depths were measured using a ruler after the ground bone samples for FTIR analysis had been removed. The area of bone underneath the white heat lines was light ivory in color, likely indicating that it had not been significantly modified by the heat.

Table 4.2. Visual analysis of white heat line (WHL) formation on burned bone.

Sheep and pig	WHL FORM		WHL WIDTH (mm)		Diaphyseal Circumference with WHL			
Metapodials	**Yes (1)**	**No (0)**	**Max**	**Min**	**< 25%**	**25 - 50%**	**50 - 75%**	**75 - 100%**
Fleshed	Notes: #1-8 are sheep metapodials; #9-18 are pig metapodials							
F1		No (0)	-	-	-	-	-	-
F2		No (0)	-	-	-	-	-	-
F3		No (0)	-	-	-	-	-	-
F4		No (0)	-	-	-	-	-	-
F5		No (0)	-	-	-	-	-	-
F6		No (0)	-	-	-	-	-	-
F7		No (0)	-	-	-	-	-	-
F8	UNBURNED CONTROL (SHEEP)							
F9	Yes (1)		8 mm	0 mm			50 - 75%	
F10	Yes (1)		6 mm	0 mm		25 - 50%		
F11	Yes (1)		7 mm	0 mm				75 – 100%
F12	Yes (1)		8 mm	0 mm				75 – 100%
F13	Yes (1)		10 mm	0 mm			50 – 75%	
F14	Yes (1)		9 mm	2 mm				75 – 100%
F15		No (0)	-	-	-	-	-	-

Sheep and pig	**WHL FORM**		**WHL WIDTH (mm)**		**Diaphyseal Circumference with WHL**			
Metapodials	**Yes (1)**	**No (0)**	**Max**	**Min**	**< 25%**	**25 - 50%**	**50 - 75%**	**75 - 100%**
F16	Yes (1)		4 mm	0 mm		25 - 50%		
F17	Yes (1)		12 mm	0 mm			50 – 75%	
F18	UNBURNED CONTROL (PIG)							
Elk	**WHL FORM**		**WHL WIDTH (mm)**		**Diaphyseal Circumference with WHL**			
Femora	**Yes (1)**	**No (0)**	**Max**	**Min**	**< 25%**	**25 - 50%**	**50 - 75%**	**75 - 100%**
Very Wet	Notes: None							
W1	Yes (1)		7 mm	0 mm			50 - 75%	
W2		No (0)	-	-	-	-	-	-
W3		No (0)	-	-	-	-	-	-
W4		No (0)	-	-	-	-	-	-
W5		No (0)	-	-	-	-	-	-
W6		No (0)	-	-	-	-	-	-
W7	Yes (1)		3 mm	0 mm	< 25%			
W8		No (0)	-	-	-	-	-	-
W9	Yes (1)		7 mm	0 mm				75 - 100%
W10		No (0)	-	-	-	-	-	-
W11		No (0)	-	-	-	-	-	-

Elk	WHL FORM		WHL WIDTH (mm)		Diaphyseal Circumference with WHL			
Femora	**Yes (1)**	**No (0)**	**Max**	**Min**	**< 25%**	**25 – 50%**	**50 – 75%**	**75 – 100%**
W12	Yes (1)		5 mm	0 mm	< 25%			
W13	Yes (1)		7 mm	0 mm			50 – 75%	
W14		No (0)	-	-	-	-	-	-
W15		No (0)	-	-	-	-	-	-
W16		No (0)	-	-	-	-	-	-
W17	Yes (1)		10 mm	0 mm		25 – 50%		
W18		No (0)	-	-	-	-	-	-
W19		No (0)	-	-	-	-	-	-
W20	Yes (1)		3 mm	0 mm	< 25%			
W21		No (0)	-	-	-	-	-	-
W22		No (0)	-	-	-	-	-	-
W23		No (0)	-	-	-	-	-	-
W24		No (0)	-	-	-	-	-	-
W25		No (0)	-	-	-	-	-	-
W26		No (0)	-	-	-	-	-	-
W27	Yes (1)		12 mm	0 mm		25 – 50%		
W28	UNBURNED CONTROL							

Elk	WHL FORM		WHL WIDTH (mm)		Diaphyseal Circumference with WHL			
Femora	**Yes (1)**	**No (0)**	**Max**	**Min**	**< 25%**	**25 – 50%**	**50 – 75%**	**75 – 100%**
W29	UNBURNED CONTROL							
W30	UNBURNED CONTROL							

Figure 4.1. Soaked bone 1, burned deer metapodial that did not develop a white heat line. Scale is in mm.

Figure 4.2. Soaked bone 2, burned deer metapodial that did not develop a white heat line. Scale is in mm.

Figure 4.3. Dry bone 7, burned deer metapodial that did not develop a white heat line. Scale is in mm.

Figure 4.4. Dry bone 11, burned deer metapodial that did not develop a white heat line. Scale is in mm.

Figure 4.5. Partially wet bone 4, burned deer metapodial that did not develop a white heat line. Scale is in mm.

Figure 4.6. Partially wet bone 14, burned deer metapodial that did not develop a white heat line. Scale is in mm.

Figure 4.7. Very wet bone 1, burned elk femur with white heat line (arrow) (maximum width of 7 mm). Scale is in mm.

Figure 4.8. Very wet bone 7, burned elk femur with white heat line (arrow) (maximum width of 3 mm). Scale is in mm.

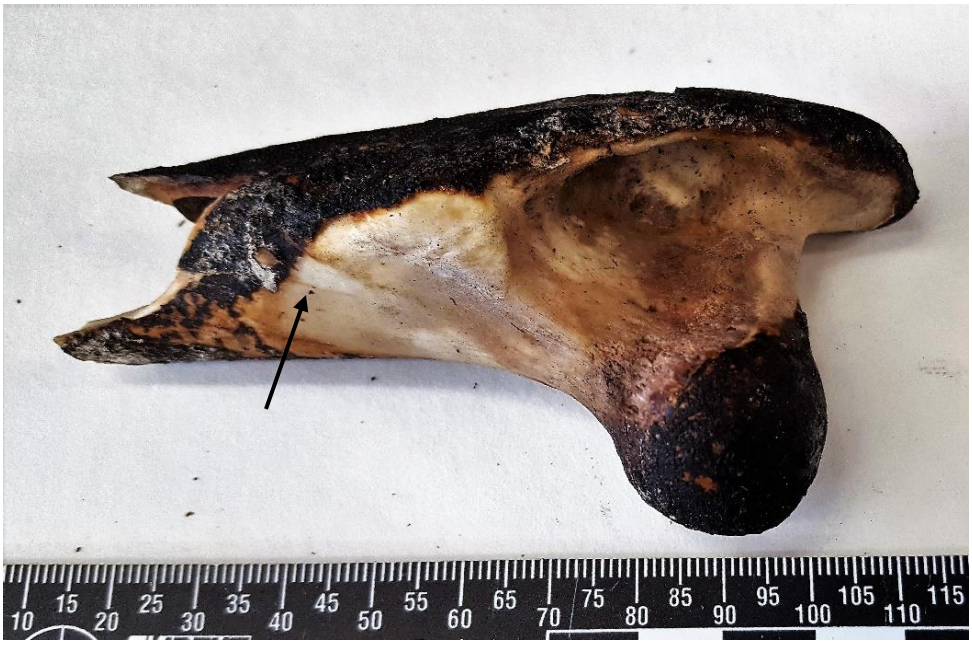

Figure 4.9. Very wet bone 9, burned elk femur with white heat line (arrow) (maximum width of 7 mm). Scale is in mm.

Figure 4.10. Very wet bone 12, burned elk femur with white heat line (arrow) (maximum width of 5 mm). Scale is in mm.

Figure 4.11. Very wet bone 13, burned elk femur with white heat line (arrow) (maximum width of 7 mm). Scale is in mm.

Figure 4.12. Very wet bone 17, burned elk femur with white heat line (arrow) (maximum width of 10 mm). Scale is in mm.

Figure 4.13. Very wet bone 20, burned elk femur with white heat line (arrow) (maximum width of 3 mm). Scale is in mm.

Figure 4.14. Very wet bone 27, burned elk femur with white heat line (arrow) (maximum width of 12 mm). Scale is in mm.

Figure 4.15. Very wet bone 3, burned elk femur that did not develop a white heat line. Scale is in mm.

Figure 4.16. Very wet bone 4, burned elk femur that did not develop a white heat line. Scale is in mm.

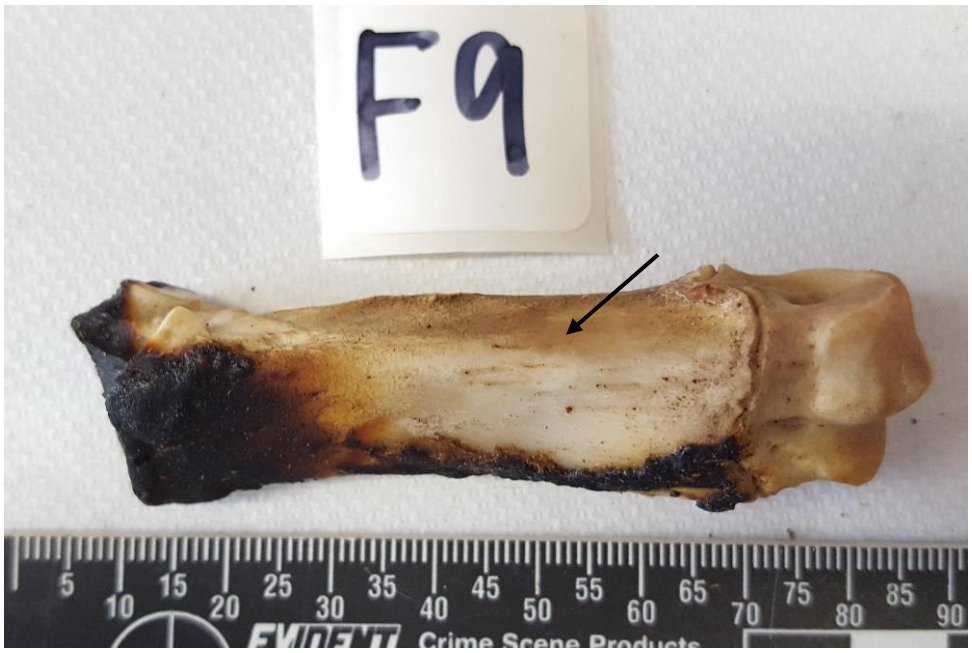

Figure 4.17. Fleshed bone 9, burned pig metapodial with white heat line (arrow) (maximum width of 8 mm). Scale is in mm.

Figure 4.18. Fleshed bone 10, burned pig metapodial with white heat line (arrow) (maximum width of 6 mm). Scale is in mm.

Figure 4.19. Fleshed bone 11, burned pig metapodial with white heat line (arrow) (maximum width of 7 mm). Scale is in mm.

Figure 4.20. Fleshed bone 12, burned pig metapodial with white heat line (arrow) (maximum width of 8 mm). Scale is in mm.

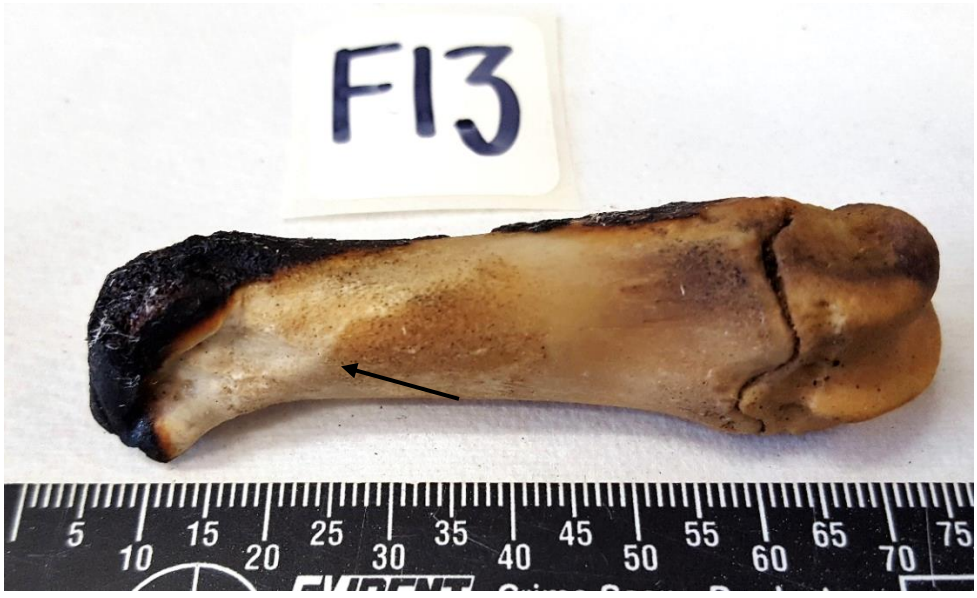

Figure 4.21. Fleshed bone 13, burned pig metapodial with white heat line (arrow) (maximum width of 10 mm). Scale is in mm.

Figure 4.22. Fleshed bone 14, burned pig metapodial with white heat line (arrow) (maximum width of 9 mm). Scale is in mm.

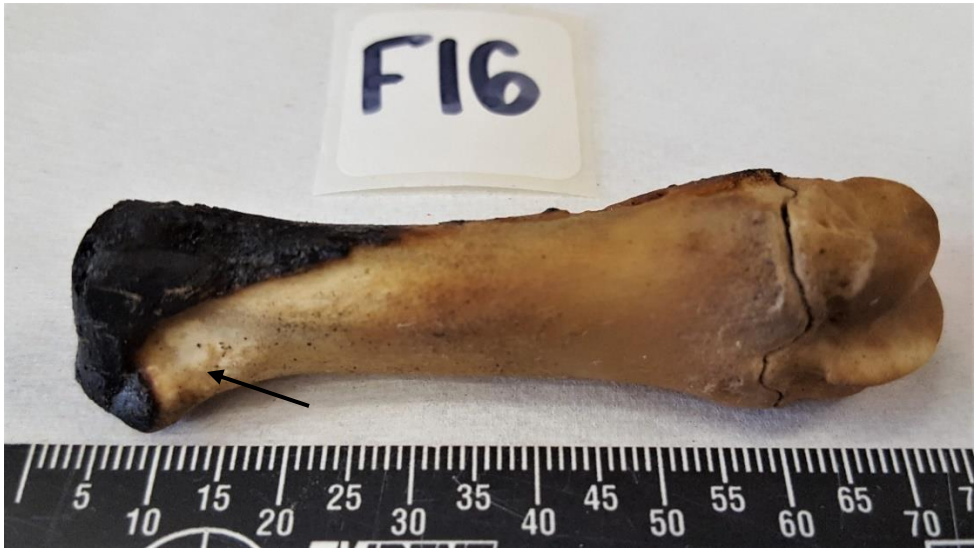

Figure 4.23. Fleshed bone 16, burned pig metapodial with white heat line (arrow) (maximum width of 4 mm). Scale is in mm.

Figure 4.24. Fleshed bone 17, burned pig metapodial with white heat line (arrow) (maximum width of 12 mm). Scale is in mm.

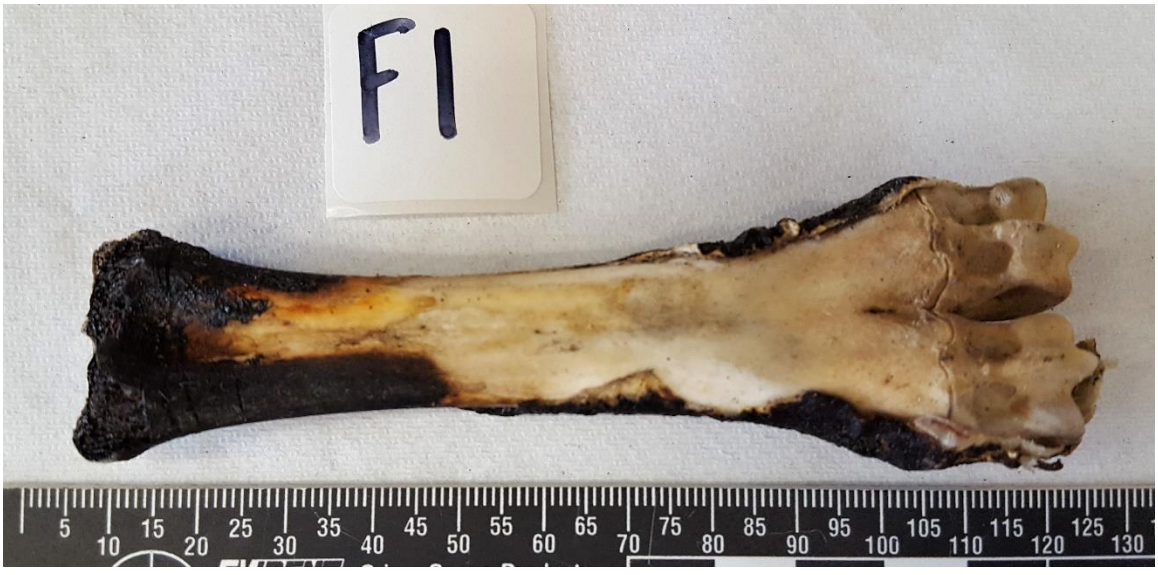

Figure 4.25. Fleshed bone 1, burned sheep metapodial that did not develop a white heat line. Scale is in mm.

Figure 4.26. Fleshed bone 15, burned pig metapodial that did not develop a white heat line. Scale is in mm.

FTIR Spectral Analysis

Results from the FTIR analysis are listed in Table 4.3 with spectral peak heights of the v3 CO_3 (1415 cm^{-1}), v3 PO_4 (1035 cm^{-1}), and amide I (1660 cm^{-1}) vibrational bands per individual bone, for the unburned controls, burned experimental bones that developed a white heat line, and the burned experimental bones that did not develop a white heat line.

Table 4.3. Spectral peak heights of v3 CO_3, v3 PO_4, and amide I per bone.

FLESHED	WHL FORM		CO_3 PEAK HEIGHT	PO_4 PEAK HEIGHT	AMIDE I PEAK HEIGHT
Sheep and pig metapodials	**Yes (1)**	**No (0)**	-	-	-
Unburned Controls	-	-	-	-	-
F8	N/A		0.151	0.258	0.21
F18	N/A		0.172	0.327	0.237
Experimental Burned	-	-	-	-	-
F1		No (0)	0.175	0.277	0.218
F2		No (0)	0.129	0.237	0.187
F3		No (0)	0.083	0.127	0.123
F4		No (0)	0.072	0.107	0.109
F5		No (0)	0.151	0.262	0.214
F6		No (0)	0.095	0.163	0.133
F7		No (0)	0.127	0.195	0.159
F9	Yes (1)		0.183	0.352	0.230
F10	Yes (1)		0.142	0.186	0.201
F11	Yes (1)		0.174	0.276	0.233
F12	Yes (1)		0.186	0.402	0.271
F13	Yes (1)		0.138	0.252	0.189
F14	Yes (1)		0.141	0.257	0.189
F15		No (0)	0.091	0.146	0.110
F16	Yes (1)		0.215	0.435	0.318
F17	Yes (1)		0.223	0.369	0.314

VERY WET	WHL FORM		CO_3 PEAK HEIGHT	PO_4 PEAK HEIGHT	AMIDE I PEAK HEIGHT
Elk Femora	**Yes (1)**	**No (0)**	-	-	-
Unburned Controls	-		-	-	-
W28	N/A		0.210	0.535	0.278
W29	N/A		0.212	0.522	0.273
W30	N/A		0.178	0.383	0.226
Experimental Burned	-		-	-	-
W1	Yes (1)		0.106	0.168	0.164
W2		No (0)	0.111	0.182	0.138
W3		No (0)	0.138	0.237	0.212
W4		No (0)	0.217	0.303	0.255
W5		No (0)	0.102	0.198	0.142
W6		No (0)	0.093	0.150	0.132
W7	Yes (1)		0.103	0.216	0.142
W8		No (0)	0.106	0.205	0.145
W9	Yes (1)		0.106	0.191	0.139
W10		No (0)	0.079	0.133	0.109
W11		No (0)	0.091	0.163	0.118
W12	Yes (1)		0.146	0.378	0.206
W13	Yes (1)		0.112	0.217	0.148
W14		No (0)	0.117	0.146	0.159
W15		No (0)	0.114	0.207	0.146
W16		No (0)	0.111	0.092	0.211
W17	Yes (1)		0.116	0.239	0.138
W18		No (0)	0.088	0.116	0.110
W19		No (0)	0.088	0.129	0.108
W20	Yes (1)		0.114	0.274	0.150
W21		No (0)	0.071	0.116	0.110
W22		No (0)	0.087	0.100	0.134
W23		No (0)	0.116	0.197	0.184
W24		No (0)	0.115	0.208	0.158
W25		No (0)	0.175	0.403	0.237

VERY WET	WHL FORM		CO_3 PEAK HEIGHT	PO_4 PEAK HEIGHT	AMIDE I PEAK HEIGHT
Elk Femora	**Yes (1)**	**No (0)**	-	-	-
W26		No (0)	0.101	0.132	0.124
W27	Yes (1)		0.131	0.279	0.176
PARTIALLY WET	**WHL FORM**		CO_3 PEAK HEIGHT	PO_4 PEAK HEIGHT	AMIDE I PEAK HEIGHT
Deer Metapodials	**Yes (1)**	**No (0)**	-	-	-
Unburned Controls	-		-	-	-
P28	N/A		0.269	0.563	0.365
P29	N/A		0.302	0.628	0.408
P30	N/A		0.297	0.425	0.339
Experimental Burned	-		-	-	-
P1		No (0)	0.153	0.346	0.212
P2		No (0)	0.362	0.853	0.482
P3		No (0)	0.366	0.816	0.486
P4		No (0)	0.204	0.441	0.273
P5		No (0)	0.245	0.535	0.313
P6		No (0)	0.178	0.417	0.238
P7		No (0)	0.276	0.581	0.394
P8		No (0)	0.245	0.548	0.319
P9		No (0)	0.173	0.344	0.229
P10		No (0)	0.184	0.387	0.247
P11		No (0)	0.318	0.629	0.421
P12		No (0)	0.228	0.567	0.309
P13		No (0)	0.267	0.618	0.347
P14		No (0)	0.200	0.345	0.242
P15		No (0)	0.185	0.387	0.246
P16		No (0)	0.202	0.555	0.281
P17		No (0)	0.266	0.601	0.230
P18		No (0)	0.180	0.419	0.230

PARTIALLY WET	WHL FORM		CO_3 PEAK HEIGHT	PO_4 PEAK HEIGHT	AMIDE I PEAK HEIGHT
Deer Metapodials	**Yes (1)**	**No (0)**	-	-	-
P19		No (0)	0.166	0.353	0.206
P20		No (0)	0.284	0.694	0.388
P21		No (0)	0.205	0.461	0.269
P22		No (0)	0.130	0.305	0.161
P23		No (0)	0.357	0.679	0.444
P24		No (0)	0.163	0.324	0.222
P25		No (0)	0.105	0.290	0.159
P26		No (0)	0.173	0.394	0.262
P27		No (0)	0.136	0.265	0.177
DRY	**WHL FORM**		**CO_3 PEAK HEIGHT**	**PO_4 PEAK HEIGHT**	**AMIDE I PEAK HEIGHT**
Deer Metapodials	**Yes (1)**	**No (0)**	-	-	-
Unburned Controls	-		-	-	-
D14	N/A		0.315	0.704	0.403
D15	N/A		0.512	1.003	0.708
Experimental Burned	-		-	-	-
D1		No (0)	0.348	1.100	0.453
D2		No (0)	0.260	0.729	0.369
D3		No (0)	0.338	0.697	0.453
D4		No (0)	0.498	0.850	0.694
D5		No (0)	0.351	0.724	0.483
D6		No (0)	0.421	0.906	0.611
D7		No (0)	0.253	0.490	0.384
D8		No (0)	0.360	1.021	0.478
D9		No (0)	0.550	1.069	0.727
D10		No (0)	0.389	0.793	0.535
D11		No (0)	0.328	0.582	0.453
D12		No (0)	0.405	0.784	0.573
D13		No (0)	0.484	1.090	0.687

SOAKED	WHL FORM		CO_3 PEAK HEIGHT	PO_4 PEAK HEIGHT	AMIDE I PEAK HEIGHT
Deer Metapodials	**Yes (1)**	**No (0)**	-	-	-
Unburned Controls	-		-	-	-
S14	N/A		0.485	0.981	0.667
S15	N/A		0.407	0.830	0.563
Experimental Burned	-		-	-	-
S1		No (0)	0.418	0.844	0.568
S2		No (0)	0.400	0.782	0.529
S3		No (0)	0.508	0.982	0.638
S4		No (0)	0.388	0.691	0.510
S5		No (0)	0.302	0.570	0.401
S6		No (0)	0.351	0.759	0.493
S7		No (0)	0.304	0.674	0.411
S8		No (0)	0.311	0.596	0.416
S9		No (0)	0.385	0.826	0.548
S10		No (0)	0.337	0.666	0.449
S11		No (0)	0.232	0.526	0.329
S12		No (0)	0.551	0.867	0.629
S13		No (0)	0.208	0.409	0.276

Figures 4.27-4.31 display the range of spectral peak heights of ν3 CO_3, ν3 PO_4, and amide I for the burned bones in each sample group, subdivided by whether a white heat line formed. A sample was considered an outlier if its spectral peak height was lower than 1.5 multiplied by the interquartile range (3^{rd} quartile subtract the 1^{st} quartile) and subtracted from the 1^{st} quartile, or higher than 1.5 multiplied by the interquartile range and added to the 3^{rd} quartile.

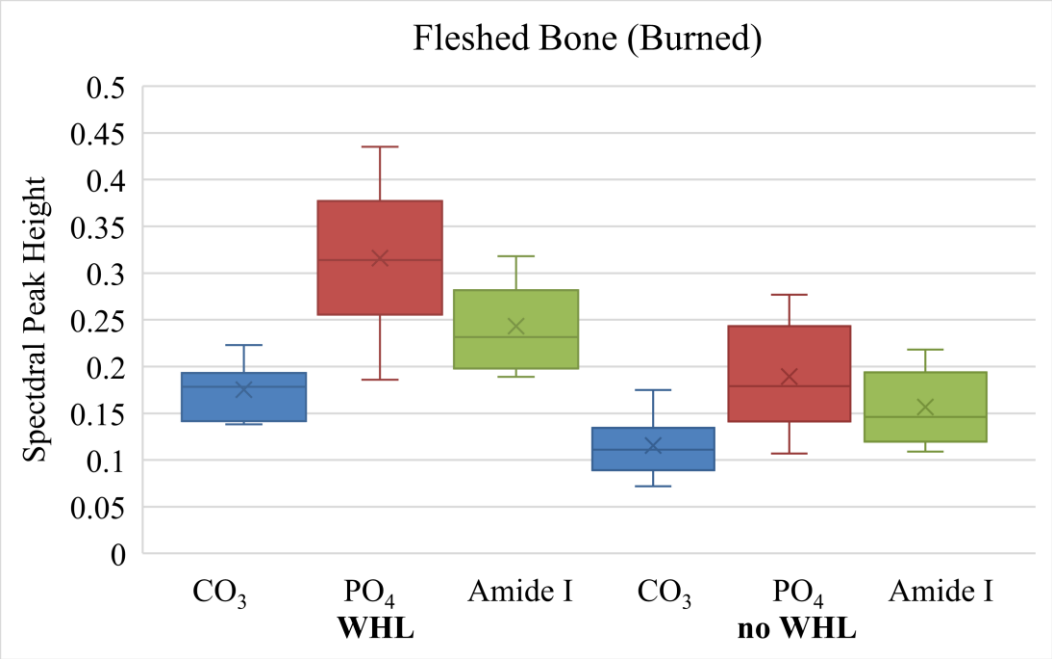

Figure 4.27. Range of spectral peak heights for carbonate (CO_3), phosphate (PO_4), and amide I in burned, fleshed bone.

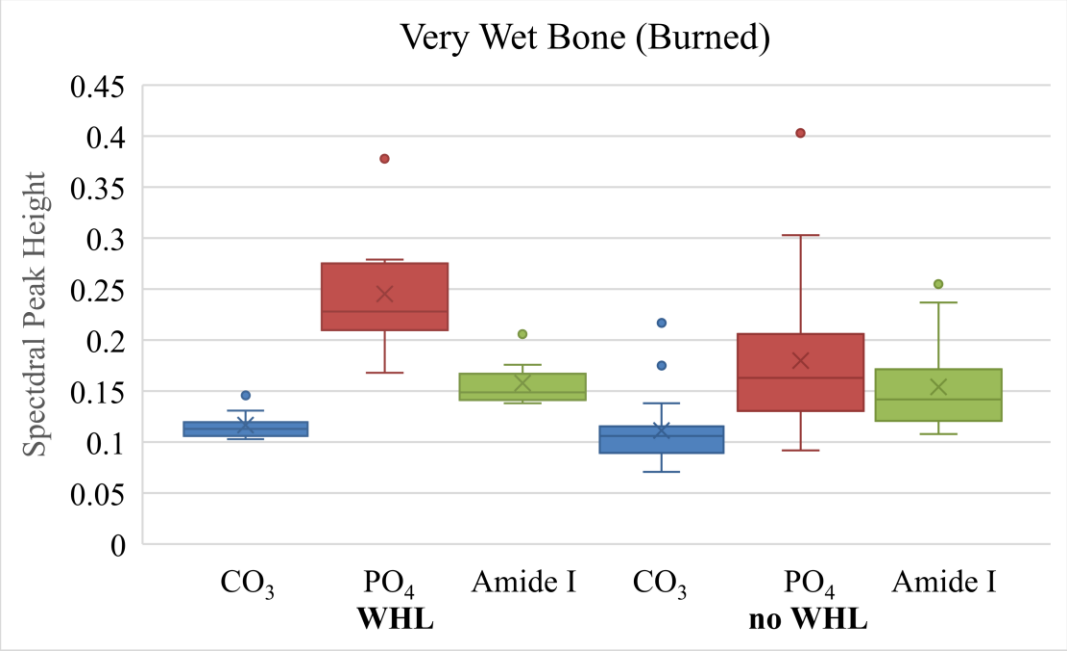

Figure 4.28. Range of spectral peak heights for carbonate (CO_3), phosphate (PO_4), and amide I in burned, very wet bone.

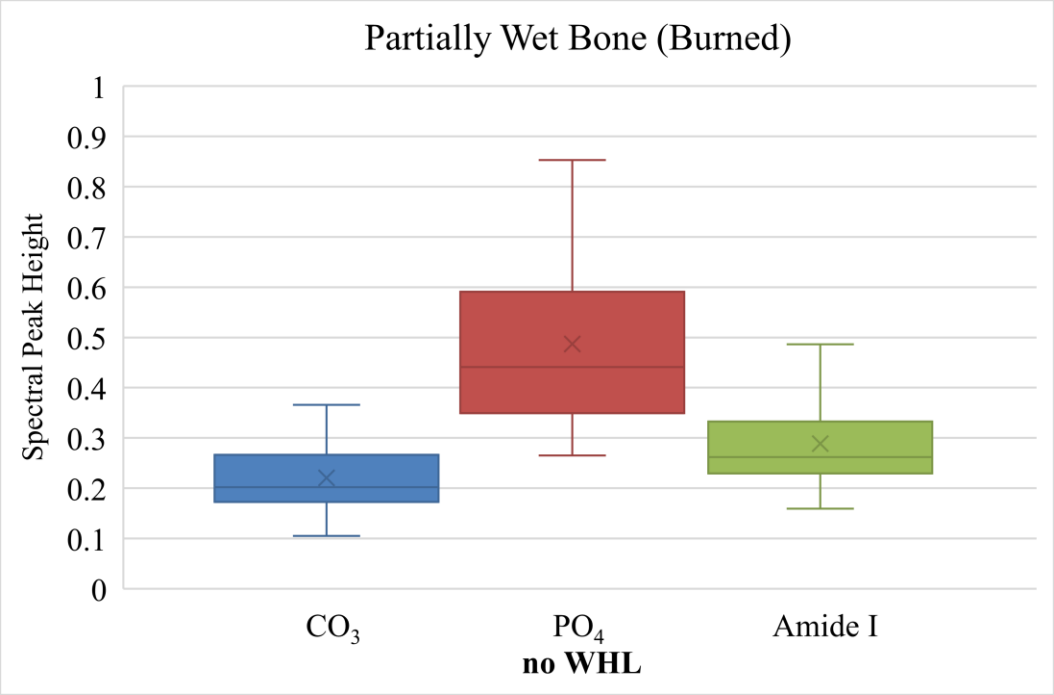

Figure 4.29. Range of spectral peak heights for carbonate (CO_3), phosphate (PO_4), and amide I in burned, partially wet bone.

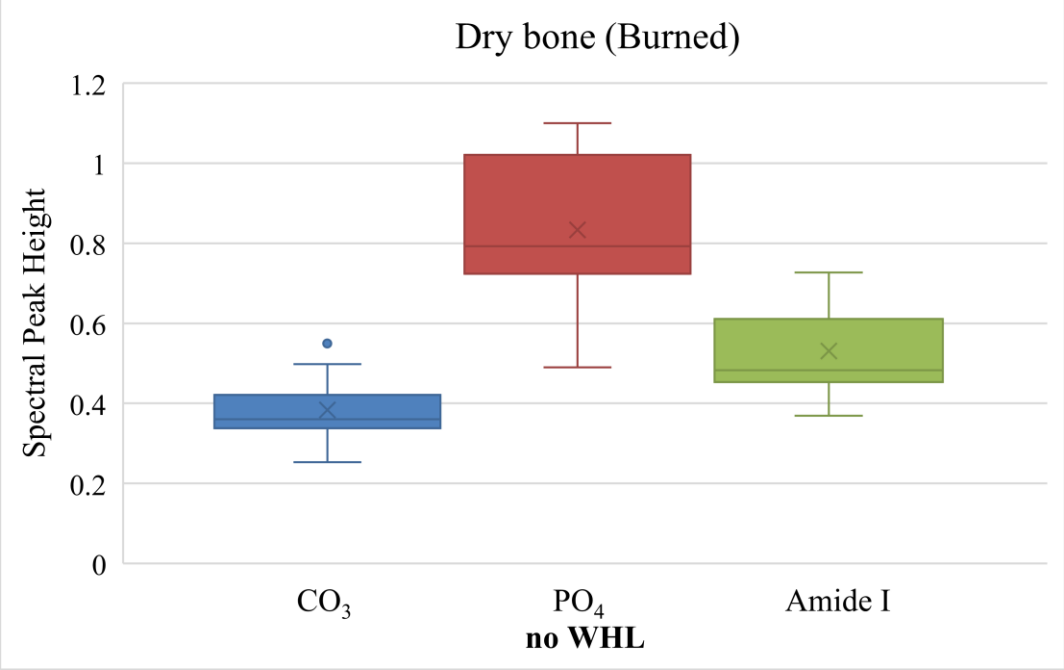

Figure 4.30. Range of spectral peak heights for carbonate (CO_3), phosphate (PO_4), and amide I in burned, dry bone.

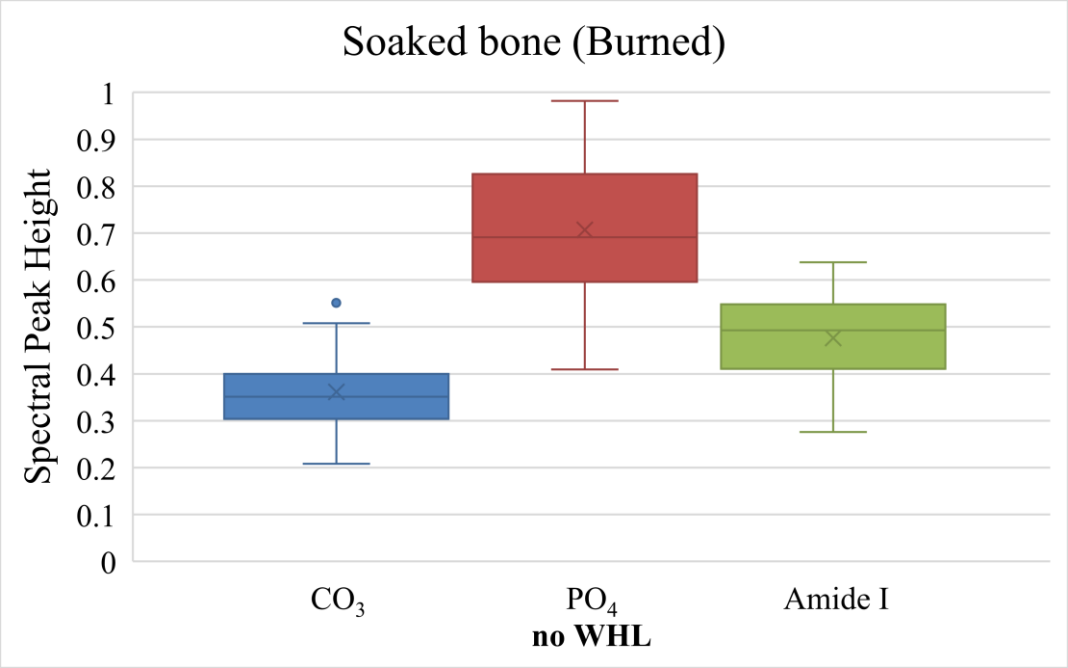

Figure 4.31. Range of spectral peak heights for carbonate (CO_3), phosphate (PO_4), and amide I in burned, soaked bone.

Mean spectral peak heights were then calculated for ν3 CO_3, ν3 PO_4, and amide I, subdivided by bone condition prior to burning (fleshed, very wet, partially wet, dry, soaked), unburned control versus burned experimental, and whether an experimental burned bone developed a white heat line after burning. The mean spectral peak heights for each bone subgroup are listed in Table 4.4. For the unburned controls, the mean ν3 CO_3, ν3 PO_4, and amide I peak heights are greatest in the soaked samples ($\bar{x}$ = 0.446, 0.9055, 0.615) and the least in the fleshed samples ($\bar{x}$ = 0.1615, 0.2925, and 0.2235). Among the burned bones that did develop a white heat line, the mean ν3 CO_3, ν3 PO_4, and amide I peak heights are greater in the fleshed samples ($\bar{x}$ = 0.17525, 0.316125, 0.2235) than in the very wet ($\bar{x}$ = 0.11675, 0.24525, 0.157875). For the burned bones

that did not develop a white heat line, the mean v3 CO_3, v3 PO_4, and amide I spectral peak heights are greatest in the dry samples ($\bar{x}$ = 0.383, 0.833, 0.531) and the least in the very wet ($\bar{x}$ = 0.112, 0.180, 0.154).

Table 4.4. Mean spectral peak heights of v3 CO_3, v3 PO_4, and amide I by bone subgroup.

	MEAN CO_3 PEAK HEIGHT	MEAN PO_4 PEAK HEIGHT	MEAN AMIDE I PEAK HEIGHT
FLESHED	-	-	-
Unburned Controls	0.162	0.293	0.224
Experimental Burned	-	-	-
WHL Formed	0.175	0.316	0.243
No WHL	0.115	0.189	0.157
VERY WET	-	-	-
Unburned Controls	0.200	0.480	0.259
Experimental Burned	-	-	-
WHL Formed	0.117	0.245	0.158
No WHL	0.112	0.180	0.154

	MEAN CO_3 PEAK HEIGHT	MEAN PO_4 PEAK HEIGHT	MEAN AMIDE I PEAK HEIGHT
PARTIALLY WET	-	-	-
Unburned Controls	0.289	0.539	0.371
Experimental Burned	-	-	-
WHL Formed	N/A	N/A	N/A
No WHL	0.220	0.487	0.288
DRY	-	-	-
Unburned Controls	0.414	0.854	0.556
Experimental Burned	-	-	-
WHL Formed	N/A	N/A	N/A
No WHL	0.383	0.833	0.531
SOAKED	-	-	-
Unburned controls	0.446	0.906	0.615
Experimental Burned	-	-	-
WHL Formed	N/A	N/A	N/A
No WHL	0.361	0.707	0.477

Figures 4.32-4.36 show the mean spectral peak heights of v3 CO_3, v3 PO_4, and amide I for the burned bones in each sample group (fleshed, very wet, partially wet, dry, oaked), subdivided by unburned control versus burned experimental, and whether an experimental burned bone developed a white heat line after burning.

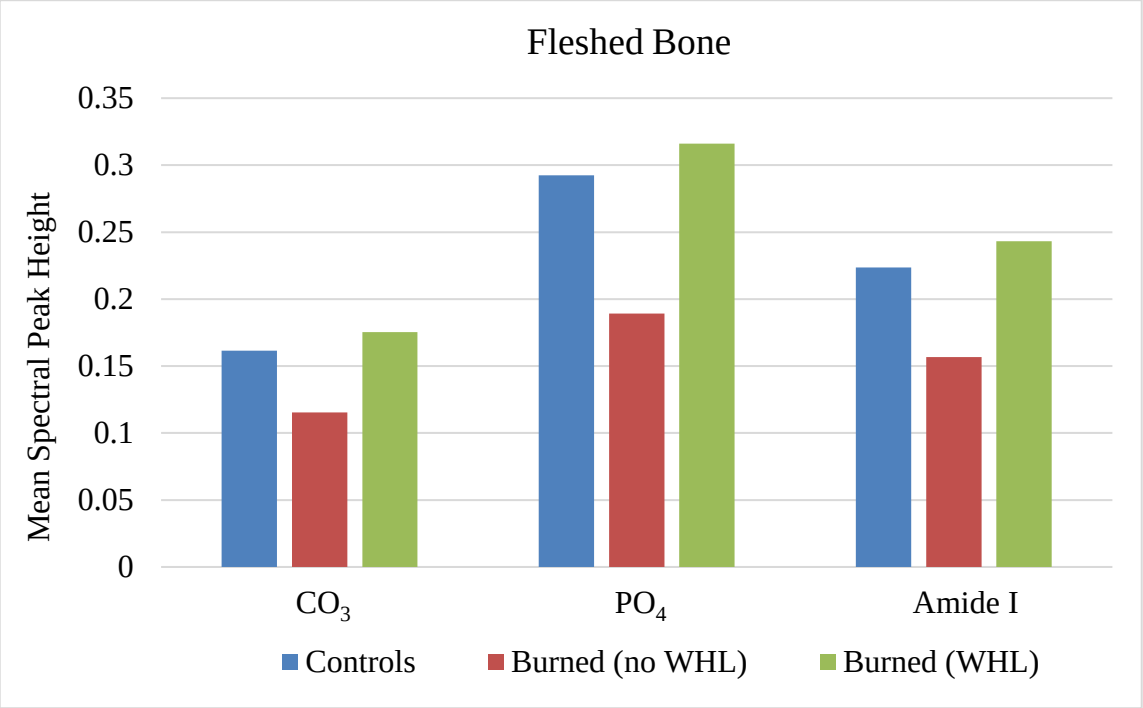

Figure 4.32. Mean spectral peak heights for carbonate (CO_3), phosphate (PO_4), and amide I in fleshed bone.

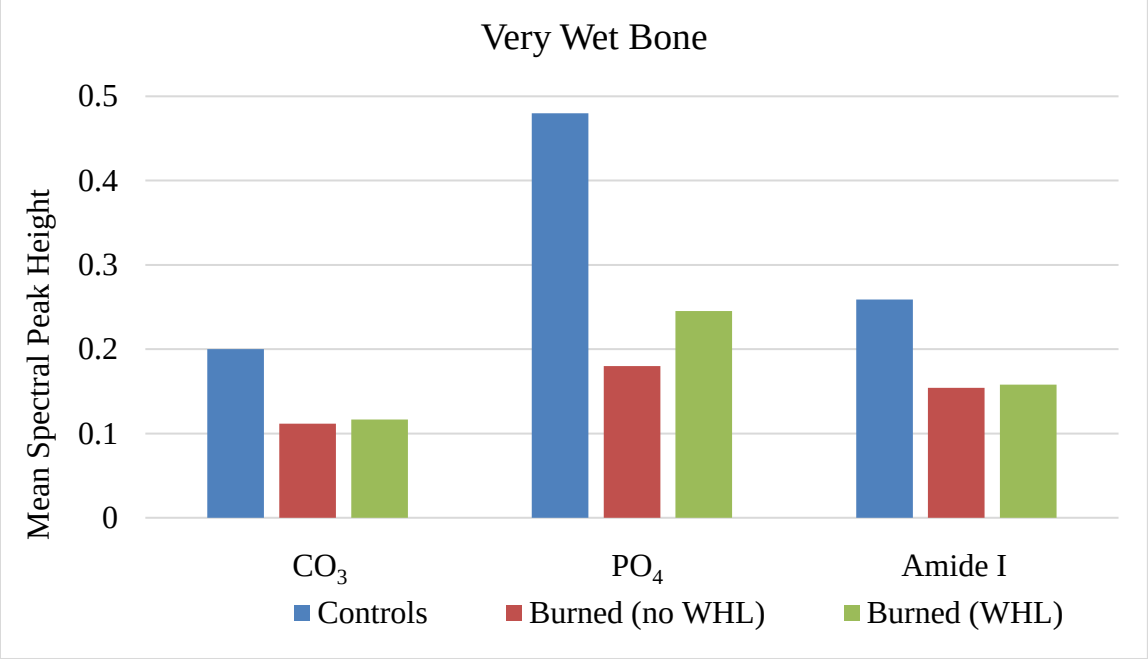

Figure 4.33. Mean spectral peak heights for carbonate (CO_3), phosphate (PO_4), and amide I in very wet bone.

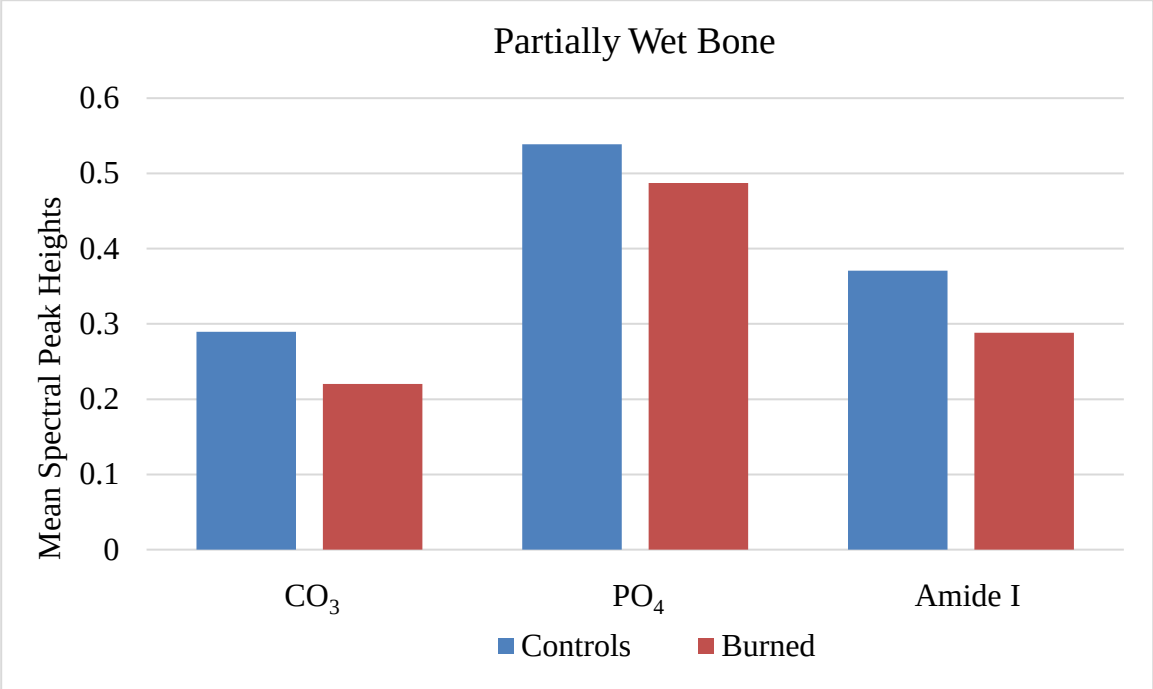

Figure 4.34. Mean spectral peak heights for carbonate (CO_3), phosphate (PO_4), and amide I in partially wet bone.

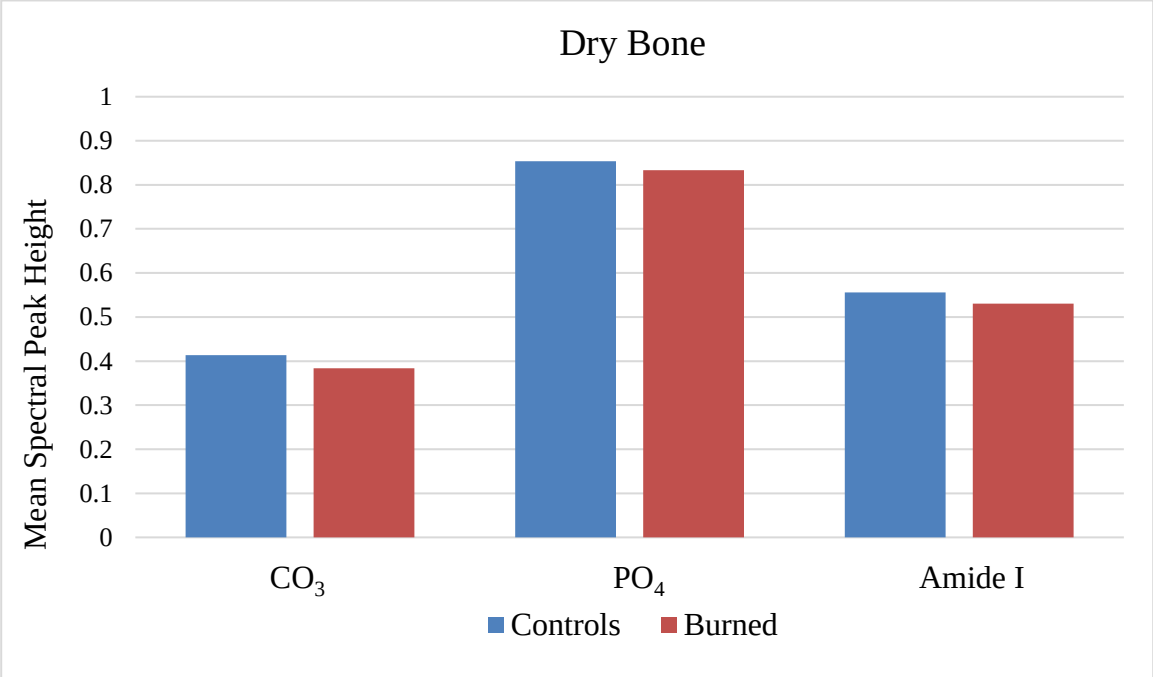

Figure 4.35. Mean spectral peak heights for carbonate (CO_3), phosphate (PO_4), and amide I in dry bone.

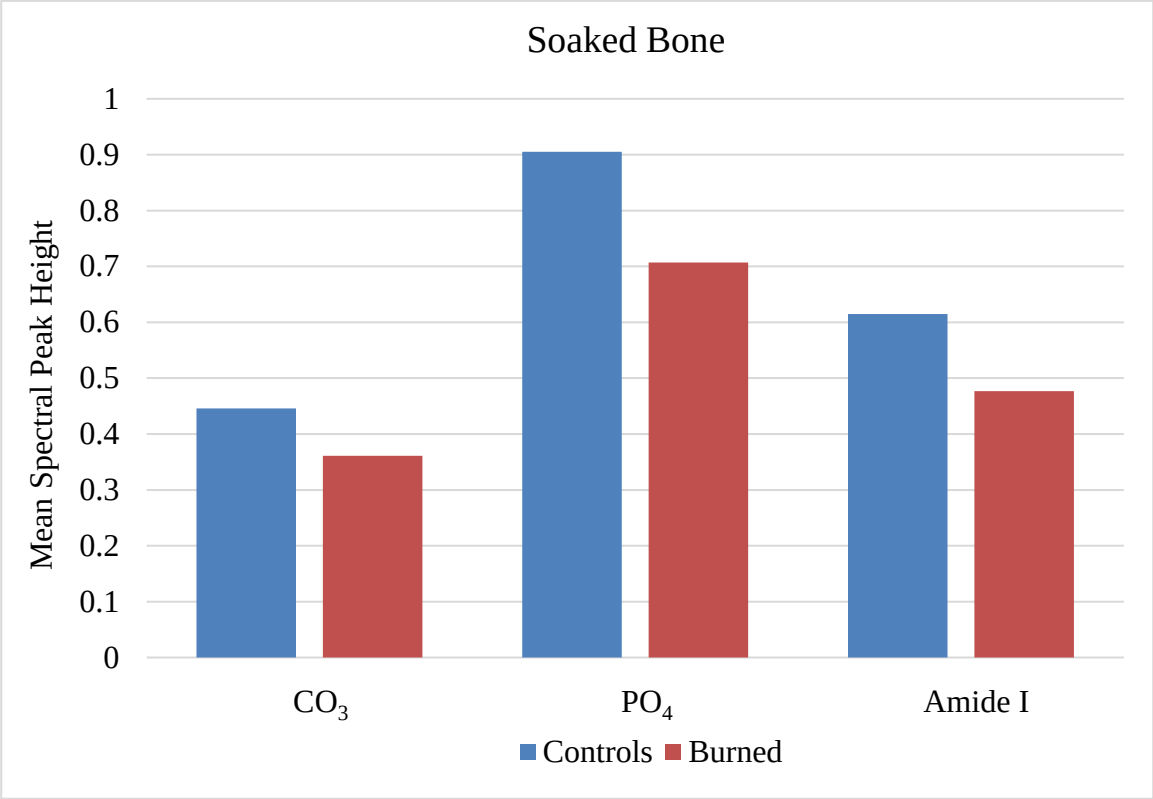

Figure 4.36. Mean spectral peak heights for carbonate (CO_3), phosphate (PO_4), and amide I in soaked bone.

Statistical Analysis

These statistical analyses were performed using the statistical software program *SPSS*, version 20 (SPSS Inc., Chicago, Illinois). For all of the statistical analyses conducted, a 5% level of significance ($\alpha = 0.05$) was utilized.

Test for Normality

Statistical normality of the data collected was assessed using a Shapiro-Wilk's W test. Spectral peak heights of ν3 CO_3, ν3 PO_4, and amide I for the fleshed, partially wet, dry, and soaked bone sample groups are normally distributed [$p > 0.05$]. However, the ν3

CO_3 [$p < 0.003$], ν3 PO_4 [$p < 0.001$], and amide I [$p < 0.004$] spectral peak heights for the very wet bone sample group do not have a normal distribution.

Correlation of Bone Condition and White Heat Line Formation

A Chi-squared (X^2) test of independence was performed to evaluate if there is a relationship between bone's physical condition prior to burning (fleshed, very wet, partially wet, dry, soaked) and white heat line formation. Results of this test are statistically significant [$p < 0.001$], indicating that bone's physical condition prior to burning and white heat line formation are not independent, but rather, that a relationship exists between these two variables.

Since a Chi-squared (X^2) test of independence only proves the existence or nonexistence of an association between variables, a Cramer's V was utilized in order to measure the strength of the relationship. The Cramer's V value is 0.527, indicating a strong relationship between bone's physical condition prior to burning (fleshed, very wet, partially wet, dry, soaked) and the formation of a white heat line.

Multivariate Correlation

Using a multivariate analysis of variance (MANOVA) test, statistically significant differences were found between groups, indicating the effect of bone's physical condition prior to burning (fleshed, very wet, partially wet, dry, soaked) on the formation of a white heat line [$F_{(4, 91)} = 8.750$, $p < 0.001$], as well as on the spectral peak heights of ν3 CO_3

[$F_{(4, 91)} = 57.327$, $p < 0.001$], ν3 PO_4 [$F_{(4, 91)} = 67.599$, $p < 0.001$], and amide I [$F_{(4, 91)} = 64.565$, $p < 0.001$].

Post-Hoc Test

Following the MANOVA, a Bonferroni post-hoc test found statistically significant differences in the formation of a white heat line between bones in the fleshed and partially wet sample groups [$p < 0.001$], fleshed and dry sample groups [$p < 0.001$], fleshed and soaked sample groups [$p < 0.001$], and the very wet and partially wet sample groups [$p < 0.012$]. The Bonferroni post-hoc test also found statistically significant differences in the spectral peak heights of ν3 CO_3 between bones in the fleshed and partially wet sample groups [$p < 0.006$], fleshed and dry sample groups [$p < 0.001$], fleshed and soaked sample groups [$p < 0.001$], very wet and partially wet sample groups [$p < 0.001$], very wet and dry sample groups [$p < 0.001$], very wet and soaked sample groups [$p < 0.001$], partially wet and dry sample groups [$p < 0.001$], and the partially wet and soaked sample groups [$p < 0.001$].

For the spectral peak heights of ν3 PO_4, the Bonferroni post-hoc test found statistically significant differences between bones in the fleshed and partially wet sample groups [$p < 0.001$], fleshed and dry sample groups [$p < 0.001$], fleshed and soaked sample groups [$p < 0.001$], very wet and partially wet sample groups [$p < 0.001$], very wet and dry sample groups [$p < 0.001$], very wet and soaked sample groups [$p < 0.001$], partially wet and dry sample groups [$p < 0.001$], and the partially wet and soaked sample groups [$p < 0.001$].

The Bonferroni post-hoc test also found statistically significant differences between bones in the spectral peak heights of amide I between bones in the fleshed and partially wet sample groups [$p < 0.012$], fleshed and dry sample groups [$p < 0.001$], fleshed and soaked sample groups [$p < 0.001$], very wet and partially wet sample groups [$p < 0.001$], very wet and dry sample groups [$p < 0.001$], very wet and soaked sample groups [$p < 0.001$], partially wet and dry sample groups [$p < 0.001$], and the partially wet and soaked sample groups [$p < 0.001$] (Figures 4.37-4.43).

In conclusion, results from the statistical analyses indicate that a strong relationship exists between bone's physical condition prior to burning and the subsequent formation of a white heat line. Bone's physical condition prior to burning also has a statistically significant impact on the spectral peak heights of ν3 CO_3, ν3 PO_4, and amide I. Specifically, statistically significant differences are present for the spectral peak heights of these three components between each of the five bone sample groups.

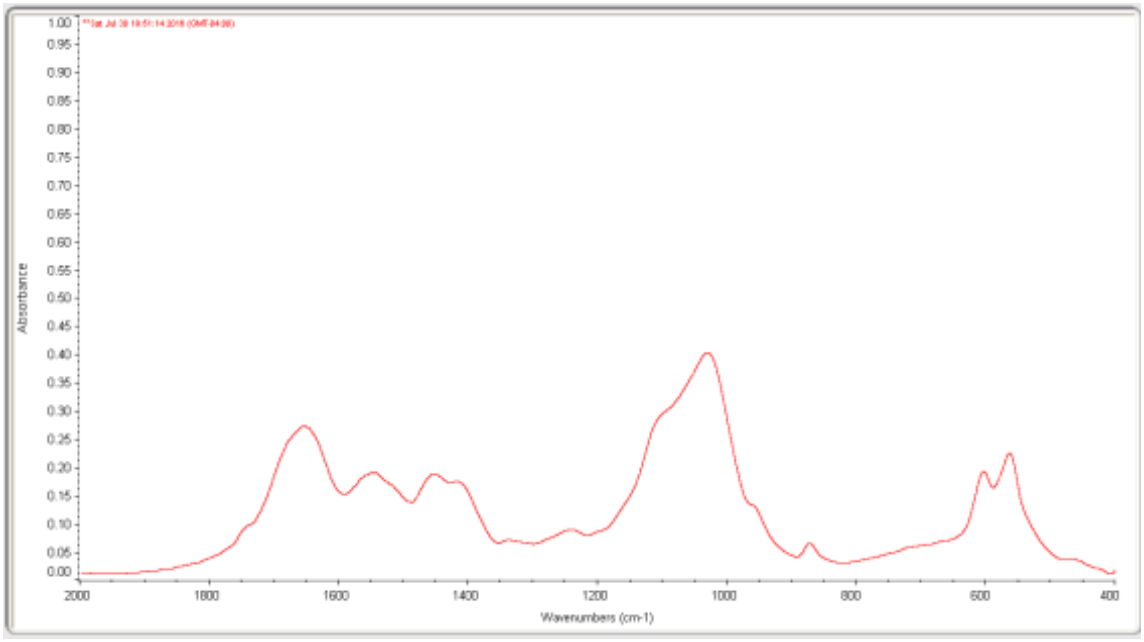

Figure 4.37. FTIR spectrum of burned, fleshed bone number 12 (white heat line formed).

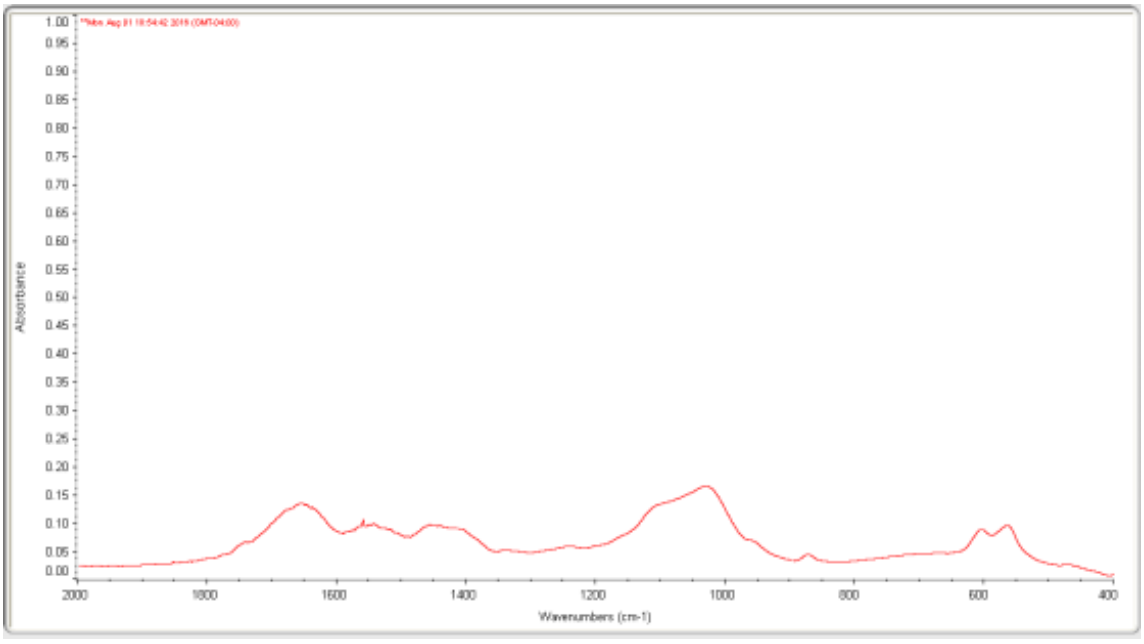

Figure 4.38. FTIR spectrum of burned, fleshed bone number 6 (white heat line did not form).

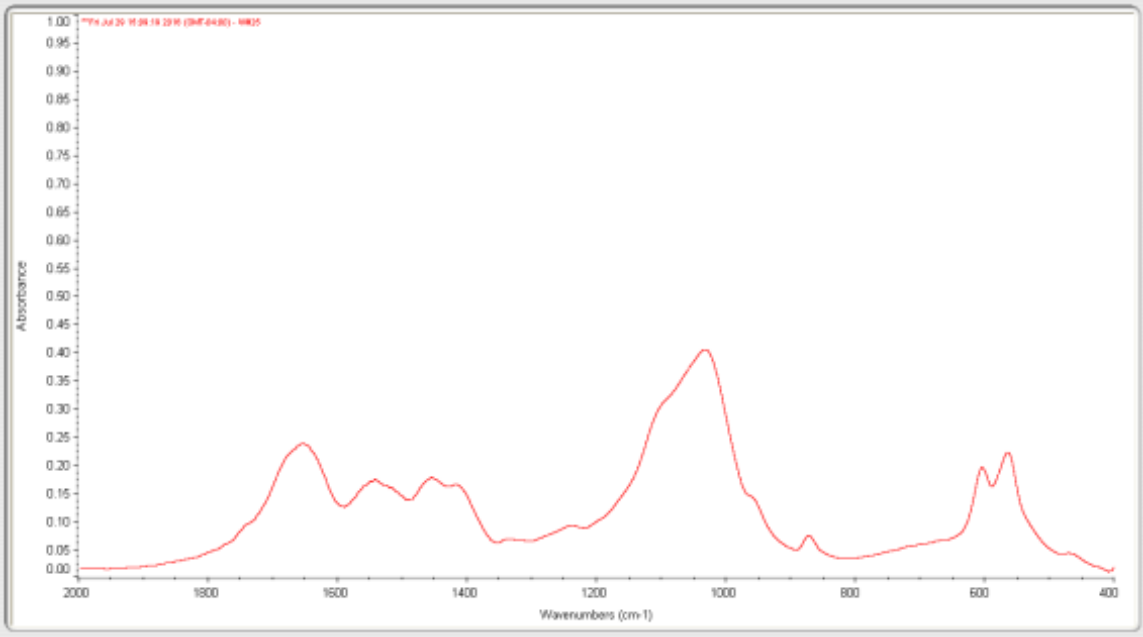

Figure 4.39. FTIR spectrum of burned, very wet bone number 25 (white heat line formed).

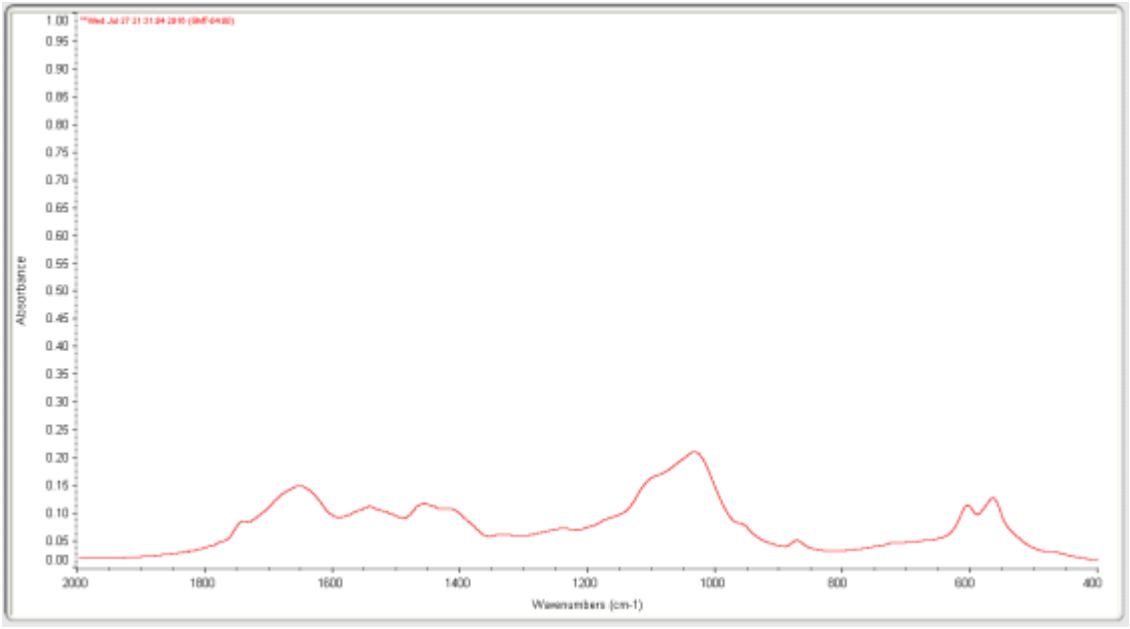

Figure 4.40. FTIR spectrum of burned, very wet bone number 15 (white heat line did not form).

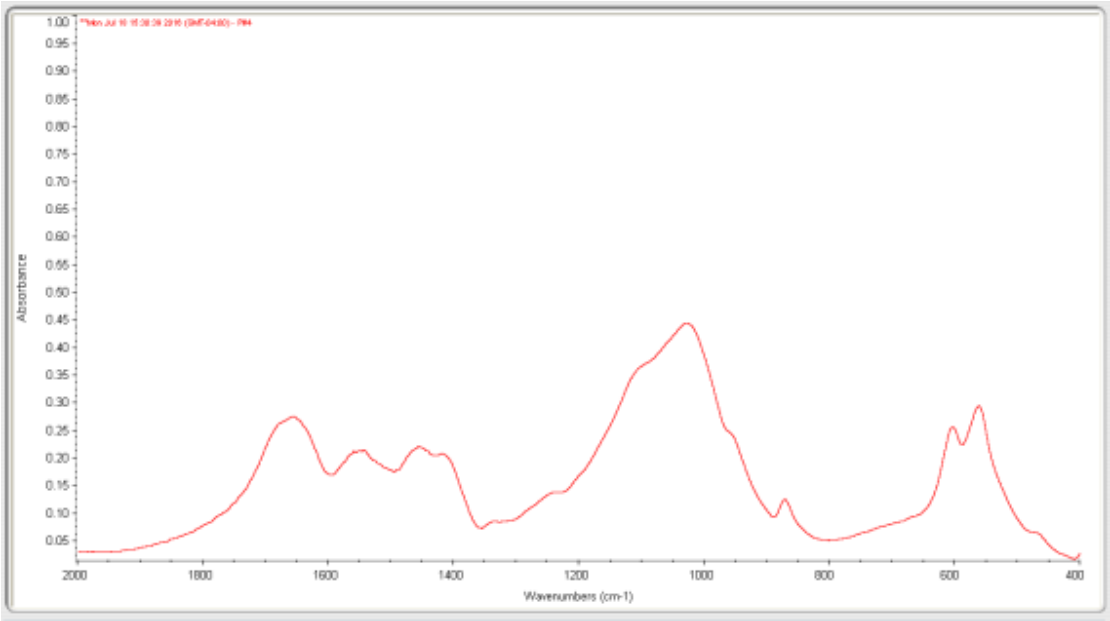

Figure 4.41. FTIR spectrum of burned, partially wet bone number 4 (white heat line did not form).

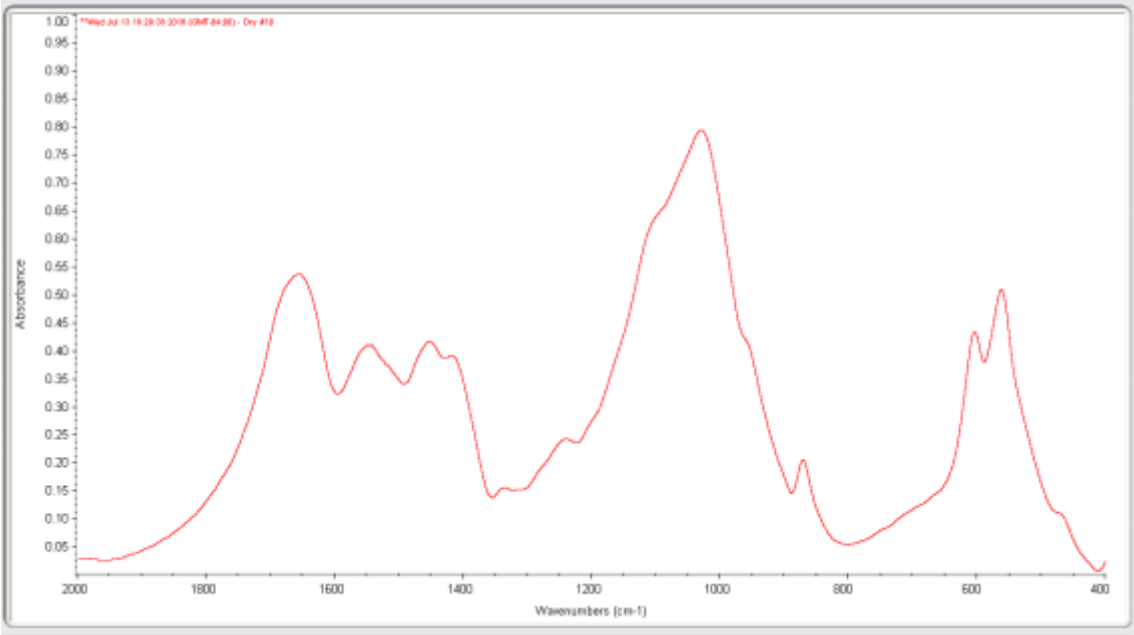

Figure 4.42. Spectrum of burned, dry bone number 10 (white heat line did not form).

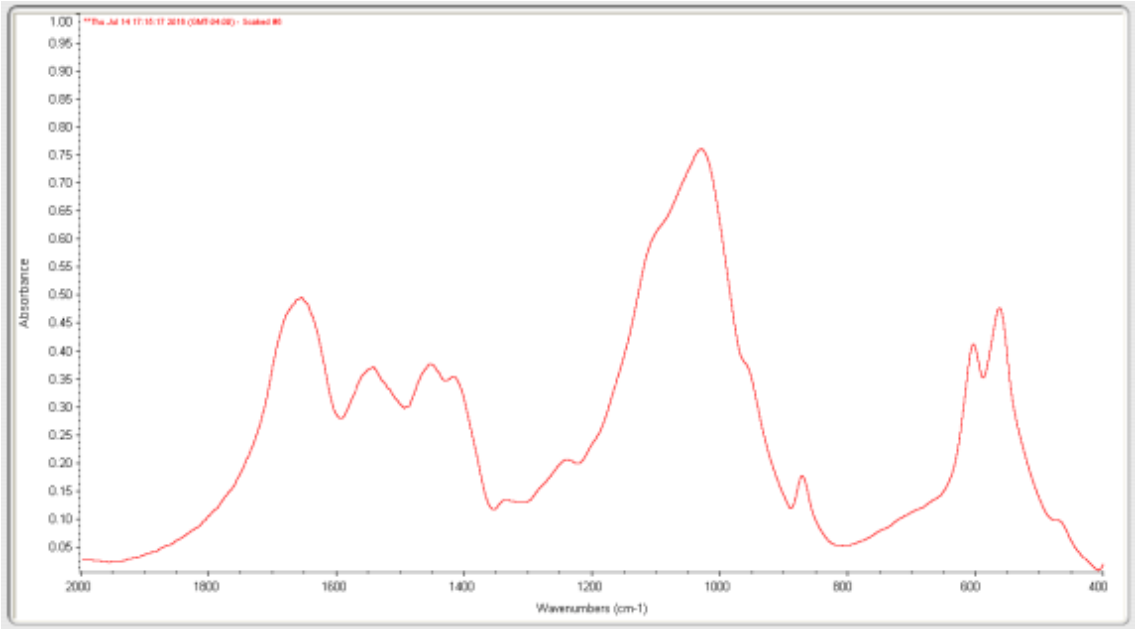

Figure 4.43. FTIR spectrum of burned, soaked bone number 6 (white heat line did not form).

CHAPTER 5: DISCUSSION

The present research examined the composition of white heat lines that may form on burned bone. Through the use of FTIR, it was determined that white heat lines contain CO_3, PO_4, and amide I, although their spectral peak heights vary between sample groups. These results do not fully support the hypothesis presented at the beginning of this project that a white heat line forms from inorganic minerals deposited on the bone's surface, resulting from the evaporation of moisture and the incineration of organic material. However, the presence of amide I may result from the inadvertent inclusion of thermally unaltered bone in the ground bone samples, and therefore, may not solely represent the composition of white heat lines.

Contrary to the hypothesis, amide I was found to make up part of the composition for all bone sampled from areas of white heat lines that formed, regardless of the bone's physical condition prior to burning, indicating that this thermal signature does not form from a total incineration of organic material. While amide I was present in all white heat line samples, the intensity varied depending on the bone sample group. For the very wet bones, while still present, the intensity of amide I decreased between the unburned controls ($\bar{x} = 0.259$) and the white heat lines that formed on the burned, experimental bones ($\bar{x} = 0.158$). The opposite is true of the fleshed bone samples, as the intensity of amide I increased between the unburned controls ($\bar{x} = 0.224$) and the burned experimental bones that developed a white heat line ($\bar{x} = 0.243$).

A similar pattern exists for the intensities of CO_3 and PO_4. While all of the white heat lines that formed were composed, in part, of these two minerals, the intensity for each varied between the fleshed and very wet bone samples. The very wet samples exhibited a relative decrease of both CO_3 and PO_4 between the unburned controls ($\bar{x}$ = 0.200, 0.480) and the burned experimental bones that developed a white heat line ($\bar{x}$ = 0.117, 0.245), contradicting the hypothesis. However, among the fleshed bone samples that developed a white heat line, the intensity of CO_3 and PO_4 increased from the unburned controls ($\bar{x}$ = 0.162, 0.293) to the burned experimental samples ($\bar{x}$ = 0.175, 0.316), supporting in part the hypothesis that a white heat line forms from inorganic minerals deposited on the bone's surface. Given these differences present between the fleshed and very wet bone samples, no definitive statement can be made for the composition of white heat lines.

In the present study, the white heat lines appeared on both fleshed and very wet bones and only formed on the outer surface of the bone. For both bone sample groups, the white heat lines appear to form superficially, as they measure approximately 1.5 mm in depth and do not penetrate deeply into the bone's surface. The bone samples taken of the white heat lines revealed bone underneath that did not appear to be thermally altered. For both the fleshed and very wet burned bones, the amide I content attributed to the white heat lines may instead originate from the organic content of the underlying unaffected bone. If so, the white heat lines that formed on fleshed bone may be an area of enriched mineral content relative to the nearby bone.

Within the fleshed sample group, which consisted of both sheep and pig metapodials, the eight bones to develop a white heat line were all pig. Aerssens *et al.*, (1998) researched interspecies differences in bone composition and found that, on average, pig cortical bone has a greater overall amount of proteins (124.6 µg/mg) than that of sheep (120.1 µg/mg). The authors divided this total amount into collagenous and non-collagenous proteins. For the collagenous proteins, which include amide I, sheep bone (25.9 µg/mg) contains a greater amount than pig bone (22.8 µg/mg). However, the opposite is true of the non-collagenous proteins, as they are present in a greater amount in the pig bone (101.8 µg/mg) than sheep bone (94.2 µg/mg). For the present study, the spectral peak heights of amide I, from proteins found in type I collagen, represent the intensity of collagenous proteins present. Since white heat lines only formed on the fleshed pig bone tested and not the sheep, this suggests that the amount of non-collagenous proteins or perhaps the total amount of proteins present in a bone may affect the formation of this thermal signature. A white heat line may be more likely to form with higher amounts of non-collagenous proteins present in the bone, or an overall greater amount of both types of proteins.

The greater amount of non-collagenous proteins present in both the pig and sheep bone, in comparison to the amount of collagenous proteins, may also explain why the spectral peak heights of amide I for the fleshed bones in the present study are lower than that of the non-fleshed bone (very wet, partially wet, dry, soaked). The non-collagenous proteins were not represented by the spectral peak heights measured for amide I.

An additional factor that may contribute to the formation of a white heat line is a bone's fat content. In the present study, white heat lines did not form on the partially wet, dry, and soaked experimental burned bones. All of the bones in these three sample groups were in Weathering Stage 0 following Behrensmeyer (1978) for bone surfaces did not display cracking, flaking, or sun bleaching due to subaerial weathering after undergoing decomposition in a forested environment. Although bone surfaces did not exhibit these physical modifications, it is possible that the weathering process had begun to affect the bones, but was not yet visible. Behrensmeyer (1978:153) defines weathering as "the process by which the original microscopic organic and inorganic components of a bone are separated from each other and destroyed by physical and chemical agents operating on the bone in situ, either on the surface or within the soil zone". The physical effects of subaerial weathering on bone include the loss of organic material (Behrensmeyer 1978; Brain 1967; Cutler *et al.*, 1999) and grease content (Junod and Pokines 2014). Prior to burning, the partially wet, dry, and soaked bones were noticeably less greasy to the touch and exhibited fewer areas of superficial fat leaching than that of the fleshed and very wet bones.

Among the burned experimental fleshed bones, differing fat content may also have contributed to white heat line formation on only the burned experimental pig metapodials and not the sheep. Field *et al.* (1974) investigated bone composition of several domestic animals, including pigs and sheep, using fresh cervical and lumbar vertebrae, ribs, and femora. The authors determined that fresh pig bone contained a larger percentage of fat, in relation to dry matter, than that of sheep bone. In their study,

fat composition for pig bone ranged from 17.61 to 27.86 percent across all of the bone types utilized. In contrast, the fat composition of sheep bone was lower, ranging from 9.35 to 22.75 percent of total osseous composition. Within each bone sample group (cervical vertebrae, lumbar vertebrae, ribs, and femora), the pig bones contained a higher fat percentage than that of their sheep counterparts. While Field *et al.* (1974) did not incorporate metapodials in their research, this trend suggests that the pig metapodials used in the present study contained a higher fat content than that of the sheep. Since white heat lines appeared on the fleshed pig bone and not the sheep, a white heat line may be more likely to form on fleshed bones with greater fat composition.

Output from the MANOVA test highlights the effect that bone's physical condition prior to burning (fleshed, very wet, partially wet, dry, soaked) has on the formation of a white heat line, as well as on the resulting spectral peak heights of CO_3, PO_4, and amide I. This variability of bone composition is seen in burned bones that did develop a white heat line and those that did not. The Bonferroni post-hoc test found statistically significant differences between most of the bone sample groups for the spectral peak heights of CO_3, PO_4, and amide I.

Results from the present study also support previous research in which the presence of a white heat line aids in determining bone's physical condition prior to burning (Keough 2013; Keough *et al.*, 2012, 2015; Symes *et al.*, 2008, 2014). For the present study, a Chi-Squared (X^2) Test of Independence confirms that a bone's physical condition prior to burning and white heat line formation are not independent, but rather a relationship exists between these two variables. Specifically, a Cramer's V value of

0.527 indicates that the relationship between bone's physical condition prior to burning (fleshed, very wet, partially wet, dry, soaked) and the formation of a white heat line is a strong association.

Previous research suggested that one may differentiate between bones burned fleshed or wet versus those burned while dry (Keough 2013; Keough *et al.*, 2012, 2015; Symes *et al.*, 2008, 2014). In the present study, white heat lines formed on fleshed and very wet bones, but not on the partially wet, dry, or soaked (although earlier research has not included the latter sample group). The development of this thermal signature on fleshed bone samples is in keeping with Symes *et al.* (2008a), who noted that a white heat line may form with fleshed burned remains, possibly occurring as the heat causes muscle and other soft tissues to retract, exposing the bone to the heat source. However, Symes *et al.* (2008a) made their observations while working with fully fleshed remains, and it is not apparent whether they also encountered bones that were burned while very wet but not fleshed. Since this thermal signature can also form on unfleshed bone, their reasoning does not explain how a white heat line manifests under other circumstances. Other researchers observed similar burn patterns in fully fleshed bodies, either fresh or in early decomposition, noting that a white heat line was not present when bone was burned in the absence of soft tissue (Keough *et al.*, 2012; Pope 2007; Symes *et al.*, 1999a).

The formation of a white heat line on both fleshed and very wet bone samples has been found previously (Keough 2013; Keough *et al.*, 2015). These studies found that distinct white heat lines formed on remains burned in early to advanced decompositional stages, with bone conditions ranging from fleshed or partially fleshed, to wet but lacking

extensive soft tissue protection. Results from the present study indicate that while this thermal signature may form on bones burned in either physical condition, it was found to occur more often on fleshed (50.0%) than on very wet bone (29.6%). Additionally, the white heat lines that formed on fleshed bone had, on average, greater maximum widths (8 mm) and extended along more of the bone's burned diaphyseal circumference (n=3 for both 50-75% and 75-100%) than those that formed on very wet bone (6.75 mm) (n=3 at less than 25%). Keough (2013) and Keough *et al.* (2015) report similar results: while white heat lines did form on partially fleshed remains or wet bone in advanced decomposition, they formed most often in fresh remains or during the early stages of decomposition when soft tissues, including muscular structures, were present.

The present study supports the conclusion of Keough *et al.* (2015) that fresh soft tissue, still adhering to the underlying bone, may be the most significant factor affecting whether a white heat line will form. This is in contrast to advanced decomposition, when the nature of degraded soft tissue and denatured periosteum may allow the tissue to burn away with less resistance, preventing the creation of this thermal signature. However, the appearance of a white heat line on very wet bone in the absence of external soft tissue, evidenced in the present study and in research conducted by both Keough (2013) and Keough *et al.* (2015), indicates that a bone's internal organic matter may also affect the formation of this thermal signature.

The present study examined the composition of white heat lines that form on burned bone. However, there are certain variables and limitations that may have affected the resulting findings. Due to difficulties in obtaining the osteological materials for this

investigation, including the number of bone samples and their requisite physical conditions, bone samples from four animal species were utilized. Ideally, in order to control for intrinsic and compositional differences, bone samples from only one animal species would be included in an experimental study.

Additionally, the use of animal models as human analogues has its own limitations. While it is common practice in experimental research due to the difficulties associated with acquiring and using human cadaveric material (Marceau 2007; Thompson 2003), one should be cautious before applying experimental results directly to situations involving human remains. Overall, animal models are useful in attempting to replicate, examine, and predict basic characteristics of heat-induced modifications in bone (Pope 2007). However, animal models cannot accurately answer questions specific to the human body. Their utility may be less useful, or even misleading, when applied at will to forensic casework because of their differential anatomy and morphology.

Another variable to consider is the use of a regulated burn, utilized in the present study, as opposed to an uncontrolled fire. Symes *et al.*, (2008a) stated that while most observations from controlled studies are also present in real-case scenarios, deviations from the normal burn pattern can occur in the former. Said deviations depend upon body orientation and limb positioning during burning, as well as the presence of obstructing material, such as debris covering a body, that shields portions of the body from burning and/or prevents the "pugilistic pose" from forming. Additional abnormalities may result from individual differences such as weight, muscle and fat composition, and pathological conditions.

The presence of a white heat line is an important source of information for forensic anthropological investigations of burned skeletal remains regarding the relative timing of burning. However, their chemical or physical composition has not been investigated, and limited research has been conducted to determine why or how white heat lines form. The present study assessed the chemical composition of this thermal signature using FTIR and found that it is comprised of CO_3, PO_4, and amide I. These findings build upon previous research, in which other authors suggest that this area of bone has undergone some dehydration and molecular alteration, resulting in a reduced organic component, due to its proximity to the heat source during a burning event (Pope 2007; Pope and Smith 2004; Symes *et al.,* 2008a). While a conclusive statement cannot be made about white heat line composition due to variations between bone samples in the present study, these initial results further the field's understanding of how fire and heat modify physical remains, specifically, with regards to the effect that bone's physical condition prior to burning has on the resulting heat-induced compositional changes. Additionally, assessing the composition of white heat lines, or in their absence the junction of unburned and charred bone, further delineates the chemical changes that bone undergoes during the beginning and middle stages of a thermal event.

Future FTIR studies could assess the other vibrational bands of CO_3, PO_4, and amide that are present in bone. While the present study utilized the amide I and ν3 vibrational bands for CO_3 and PO_4, other researchers have used the amide II (Boskey and Camacho 2007; Paschalis *et al.,* 1997, 2001), ν2 CO_3 (Boskey and Camacho 2007; Camacho *et al.,* 1995; Gourion-Arsquaud *et al.,* 2013; Paschalis *et al.,* 1996; Pienkowski

et al., 1997; Stiner *et al.,* 1995, 2001; Turunen *et al.,* 2010, 2014), ν1ν3 PO_4 (Alvarez-Llortet *et al.,* 2006; Boskey and Camacho 2007; Camacho *et al.,* 1995; Paschalis *et al.,* 1996; Pienkowski *et al.,* 1997; Turunen *et al.,* 2010, 2014), and the ν4 PO_4 vibrational bands (Lebon *et al.,* 2010; Piga *et al.,* 2016) to analyze bone composition. These other vibrational bands should be assessed to determine if additional amounts of CO_3, PO_4, and amide, those not represented by the spectral peak heights measured for in the present study, make up the composition of white heat lines.

CHAPTER 6: CONCLUSION

Forensic anthropologists are frequently confronted with the need to interpret burned skeletal remains. Fire can be the cause of death, through either criminal or accidental means, or a method used to conceal a crime and destroy physical evidence (Symes et al., 2008a). The presence of burned bone raises additional analytical concerns as to the sequence of events leading from the time of death until discovery, including the relative timing of the thermal event and physical condition of the body prior to burning (Ellingham *et al*, 2015; Keough 2013; Keough *et al*., 2015; Ubelaker 2009). Regardless of the nature of the thermal event, bodies exposed to fire and heat undergo a wide array of postmortem effects and may become heavily fractured, fragile, and discolored (Bohnert *et al.*, 1998; Christensen 2002; Pope 2007; Pope and Smith 2004; Porta *et al.*, 2013).

The burning process of soft and hard tissues proceeds in a consistent, identifiable, and predictable pattern (Adelson 1955; Bass 1984; Bohnert 1998; DeHaan 2012; Icove and DeHaan 2004; Pope 2007; Pope and Smith 2004). Combustion of physical remains starts with the superficial soft tissue layers, beginning with the skin and progressing inwards to the subcutaneous fat, muscles, and other deeper tissue layers, and lastly the underlying bone as the thermal event continues (Pope 2007). During a thermal event, the gradual shrinkage and destruction of soft tissues causes bone to undergo a series of visible color changes as it dehydrates and becomes exposed to the heat source (Buikstra and Swegle 1989; Nicholson 1993; Pope 2007; Pope and Smith 2004; Shipman *et al.*,

1984). Heat-induced color changes occur in set stages as the burning event progresses and the heat exposure continues to modify and reduce bone's organic material (Bonucci and Graziani 1975). Symes *et al.* (2008a) categorize this color change as initial unaltered bone that progresses to a white heat line, heat border, charring, and lastly, calcination. An opaque white heat line, the first area of heat-modified bone, is an occasionally occurring thermal signature that, when it forms, is the area of initial transition from unaltered to thermally altered bone (Keough 2013; Keough *et al.*, 2012, 2015; Symes *et al*., 1999a, 1999b, 2008a, 2014a).

Recent studies indicate that the formation of a white heat line aids in determining a bone's physical condition prior to burning (Keough 2013; Keough *et al.*, 2012, 2015; Symes *et al.*, 2008, 2014). Notably, experiments suggest that one may differentiate between bones burned fleshed (fresh bones encased in adhering soft tissue) or wet (defleshed shortly before burning, greasy) versus dry (defleshed and degreased) (Keough *et al.*, 2012; Keough 2013; Keough *et al.* 2015; Pope 2007; Symes *et al.*, 1999a). Knowledge of a bone's prior physical condition contributes to anthropological examinations of burned skeletonized remains and interpretation of the sequence of events leading to the thermal modification (Ellingham *et al.*, 2015; Ubelaker 2009). However, while the relationship between bone's physical condition prior to burning and white heat line formation has been studied, there is a lack of research concerning the chemical or physical composition of this thermal signature.

The present study investigated the effects of soft tissue and the retention of bone's organic material, including naturally-occurring grease and water, on the development and

appearance of a white heat line for bones thermally altered by burning. Skeletal remains for the present project consisted of 108 isolated long bones from four animal species: white-tailed deer, elk, sheep, and pig. The purpose of the present investigation was to assess the chemical composition of white heat lines that form on burned bone using FTIR and by analyzing the spectral peak heights of the ν3 CO_3 (1415 cm^{-1}), ν3 PO_4 (1035 cm^{-1}), and amide I (1660 cm^{-1}) vibrational bands.

For both the fleshed and very wet samples, the shape and width of white heat lines varied among the bones. Generally, the white heat lines that formed on the fleshed samples were sharply defined, with a greater contrast to the surrounding bone, and exhibited a more uniform width. Conversely, the white heat lines that formed on the very wet samples were more irregular in shape, variable in their width per bone, and often presented with an adjacent heat border. For both bone sample groups, the white heat lines appear to form superficially, measuring approximately 1.5 mm in depth, and do not penetrate deeply into the bone's surface. After the white heat lines were ground and removed for FTIR analysis, the underlying bone was light ivory in color, likely indicating that this area had not been significantly modified by the heat (Mayne Correia, 1997).

Results from the Chi-Squared (X^2) test of independence confirm that a bone's physical condition prior to burning and white heat line formation are not independent, but rather, that a relationship exists between these two variables. This statistical analysis supports findings from previous research in which the presence of a white heat line aids in determining bone's physical condition prior to burning (Keough *et al.*, 2012; Keough 2013; Keough *et al.* 2015; Pope 2007; Symes *et al.*, 1999a). Specifically, one can

differentiate between bones burned fleshed or very wet, versus those burned partially wet, dry, or soaked (although earlier research does not include the last sample group).

Results from the present study indicate that while this thermal signature may form on bones burned in either physical condition, white heat lines formed more often on fleshed than on very wet bone. For both fleshed and very wet bone, white heat lines consisted of CO_3, PO_4, and amide I, although their spectral peak heights varied between the two sample groups. White heat lines that formed on fleshed bone had an increased intensity of CO_3, PO_4, and amide I in comparison to their unburned controls. Conversely, white heat lines that formed on very wet bone were composed of a decreased intensity of CO_3, PO_4, and amide I in comparison to their unburned controls. The white heat lines that formed on fleshed bone also exhibit larger maximum widths and cover more of the bone's burned diaphyseal circumference than those that developed on very wet bone. Statistical analysis shows that bone's physical condition prior to burning (fleshed, very wet, partially wet, dry, soaked) affects not only the formation of a white heat line, but also the resulting spectral peak heights of CO_3, PO_4, and amide I. This variability of bone composition is apparent through the FTIR analysis of burned bones that did develop a white heat line and those that did not.

At the beginning of the present study, it was hypothesized that a white heat line forms from inorganic minerals deposited on or near the bone's surface, resulting from the evaporation of moisture and the incineration of organic material. However, the results do not fully support this hypothesis. Given the differing spectral peak heights of CO_3, PO_4, and amide I present between the fleshed and very wet bone samples that developed this

thermal signature, no definitive statement can be made for the origin or composition of white heat lines at this time.

There are certain variables and limitations that may have affected the resulting data. Due to difficulties in obtaining the osteological materials for the present investigation, including the number of bone samples and their requisite physical conditions, bone samples from four nonhuman animal species were utilized. Ideally, bone samples from only one animal species would be included in an experimental study in order to control for species-dependent compositional differences. Additionally, one should be cautious before applying experimental results directly to situations involving human remains for animal models cannot accurately answer questions specific to the human body. Their utility may be reduced, or even misleading, when applied at will to forensic casework because of their differential anatomy and morphology.

An additional variable to consider is the use of a regulated burn instead of an uncontrolled fire. Symes *et al.*, (2008a) state that while most observations from controlled studies are also present in real-case scenarios, deviations from the normal burn pattern can occur in the former.

The present study is the first to investigate the chemical composition of white heat lines that form on bone thermally altered by burning. These findings further our knowledge of how fire and heat modify physical remains with regards to the effect that bone's physical condition prior to burning, including the presence of soft tissue and naturally-occurring organic material, has on the development and appearance of a white heat line and the resulting heat-induced compositional changes. The presence of this

thermal signature is utilized in forensic anthropological investigations of thermally altered remains regarding the relative timing of burning and yet limited research has been conducted to determine why or how it forms. Assessing the composition of white heat lines, or in their absence the junction of unburned and charred bone, further delineates the chemical changes that bone undergoes during the beginning and middle stages of a thermal event.

Continuing thermal alteration research is needed in order to build upon the initial results gained from the present study. Specifically, further research is necessary to determine compositional differences between white heat lines that form on fleshed versus very wet burned bone. Future studies should also investigate a bone's fat content as a possible contributing factor to the formation of a white heat line. Furthermore, additional FTIR research is needed to assess the other vibrational bands of CO_3, PO_4, and amide that are present in bone. Analyzing these added vibrational bands will enable a more thorough determination of the mineral and organic content of this thermal signature relative to thermally unaltered bone and burned bone that do not develop a white heat line.

APPENDIX A

Figure A.1. Fleshed sheep metapodials burning on the 55-gallon drum.

Figure A.2. Fleshed pig metapodials burning on the 55-gallon drum.

Figure A.3. Very wet elk femora (third group) burning on the 55-gallon drum.

Figure A.4. Partially wet deer metapodials (second group) burning on the 55-gallon drum.

Figure A.5. Dry deer metapodials burning on the 55-gallon drum.

LIST OF JOURNAL ABBREVIATIONS

Am J Anat	American Journal of Anatomy
Am J Foren Med Path	American Journal of Forensic Medicine and Pathology
Am J Phys Anthropol	American Journal of Physical Anthropology
Anthrop Anz	Anthropologischer Anzeiger
Appl Geochem	Applied Geochemistry
Appl Spectrosc	Applied Spectroscopy
Biomed Environ Sci	Biomedical and Environmental Sciences
Bull Soc Chim Fr	Bulletin de la Société Chimique de France
Calcified Tissue Int	Calcified Tissue International
Ceram Int	Ceramics International
Clin Orthop Relat Res	Clinical Orthopaedics and Related Research
Cornell Vet	Cornell Veterinarian
Forensic Sci Int	Forensic Science International
Geoarchaeology	Geoarchaeology – An International Journal
Homo	HOMO-Journal of Comparative Human Biology
Int J Legal Med	International Journal of Legal Medicine
Int J Spectroscopy	International Journal of Spectroscopy
Int J Osteoarchaeol	International Journal of Osteoarchaeology
J Anim Sci	Journal of Animal Science

J Archaeol Sci	Journal of Archaeological Science
J Bone Miner Res	Journal of Bone and Mineral Research
J Biomech	Journal of Biomechanics
J Biomed Opt	Journal of Biomedical Optics
J Bone Joint Surg	Journal of Bone and Joint Surgery
J Cell Sci	Journal of Cell Science
J Crim Law Criminol	Journal of Criminal Law, Criminology, and Police Studies
J Dent Res	Journal of Dental Research
J Field Archaeol	Journal of Field Archaeology
J Forensic Sci	Journal of Forensic Sciences
J Hard Tissue Biol	Journal of Hard Tissue Biology
J Hum Evol	Journal of Human Evolution
J Inorg Biochem	Journal of Inorganic Biochemistry
J Mater Eng Perform	Journal of Materials Engineering and Performance
J Mater Sci	Journal of Materials Science
J Med Entomol	Journal of Medical Entomology
Mater Sci Eng	Materials, Science, and Engineering
Meas Sci Technol	Measurement Science and Technology
Mediterr Archaeol Ar	Mediterranean Archaeology and Archaeometry
Med Sci Law	Medicine, Science, and the Law
Metab Bone Dis Relat	Metabolic Bone Disease and Related Research
Nat Mater	Nature Materials

Osteoporosis Int	Osteoporosis International
Palaeogeogr Palaeocl	Palaeogeography, Palaeoclimatology, Palaeoecology
Rev Chim-Bucharest	Revista De Chimie
S Afr J Sci	South African Journal of Science
Sci Justice	Science and Justice
Sci Rep	Science Reports
Tex J Sci	Texas Journal of Science
Yearb Phys Anthropol	Yearbook of Physical Anthropology

REFERENCES

Abdel-Maksoud G. 2010. Comparison between the properties of "accelerated-aged" bones and archaeological bones. Mediterr Archaeol Ar 10(1):89.

Absolonová K, Dobisiková M, Beran M, Zocová J, Velemínský P. 2012. The temperature of cremation and its effect on the microstructure of the human rib compact bone. Anthrop Anz 69(4):439-460.

Adelson L. 1955. Role of the pathologist in arson investigation. J Crim Law Criminol 45(6):760-768.

Aerssens J, Boonen S, Lowet G, Dequeker J. 1998. Interspecies differences in bone composition, density, and quality: Potential implications for in vivo bone research. Endocrinology 139(2):663-670.

Alunni V, Grevin G, Buchet L, Quatrehomme G. 2014. Forensic aspect of cremations on wooden pyre. Forensic Sci Int 241:167-172.

Álvarez-Lloret P, Rodríguez-Navarro AB, Romanek CS, Gaines KF, Congdon YJ. 2006. Quantitative analysis of bone mineral using FTIR. Macla 6:45-47.

Asmussen B. 2009. Intentional or incidental thermal modification? Analysing site occupation via burned bone. J Archaeol Sci 36(2):528-536.

Baby RS. 1954. Hopewell cremation practices. The Ohio Historical Society Papers in Archaeology 1:1–7.

Bass WM. 1984. Is it possible to consume a body completely in a fire? In Rathbun T, Buikstra J, editors. Human Identification: Case Studies in Forensic Anthropology. Springfield (IL): Charles C Thomas. pp 159-167.

Beasley MM, Bartelink EJ, Taylor L, Miller RM. 2014. Comparison of transmission FTIR, ATR, and DRIFT spectra: implications for assessment of bone bioapatite diagenesis. J Archaeol Sci 46(1):16-22.

Behrensmeyer AK. 1978. Taphonomic and ecologic information from bone weathering. Paleobiology 4(2):150-162.

Bell LS, Cox G, Sealy JC. 2001. Determining life history trajectories using bone density fractionation and stable light isotope analysis: a new approach. Am J Phys Anthrop 116(1):66–79.

Bennett JL. 1999. Thermal alteration of buried bone. J Archaeol Sci 26(1):1-8.

Bigi A, Cojazzi G, Panzavolta S, Ripamonti A, Roveri N, Romanello M, Suarez KN, Moro L. 1997. Chemical and structural characterization of the mineral phase from cortical and trabecular bone. J Inorg Biochem 68(1):45-51.

Binford LR. 1963. An analysis of cremations from three Michigan sites. Wisconsin Archaeologist 44(2):98–110.

Bohnert M, Rost T, Pollak S. 1998. The degree of destruction of human bodies in relation to the duration of the fire. Forensic Sci Int 95(1):11-21.

Bonucci E and Graziani G. 1975. Comparative thermogravimetric X-ray diffraction and electron microscope investigations of burnt bones from recent, ancient and prehistoric age. Atti della accademia Nazionale dei Lincei, Rendiconti, classe di scienze fisiche, matematiche e naturali 59: 517-32.

Boskey A, Mendelsohn R. 2005. Infrared analysis of bone in health and disease. J Biomed Opt 10(3): 0311021-0311029.

Boskey A, Camacho NP. 2007. FT-IR imaging of native and tissue-engineered bone and cartilage. Biomaterials 28(15):2465-2478.

Boyde A. 1980. Electron microscopy of the mineralizing front. Metab Bone Dis Relat 2(Suppl):69–78.

Bradtmiller B, Buikstra JE. 1984. Effects of burning on human bone microstructure: a preliminary study. J Forensic Sci 29(2):535-540.

Brain CK. 1967. Bone weathering and the problem of bone pseudo-tools. S Afr J Sci 63(3):97-99.

Buikstra JE, Swegle M. 1989. Bone modification due to burning: experimental evidence. In: Bonnichsen R, Sorg M, editors. Bone Modification. Orno: Center for the Study of the First Americans. pp 247-258.

Butler DH, Dawson PC. 2013. Accessing hunter-gatherer site structures using Fourier transform infrared spectroscopy: applications at a Taltheilei settlement in the Canadian sub-Arctic. J Archaeol Sci 40(4):1731-1742.

Cain CR. 2005. Using burned animal bone to look at Middle Stone Age occupation and behavior. J Archaeol Sci 32(6):873-884.

Carden A, Morris MD. 2000. Application of vibration spectroscopy to the study of mineralized tissues (review). J Biomed Opt 5(3):259-268.

Christensen AM. 2002. Experiments in the combustibility of the human body. J Forensic Sci 47(3):466-470.

Civjan S, Selting WJ, de Simon LB, Battistone GC, Grower MF. 1971. Characterization of osseous tissues by thermogravimetric and physical techniques. J Dent Res 51(2):539–542

Cordner SM, Woodford N, Bassed R. 2011. Forensic aspects of the 2009 Victorian Bushfires disaster. Forensic Sci Int 205(1):2-7.

Crow DM, Glassman RM. 1996. Standardization model for describing the extent of burn injury to human remains. J Forensic Sci 41(1):152-154.

Currey JD. 1960. Differences in the blood-supply of bone of different histological types. J Cell Sci 3(55):351–370.

Currey JD. 2002. The structure of bone tissue. In: Currey JD, editor. Bones: Structure and Mechanics. Princeton (NJ):Princeton University Press. pp 3-26.l

Currey JD. 2003. The many adaptations of bone. J Biomech 36(10):1487–95.

de Ricqlès A. 1977. Recherches paleohistologiques sur les os longs des t´etra-podes VII (deuxi`eme partie, fin). Annales de paleontology 63:133–60.

de Gruchy S, Rogers TL. 2002. Identifying chop marks on cremated bone: a preliminary study. J Forensic Sci 47(5): 1-4.

Cutler AH, Behrensmeyer AK, Chapman RE. 1999. Environmental information in a recent bone assemblage: roles of taphonomic processes and ecological change. Palaeogeogr Palaeocl 149(1-4): 359-372.

DeHaan JD. 1997. A case of not-so-spontaneous human combustion. Fire and Arson Investigator 47(4): 14-16.

DeHaan J. 2006. Fire-Related Deaths and Injuries. In: DeHaan, J. editor. Kirk's Fire Investigation (6th ed.). Upper Saddle River (NJ): Prentice Hall Inc. pp. 363-393.

DeHaan JD. 2012. Sustained combustion of bodies: Some observations. J Forensic Sci 57(6):1578-1584.

DeHaan JD and Nurbakhsh S. 2001. Sustained combustion of an animal carcass and its implications for the consumption of human bodies in fire. J Forensic Sci 46(5):1076-1081.

DeHaan J, Campbell S, Nurbakhsh S. 1999. Combustion of animal fat and its implications for the consumption of human bodies in fires. Sci Justice 39(1):27-38.

Dekeirsschieter J, Verheggen FJ, Gohy M, Hubrecht F, Bourguignon L, Lognay G, Haubruge E. 2009. Cadaveric volatile organic compounds released by decaying pig carcasses (Sus domesticus L.) in different biotopes. Forensic Sci Int 189(1):46-53.

D'Elia M, Gianfrate G, Quarta G, Giotta L, Giancane G, Calcagnile L. 2007. Evaluation of possible contamination in the 14C analysis of bone samples by FTIR spectroscopy. Radiocarbon 49(2):201-210.

Devlin JB, Kroman AM, Symes SA. 2006. Time, temperature, and color: Heat intensity vs. exposure duration. Part I: Macroscopic influence on burned bone. Proceedings of the American Academy of Forensic Sciences 12:311-312.

Dirkmaat DC, Cabo LL, Ousley SD, Symes SA. 2008. New perspectives in forensic anthropology. Yearb Phys Anthropol 51:33-52.

Dirkmaat DC, Olson GO, Klales AR, Getz S. 2012. The role of forensic anthropology in the recovery and interpretation of the fatal-fire victim. In: Dirkmaat DC, editor. A Companion to Forensic Anthropology (1st ed.). Malden, MA: Wiley-Blackwell. pp 113-135.

Donnelly E. 2011. Methods for assessing bone quality: a review. Clin Orthop Relat Res 469(8):2128-2138.

Dunlop JM. 1978. Traffic light discoloration in cremated bones. Med Sci Law 18(3):163–173.

Eckert WG, James S, Katchis S. 1988. Investigation of cremations and severely burned bodies. Am J Foren Med Path 9(3): 188-200.

Ellingham ST, Thompson TJ, Islam M, Taylor G. 2015. Estimating temperature exposure of burnt bone: a methodological review. Sci Justice 55(3):181-188.

Ellingham ST, Thompson TJ, Islam M. 2016. The effect of soft tissue on temperature estimation from burnt bone using Fourier transform infrared spectroscopy. J Forensic Sci 61(1):153-159.

Enlow DH and Brown SO. 1956. A comparative histological study of fossil and recent bone tissues. Part I. Tex J Sci 8:405–443.

Enlow DH and Brown SO. 1957. A comparative histological study of fossil and recent bone tissues. Part II. Tex J Sci 9(2):186–204.

Enow DH and Brown SO. 1958. A comparative histological study of fossil and recent bone tissues. Part III. Tex J of Sci 10(2):187–230.

Enlow DH. 1962. Functions of the Haversian system. Am J Anat 110(3):269-305.

Etok SE, Valsami-Jones E, Wess TJ, Hiller JC, Maxwell CA, Rogers KD, Manning DAC, White ML, Lopez-Capel E, Collins MJ, Buckley M, Penkman KEH, Woodgate SL. 2007. Structural and chemical changes of thermally treated bone apatite. J Mater Sci 42(23):9807-9816.

Fairgrieve SI. 2008. Forensic Cremation Recovery and Analysis. Boca Raton, FL: CRC Press.

Farlay D and Boivin G. 2012. Bone mineral quality. In: Dionyssiotis Y, editor. Osteoporosis. InTech Open Access Publisher pp 3-32.

Field RA, Riley ML, Mello FC, Corbridge JH, Kotula AW. 1974. Bone composition in cattle, pigs, sheep and poultry. J Anim Sci 39(3):493-9.

Figueiredo M, Fernando A, Martins G, Freitas J, Judas F, Figueiredo H. 2010. Effect of the calcination temperature on the composition and microstructure of hydroxyapatite derived from human and animal bone. Ceram Int 36(8):2383-2393.

Fojas CC, Rainwater W, Symes SA. 2011. Using spatial analysis to recognize normal and abnormal patterns in burned bodies. Proceedings of the American Academy of Forensic Sciences 17:367-368.

Forbes SL, Dent BB, Stuart BH. 2005a. The effect of soil type on adipocere formation. Forensic Sci Int 154(1):35-43.

Forbes SL, Stuart BH, Dent BB. 2005b. The effect of the burial environment on adipocere formation. Forensic Sci Int 54(1):24-34.

Forbes SL, Stuart BH, Dent BB. 2005c. The effect of the method of burial on adipocere formation. Forensic Sci Int 154(1):44-52.

France DL, Griffin TJ, Swanburg JG, Lindemann JW, Davenport GC, Trammell V, Armbrust CT, Kondratieff B, Nelson A, Castellano K, Hopkins D. 1992. A multidisciplinary approach to the detection of clandestine graves. J Forensic Sci 37 (6):1445–1458.

Gadaleta SJ, Paschalis EP, Betts F, Mendelsohn R, Boskey AL. 1996. Fourier transform infrared spectroscopy of the solution-mediated conversion of amorphous calcium phosphate to hydroxyapatite: new correlations between x-ray diffraction and infrared data. Calcified Tissue Int 58(1):9-16.

Gamsjäger S, Zoehrer R, Roschger P, Fratzl P, Klaushofer K, Mendelsohn R, Paschalis EP. 2009. Vibrational spectroscopy in biomedical science: bone. Proceedings of the International Society for Optics and Photonics, Optics in Bone Biology and Diagnostics, February 18, San Jose.

Gilchrist R, Mytum HC. 1986. Experimental archaeology and burnt animal bone from archaeological sites. Circaea 4(1):29-38.

Gonçalves D, Thompson TJ, Cunha E. 2011. Implications of heat-induced changes in bone on the interpretation of funerary behavior and practice. J Archaeol Sci 38(6):1308-1313.

Gourion-Arsiquaud S, Lukashova L, Power J, Loveridge N, Reeve J, Boskey AL. 2013. Fourier transform infrared imaging of femoral neck bone: reduced heterogeneity of miner-to-matrix and carbonate-to-phosphate and more variable crystallinity in treatment-naïve fracture cases compared with fracture-free controls. J Bone Miner Res 28(1):150-1161.

Grassberger M, Frank C. 2004. Initial study of arthropod succession on pig carrion in a central European urban habitat. J Med Entomol 41(3):511-523.

Griffiths P, de Haseth J. 2007. Introduction to vibrational spectroscopy. In: Griffiths P, Haseth J, editors. Fourier Transform Infrared Spectroscopy (2nd ed.). Hoboken (NJ): Wiley-Interscience. pp 1-18.

Grupe G, Hummel S. 1991. Trace element studies on experimentally cremated bone. I. Alteration of the chemical composition at high temperatures. J Archaeol Sci 18(2):177-186.

Han YM, Peteet D, Arimoto R, Cao JJ, An ZS, Sritrairat S, Yan BZ. 2016. Climate and fuel controls on North American paleofires: flaming and smoldering in the Late-glacial-Holocene transition. Sci Rep 6(20719):1-8.

Hanson M and Cain CR. 2007. Examining histology to identify burned bone. J Archaeol Sci 34(11): 1902-1913.

Harbeck M, Schleuder R, Schneider J, Wiechmann I, Schmahl WW, Grupe G. 2011. Research potential and limitations of trace analyses of cremated remains. Forensic Sci Int 204(1-3): 191-200.

Herrmann B. 1970. Anthropologische bearbeitung der leichenbränden von Berlin-Rudow. Ausgrabungen in Berlin 1:61-71.

Herrmann B. 1977. On histological investigations of cremated human remains. J Hum Evol 6(2):101-103.

Herrmann N, Bennett J. 1999. The differentiation of traumatic and heat-related fractures in burned bone. J Forensic Sci 44(3):461-469.

Hillier ML, Bell LS. 2007. Differentiating human bone from animal bone: A review of histological methods. J Forensic Sci 52(2):249-263.

Holck P. 2005. Cremated bones. Anatomical Institute, University of Oslo, Oslo, pp. 113-119.

Holden JL, Phakey PP, Clement JG. 1995a. Scanning electron microscope observations of heat-treated human bone. Forensic Sci Int 74(1-2):29-45.

Holden JL, Phakey PP, Clement JG. 1995b. Scanning electron microscope observations of incinerated human femoral bone: a case study. Forensic Sci Int 74(1):17-28.

Howes JM, Stuary BH, Thomas PS, Raja S, O'Brien C. 2012. An investigation of model forensic bone in soil environments studied using infrared spectroscopy. J Forensic Sci 57(5):1161-1167.

Icove DJ and DeHaan JD. 2004. Forensic Fire Scene Reconstruction. Upper Saddle River (NJ):Prentice Hall Inc.

Isaksson H, Turunen MJ, Rieppo L, Saarakkala S, Tamminen IS, Rieppo J, Kröger H, Jurvelin JS. 2010. Infrared spectroscopy indicates altered bone turnover and remodeling activity in renal osteodystrophy. J Bone Miner Res 25(6):1360-1366.

Jowsey J. 1968. Age and species differences in bone. Cornell Vet 58(Suppl): 74-94.

Junod CA, Pokines JT. 2014. Subaerial weathering. In: Pokines JT, Symes SA, editors. Manual of Forensic Taphonomy. Boca Raton (FL): CRC Press. pp 287-314.

Kennedy KAR. 1996. The wrong urn: Commingling of cremains in mortuary practices. J Forensic Sci 41(4):689-692.

Keough N. 2013. Skeletal Changes after Post-Mortem Exposure to Fire as an Indicator of Decomposition Stage. (Unpublished Doctoral dissertation). University of Pretoria, Pretoria, South Africa.

Keough N, Colman K, L'Abbé EN, Symes SA, Cabo L. 2012. Distinguishing features of thermal destruction on fleshed, wet and dry remains. Proceedings of the American Academy of Forensic Sciences 18:386.

Keough N, L'Abbé EN, Steyn M, Pretorius S. 2015. Assessment of skeletal changes after post-mortem exposure to fire as an indicator of decomposition stage. Forensic Sci Int 246:17-24.

Koon HEC, Nicholson RA, Collins MJ. 2003. A practical approach to the identification of low temperature heated bone using TEM. J Archaeol Sci 30(11):1393-1399.

Krogman WM. 1943a. Role of the physical anthropologist in the identification of human skeletal remains, Part I. FBI Law Enforcement Bulletin 12(4):17-40.

Krogman WM. 1943b. Role of the physical anthropologist in the identification of human skeletal remains, Part II. FBI Law Enforcement Bulletin 12(5):12-28.

Kuhn LT, Grynpas MD, Rey CC, Wu Y, Ackerman JL, Glimcher MJ. 2008. A comparison of the physical and chemical differences between cancellous and cortical bovine bone mineral at two ages. Calcified Tissue Int 83(2):146-154.

Lebon M, Reiche I, Bahain JJ, Chadefaux C, Moigne AM, Fröhlich F, Sémah F, Schwarcz HP, Falguères C. 2010. New parameters for the characterization of diagenetic alterations and heat-induced changes of fossil bone mineral using Fourier transform infrared spectrometry. J Archaeol Sci 37(9):2265-2276.

LeGeros RZ and LeGeros J.P. 1983. Carbonate analysis of synthetic mineral and biological apatites. J Dent Res 62:259.

LeGeros RZ, Trautz OR, Legeros JP, Klein E. 1968. Carbonate substitution in the apatitic structure. Bull Soc Chim Fr 4:1712-1718.

Marceau CM. 2007. Bone Weathering in a Cold Climate: Forensic Applications of a Field Experiment Using Animal Models. (Unpublished Master's thesis). University of Alberta, Alberta, Canada.

Mayne PM. 1990. The Identification of Precremation Trauma in Cremated Bone. (Unpublished Master's thesis). University of Alberta, Alberta, Canada.

Mayne Correia PM. 1997. Fire modification of bone: a review of the literature. In: Haglund WD, Sorg MH, editors. Forensic Taphonomy: The Postmortem Fate of Human Remains. Boca Raton (Fl): CRC Press. pp 275-293.

Michel V, Ildefonse P, Morin G. 1995. Chemical and structural changes in Cervus elaphus tooth enamels during fossilization (Lazaret Cave): a combined IR and XRD Rietveld analysis. Appl Geochem 10:145-159.

Miller A and Parker SB. 1984. Collagen: the organic matrix of bone [and discussion]. Philosophical Transactions of the Royal Society of London B: Biological Sciences 304(1121), 455-477.

Mkukuma LD, Skakle JM, Gibson IR, Imrie CT, Aspden RM, Hukins DW. 2004. Effect of the proportion of organic material in bone on thermal decomposition of bone mineral: an investigation of a variety of bones from different species using thermogravimetric analysis coupled to mass spectrometry, high-temperature x-ray diffraction, and Fourier transform infrared spectroscopy. Calcif Tissue Int 75(4):321-328.

Morris MD, Finney WF. 2004. Recent developments in Raman and infrared spectroscopy and imaging of bone tissue. Spectroscopy 18(2):155-159.

Munro LE, Longstagge FJ, White CD. 2007. Burning and boiling of modern deer bone: effects on crystallinity and oxygen isotope composition of bioapatite phosphate. Palaeogeogr Palaeocl 249(1):90-102.

Munro LE, Longstaffe FJ, White CD. 2008. Effects of heating on the carbon and oxygen-isotope compositions of structural carbonate in bioapatite from modern deer bone. Palaeogeogr Palaeocl 266(3):142-50.

Munsell Soil Color Book. 2012. 2009 Revised ed. Grand Rapids (MI): Munsell Color X-Rite.

Nagy G, Lorand T, Patonai Z, Montsko G, Bajnoczky I, Marcsik A, Mark L. 2008. Analysis of pathological and non-pathological human skeletal remains by FT-IR spectroscopy. Forensic Sci Int 175(1):55-60.

Nakada H, Numata Y, Sakae T, Kimura-Suda H, Tanimoto Y, Sawki H, Teranishi M, Kato T, LeGeros RZ. 2010. Changes in bone quality associated with the mineralization of new bone formed around implants – using XPS, polarized microscopy, and FTIR imaging. J Hard Tissue Biol 19(20):101-110.

Nalla RK, Kinney JH, Ritchie RO. 2003. Mechanistic fracture criteria for the failure of human cortical bone. Nat Mater 2(3):164-168.

Nawrocki SP. 2009. Forensic taphonomy. In: Blau J, Ubelaker DH, editors. Handbook of Forensic Anthropology and Archaeology. Walnut Creek (CA): Left Coast Press. pp 284-295.

Nelson R. 1992. A microscopic comparison of fresh and burned bone. J Forensic Sci 37(4):1055-1060.

Nicholson RA. 1993. A morphological investigation of burnt animal bone and an evaluation of its utility in archaeology. J Archaeol Sci 20(4):411-428.

Olsen J, Heinemeier J, Bennike P, Krause C, Hornstrup KM, Thrane H. 2008. Characterisation and blind testing of radiocarbon dating of cremated bone. J Archaeol Sci 35(3):791-800.

Ou SF, Chiou SY, Ou KL. 2013. Phase transformation on hydroxyapatite decomposition. Cram Int 39(4):3809-3816.

Park DK, Park KH, Ko JS, Kim YS, Chung NE, Ahn YW, Han SH. 2009. The role of forensic anthropology in the examination of the Daegu subway disaster (2003, Korea). J Forensic Sci 54(3):513-8.

Paschalis EP, DiCarlo E, Betts F, Sherman P, Mendelsohn R, Boskey AL. 1996. FTIR microspectroscopic analysis of human osteonal bone. Calcified Tissue Int 59(6):480-487.

Paschalis EP, Betts F, Mendelsohn R, Boskey AL. 1997. FTIR microspectroscopic analysis of normal human cortical and trabecular bone. Calcified Tissue Int 61 (6):480-486.

Paschalis EP. 2009. Fourier transform infrared analysis and bone. Osteoporosis Int 20(6):1043-1047.

Paschalis EP, Verdelis K., Doty SB, Boskey AL, Mendelsohn R, Yamauchi M. 2001. Spectroscopic characterization of collagen cross-links in bone. J Bone Miner Res 16(10):1821-1828.

Paschalis EP, Mendelsohn R, Boskey AL. 2011. Infrared assessment of bone quality: A Review. Clin Orthop Relat Res 469(8):2170-2178.

Patonai Z, Maasz G, Avar P, Schmidt J, Lorand T, Bajnoczky I, Mark L. 2013. Novel dating method to distinguish between forensic and archaeological human skeletal remains by bone mineralization indexes. Int J Legal Med 127(2):529-533.

Pearson OM and Lieberman DE. 2004. The aging of Wolff's "Law": ontogeny and responses to mechanical loading in cortical bone. Yearb Phys Anthropol 47(S39):63-99.

Pestle WJ, Ahmad F, Vesper BJ, Cordell GA, Colvard MD. 2014. Ancient bone collagen assessment by hand-held vibrational spectroscopy. J Archaeol Sci 42(1):381-389.

Piga G, Hernández-Gasch J, Malgosa A, Ganadu ML, Enzo S. 2010. Cremation practices coexisting at the S'Illot des Porros Necropolis during the Second Iron Age in the Balearic Islands (Spain). Homo 61(6):440-452.

Piga G, Malgosa A, Thompson TJ, Guirguis M, Enzo S. 2015. A unique case of prone position in the primary cremation tomb 252 of *Monte Sirai* necropolis (Carbonia, Sardinia, Italy). Int J Osteoarchaeol 25(2):146-159.

Piga G, Gonçalves, Thompson TJ, Brunetti A, Malgosa A, Enzo S. 2016. Understanding the crystallinity indices behavior of burned bones and teeth by ATR-IR and XRD in the presence of bioapatite mixed with other phosphate and carbonate phases. Int J Spectroscopy 2016(Article ID 4810149).

Pope EJ. 2007. The Effects of Fire on Human Remains: Characteristics of Taphonomy and Trauma. (Unpublished Doctoral dissertation). University of Arkansas, Fayetteville, Arkansas.

Pope EJ, Smith OC. 2004. Identification of traumatic injury in burned cranial bone: An experimental approach. J Forensic Sci 49(3):431-440.

Porta D, Poppa P, Regazzola V, Gibelli D, Schillaci DR, Amadasi A, Magli F, Cattaneo C. 2013. The importance of an anthropological scene of crime investigation in the case of burnt remains in vehicles: 3 case studies. AM J Foren Med Path 34(3):195-200.

Quatrehomme G, Bolla M, Muller M, Rocca JP, Grévin G, Bailer P, Ollier A. 1998. Experimental single controlled study of burned bones: contribution of scanning electron microscopy. J Forensic Sci 43(2):417-422.

Reiche I, Favre-Quattropani L, Vignaud C, Bocherens H, Charlet L, Menu M. 2003. A multi-analytical study of bone diagenesis: the Neolithic site of Bercy (Paris, France). Meas Sci Technol 14(9):1-12.

Reilly DT, Burnstein AH. 1974. The mechanical properties of cortical bone. J Bone Joint Surg 56(5):1001-1022.

Rey C, Collins B, Goehl T, Dickson IR, Glimcher MJ. 1989. The carbonate environment in bone mineral: a resolution-enhanced Fourier transform infrared spectroscopy study. Calcif Tissue Int 45(3):157-164.

Richards NF. 1977. Fire investigation—destruction of corpses. Med Sci Law.17(2):79-82.

Rodriguez WC, Bass WM. 1985. Decomposition of buried bodies and methods that may aid in their location. J Forensic Sci 30(3):836-852.

Salesse K, Dufour E, Lebon M, Wurster C, Castex D, Bruzek J, Zazzo A. 2014. Variability of bone preservation in a confined environment: the case of the catacomb of Sts Peter and Marcellinus (Rome, Italy). Palaeogeogr Palaeocl 416:43-54.

Schiegl S, Goldberg P, Pfretzschner H, Conard N. 2003. Paleolithic burnt bone horizons from the Swabian Jura: distinguishing between *in situ* fireplaces and dumping areas. Geoarchaeology 18(5):541-565.

Schoenly K, Griest K, Rhine S. 1991. An experimental field protocol for investigation of postmortem interval using multidisciplinary indicators. J Forensic Sci 36(5):1395-1415.

Schotsmans EM, Denton J, Dekeirsschieter J, Ivaneanu T, Leentjes S, Janaway RC, Wilson AS. 2012. Effects of hydrated lime and quicklime on the decay of buried human remains using pig cadavers as human body analogues. Forensic Sci Int 217(1):50-59.

Schotsmans EM, Fletcher JN, Denton J, Janaway RC, Wilson AS. 2014. Long-term effects of hydrated lime and quicklime on the decay of human remains using pig cadavers as human body analogues: field experiments. Forensic Sci Int 238:141.e1–141e.13.

Shahack-Gross R, Bar-Yosef O, Weiner S. 1997. Black-coloured bones in Hayonim Cave, Israel: differentiating between burning and oxide staining. J Archaeol Sci 24(5):439-446.

Shipman P, Foster G, Schoeninger M. 1984. Burnt bones and teeth: an experimental study of color, morphology, crystal structure and shrinkage. J Archaeol Sci 11(4):307-325.

Snoeck C, Lee-Thorp JA, Schulting RJ. 2014. From bone to ash: compositional and structural changes in burned modern and archaeological bone. Palaeogeogr Palaeocl 416:55-68.

Snoeck C, Schulting RJ, Lee-Thorp JA, Lebon M, Zazzo A. 2016. Impact of heating conditions on the carbon and oxygen isotope composition of calcined bone. J Archaeol Sci 65:32-43.

Spennemann D and Colley S. 1989. Fire in a pit: the effects of burning on faunal remains. Archaeozoologia 3(1-2):51-64.

Squires KE, Thompson TJ, Islam M, Chamberlain A. 2011. The application of histomorphometry and Fourier Transform Infrared Spectroscopy to the analysis of early Anglo-Saxon burned bone. J Archaeol Sci 38(9):2399-2409.

Stiner MC, Kuhn SL, Weiner S, Bar-Yosef O. 1995. Differential burning, recrystallization, and fragmentation of archaeological bone. J Archaeol Sci 22(2):223-237.

Stiner MC, Kuhn SL, Surovell TA, Goldber P, Meignen L, Weiner S, Bar-Yosef O. 2001. Bone preservation in Hayonim Cave (Israel): a macroscopic and mineralogical study. J Archaeol Sci 28(6):643-659.

Stover SM, Pool RR, Martin RB, Morgan JP. 1992. Histological features of the dorsal cortex of the third metacarpal bone mid-diaphysis during postnatal growth in thoroughbred horses. Journal of Anatomy 181:455-469.

Stuart B. 2004. Introduction. In: Stuart B, editor. Infrared Spectroscopy: Fundamentals and Applications. Chichester (UK): John Wiley & Sons. pp 1 -14.

Stuart BH, Dent BB, Fenwick-Mulcahy S, Forbes SL. 2005. Characterization of adipocere formation in animal species. J Forensic Sci 50(3):1-8.

Surovell TA, Stiner MC. 2001. Standardizing infra-red measures of bone mineral crystallinity: an experimental approach. J Archaeol Sci 28(6):633-642.

Symes SA, Smith OC, Berryman H, Peters CE, Rockhold LA, Haun SJ, Francisco JT, Sutton TP. 1996. Bones: bullets, burns, bludgeons, blunders, and why (Workshop). Proceedings of the American Academy of Forensic Sciences 2:10-11.

Symes SA, Smith OC, Berryman H, Pope EJ. 1999a. Patterned thermal destruction of human remains. Paper presented to the 30th anniversary of the T.D. Stewart "Personal Identification in Mass Disasters" Central Identification Laboratory, Hawaii.

Symes SA, Smith OC, Gardner CD, Francisco JT, Horton GA. 1999b. Anthropological and pathological analyses of sharp trauma in autopsy. Proceedings of the American Academy of Forensic Sciences 5:177-178.

Symes SA, Pope EJ, Smith OC, Gardener CD, Zephro LA. 2001. Burning observations III: Analysis of fracture patterns in burned human remains. Proceedings of the American Academy of Forensic Sciences 7:278.

Symes SA, Rainwater CW, Chapman EN, Gipson DR, Piper AL. 2008a. Patterned thermal destruction of human remains in a forensic setting. In: Schmidt CW, Symes SA, editors. The Analysis of Burned Human Remains. Amsterdam, the Netherlands: Academic Press. pp 15-54.

Symes SA, Rainwater CW, Chapman EN, Stull K. 2008b. Recognizing patterned fire and heat damage to bone. A Presentation before the 60th Anniversary Meeting of the American Academy of Forensic Sciences, February 18-23, Washington, D.C.

Symes SA, Dirkmaat DC, Ousley S, Chapman EN, Cabe L. 2012. Recovery and interpretation of burned human remains. Technical report prepared for the National Institute of Justice, Department of Justice. Funded by the National Institute of Justice Award No. 2008-DN-BX-K131.

Symes SA, L'Abbé EN, Pokines JT, Yuzwa T, Messer D, Stromquist A, Keough N. 2014a. Thermal alteration to bone. In: Pokines JT, Symes SA, editors. Manual of Forensic Taphonomy. Boca Raton (FL): CRC Press. pp 367-402.

Symes SA, L'Abbé EN , Stull KE, Lacroix M, Pokines JT. 2014b. Taphonomy and the timing of bone fractures in trauma analysis. In: Pokines JT, Symes SA, editors. Manual of Forensic Taphonomy. Boca Raton (FL): CRC Press. pp 341-366.

Tanasescu RN, Fulias A, Ledeti I, Miron MI, Matusz P. 2015. Evaluation of mineral composition in the area of the cortical osteoporotic bone: a Fourier transform infrared spectroscopy (FTIR) and scanning electronic microscopy (SEM) study. Rev Chim-Bucharest 66(12):2047-2050.

Thompson TJ, 2002. The assessment of sex in cremated individuals: some cautionary notes. Canadian Society of Forensic Science Journal 35(2):49-56.

Thompson TJ. 2003. An Experimental Study of the Effects of Heating and Burning on the Hard Tissues of the Human Body, and its Implications for Anthropology and Forensic Science. (Unpublished Doctoral dissertation). University of Sheffield, Sheffield, England.

Thompson TJ. 2004. Recent advances in the study of burned bone and their implications for forensic anthropology. Forensic Sci Int 146S:S203-S205.

Thompson TJ. 2005. Heat-induced dimensional changes in bone and their consequences for forensic anthropology. J Forensic Sci 50(5):1-8.

Thompson TJ and Chudek JA. 2007. A novel approach to the visualisation of heat-induced structural change in bone. Science Justice 47(2): 99-104.

Thompson TJ, Gauthier M, Islam M. 2009. The application of a new method of Fourier transform infrared spectroscopy to the analysis of burned bone. J Archaeol Sci 36(3):910-914.

Thompson TJ, Islam M, Piduru K, Marcel A. 2011. An investigation into the internal and external variables acting on crystallinity index using Fourier transform infrared spectroscopy on unaltered and burned bone. Palaeogeogr Palaeocl 299(1):168-174.

Thompson TJ, Islam M, Bonniere M. 2013. A new statistical approach for determining the crystallinity of heat-altered bone mineral from FTIR spectra. J Archaeol Sci 40(1):416-422.

Thurman M and Willmore LJ. 1980. A replicative cremation experiment. N Am Archaeol 2(4):275-283.

Turunen MJ, Saarakkala S, Rieppo L, Helminen HJ, Jurvelin JS, Isaksson H. 2011. Comparison between infrared and Raman spectroscopoic analysis of maturing rabbit cortical bone. Appl Spectrosc 65(6):595-603.

Turunen MJ, Lages S, Labrador A, Olsson U, Tagil M, Jurvelin JS, Isaksson H. 2014. Evaluation of composition and mineral structure of callus tissue in rat femoral fracture. J Biomed Opt 19(2):0250031-0250038.

Ubelaker DH. 2009. The forensic evaluation of burned skeletal remains: a synthesis. Forensic Sci Int 183(1-3):1-5.

Ubelaker DH, Owsley DW, Houck MM, Craig E, Grant W, Woltanski T, Fram R, Sandness K, Peerwani N. 1995. The role of forensic anthropology in the recovery and analysis of branch Davidian Compound victims: recovery procedures and characteristics of the victims. J Forensic Sci 40(3):335-340.

Van Strydonck MV, Decq L, Van Den Brande T, Boudin M, Ramis D, Borms H, De Mulder G. 2015. The protohistoric ‘quicklime burials’ from the Balearic Islands: cremation or inhumation. Int J Osteoarchaeol 25(4):392-400.

Walker PL, Miller KP. 2005. Time, temperature, and oxygen availability: an experimental study of the effects of environmental conditions on the color and organic content of cremated bone. Am J Phys Anthropol S40:216-217.

Walters MA, Leung YC, Blumenthal NC, LeGeros RZ, Konsker KA. 1990. A Raman and infrared spectroscopic investigation of biological hydroxyapatite. J Inorg Biochem 39(3):193-200.

Wang XY, Zuo Y, Huang D, Hou X, Li Y. 2010. Comparative study on inorganic composition and crystallographic properties of cortical and cancellous bone. Biomed Environ Sci 23(6):473-480.

Webb WS and Snow CE. 1945. The Adena People. The Adena People. University of Kentucky Reports in Anthropology and Archaeology 6: 1-369. University of Kentucky, Lexington.

Weiner S, Bar-Yosef, O. 1990. States of preservation of bones from prehistoric sites in the near east: a survey. J Archaeol Sci 17(2):187-196.

Weiner S, Goldberg P, Bar-Yosef O. 1993. Bone preservation in Kebara Cave, Israel using on-site Fourier transform infrared spectrometry. J Archaeol Sci 20(6):613-627.

Wells C. 1960. A study of cremation. Antiquity 34(133):29-37.

White TD, Black MT, Folkens PA. 2012. Human osteology (3rd ed.). Burlington (MA): Academic press.

Wilson AS, Janaway RC, Holland AD, Dodson HI, Baran E, Pollard AM, Tobin DJ. 2007. Modelling the buried human body environment in upland climes using three contrasting field sites. Forensic Sci Int 169(1):6-18.

Whyte TR. 2001. Distinguishing remains of human cremations from burned animal bones, J. Field Archaeol. 28 (3-4):437-448.

Van Vark GN. 1970. Some statistical procedures for the investigation of prehistoric skeletal material. (Unpublished doctoral dissertation). Rijksuniversiteit de Groningen, Groningen, Netherlands.

Wright LE, Schwarcz HP. 1996. Infrared and isotopic evidence for diagenesis of bone apatite at Dos Pilas, Guatemala: palaeodietary implications. J Archaeol Sci 23(6):933-944.

Wopenka B and Pasteris J.D. 2005. A mineralogical perspective on the apatite in bone. Mater Sci Eng: C 25(2):131-143.

Younesi M, Javadpour S, Bahrololoom ME. 2011. Effect of heat treatment temperature on chemical compositions of extracted hydroxyapatite from bovine bone ash. J Mater Eng Perform 20(8):1484-1490.

CURRICULUM VITAE